Basement Membrane Homeostasis and Repair

By
Angela Marie Howard

Dissertation
Submitted to the Faculty of the
Graduate School of Vanderbilt University
in partial fulfillment of the requirements
for the degree of
DOCTOR OF PHILOSOPHY
in
Cell and Developmental Biology
May 10th, 2019
Nashville, Tennessee

Approved:
Andrea Page-McCaw, Ph.D.
Alissa M. Weaver, Ph.D.
Gautam Bhave, Ph.D.
Chin Chiang, Ph.D.
Matthew Tyska, Ph.D.

Acknowledgements

First and foremost, thank you to my academic advisor, Andrea Page-McCaw. She has provided me with ample amounts of support and advice throughout the course of my thesis work. I also appreciate the feedback I have received from my thesis committee- Alissa Weaver, Gautam Bhave, Ching Chiang, and Matthew Tyska. Lastly, thank you Dr. Christopher Wright for his insight into the scientific community and for his mentorship.

Thank you to my lab mates, both past and present. They have been an amazing sounding board for my experimental woes as well as providing ample laughs to get me through my weeks. Our lab manager, Kimi, has been instrumental in helping me with a multitude of experiments over the years.

My parents, Robert and Theresa Howard, have played an extremely influential role in where I am today. I could honestly never thank them enough for all they have done for me. A colossal thank you goes to my mother for her kind words and extraordinary amount of patience as I have ventured through this graduate school journey. Thank you for always answering my calls, even when it was the fifth one that day and I ranted about the same thing as the other four calls.

A major shout out to all my friends for their incredible amount of emotional support. Graduate school would have been insurmountable without their encouragement. Thank you for all the visits, good times, and listening ears throughout my years here.

Last, but not least thank you to my fur children, Charles Daniel, Benjamin, and Nutmegan, for all their help along the way. Their comforting cuddles and meticulous editing skills were imperative, especially over these last few months.

List of Figures

List of Tables

List of Abbreviations

DSS = Dextran Sodium Sulfate

Table of Contents

Chapter 1

A brief review of basement membrane, its repair, and damage models

Review of the basement membrane

Basement membrane is a sheet-like extracellular matrix essential for anchoring epithelial cells. The basement membrane surrounds blood vessels, muscles, and organs, and it underlies epithelia. Yet very little is understood about how the basement membrane is altered in response to tissue changes: for example, repair and changing size. The basement membrane is a dynamic system with assembly and disassembly mechanisms that can account for its expansion, shrinkage, repair, and – when these processes are balanced – homeostasis (Avery and Horvitz 1989; Haigo and Bilder 2011; Pastor-Pareja and Xu 2011; Ihara et al. 2011)

Basement membrane assembly

One aspect of basement-membrane dynamics is its assembly. Collagen IV is the most abundant protein in the basement membrane. It serves as a scaffold for the assembly of macromolecules, and it can interact with cell surface receptors such as integrins to control cell adhesion, migration, proliferation, and differentiation (Pöschl et al. 2004; Yurchenco and Furthmayr 1984). Collagen IV assembly begins with the translation of three alpha chains with a 7S domain at the N-terminus, a central collagenous region, and a globular NC1 domain at the C-terminus. In the Golgi apparatus, these three chains wrap around each other in a zipper like fashion to form a

triple-helical protomer. While in the Golgi, some of the lysine and proline amino acids of Collagen IV are hydroxylated, and some of these hydroxylysines are then glycosylated (Sricholpech et al. 2012; Kivirikko et al. 1973; Risteli and Kivirikko 1974; R. G. Spiro and Spiro 1971; Liefhebber et al. 2010; Schegg et al. 2009).

These protomers are secreted and then incorporated extracellularly into an extended and continuous lattice within the basement membrane. Three kinds of intermolecular interactions participate in this assembly: the 7S domains form tetramers, NC1 domains form head-to-head dimers, and the triple-helix regions form lateral associations. Remarkably, purified collagen IV can self-assemble into an extended lattice that can be visualized by EM rotary shadowing (Yurchenco and Furthmayr 1984). The collagen IV NC1 domain undergoes a chloride ion dependent conformational change outside of the cells it was produced in, which triggers the assembly of Collagen IV networks (Cummings et al. 2016). Chloride levels are at increased concentrations outside the cells, which is thought to cause the Collagen IV assembly activation. The NC1 domains are observed to associate head-to-head. The 7S amino-terminus of one Collagen IV protomer comes together with the amino-termini of three other protomers to form a tetramer (TIMPL and GLANVILLE 1981; Kühn and Kraehenbuhl 1981; J. H. Fessler, Shigaki, and Fessler 1985), and lateral associations are observed. Thus, it appears that a collagen IV scaffold can self-assemble from secreted material from cells, and few if any regulatory steps are required after secretion into the extracellular environment.

Like collagen IV, laminin also forms an extended network from an initial trimer. Using rotary shadowing, it was shown that purified laminin from EHS tumors forms a

trimer from 1 alpha-chain, 1-beta chain and 1-gamma chain to create a cross-like shape of one long and three similar short arms (Engel et al. 1981). The heterotrimer and its posttranslational modifications occur in the Golgi. Upon secretion to the necessary location, the laminin N-terminal (LN) domains of the short arms of laminin interact to form ternary nodes (Hohenester and Yurchenco 2013). In vitro studies showed laminin can self-assemble in a two-step process when the chains of laminin are warmed to 21-35 ^{o}C in a neutral phosphate buffer then calcium ions were dialyzed into the laminin to form the laminin heterotrimer (Yurchenco et al. 1985).

Nidogen consists of three globes, which are connected by a thin rod-like segment. Nidogen forms a stable complex with both laminin and collagen IV in the basement membrane with distinct binding sites for the two different proteins (Fox et al. 1991). Perlecan is the fourth conserved component of the basement membrane. Using rotary shadowing electron micrographs, it was revealed that perlecan looked like "beads on a string," with globules separated by thin segments. Perlecan is able to not only self-aggregate, but also bind to laminin through its non-heparan sulfate-containing terminal globule (Noonan et al. 1991)

Order of basement membrane assembly

As the assembly is important for proper formation of the components, the order of basement membrane assembly is important for proper basement membrane formation. Previous work on the basement membrane has shown laminin deposition is needed for the formation of the basement membrane (Pöschl et al. 2004). If laminin is mutated then no other basement membrane components are able to come together to

form a complete basement membrane. Collagen IV deposition is dependent on laminin being laid down (Li et al., 2002) (Murray and Edgar, 2000) . With the ectopic addition of laminin to laminin mutant embryoid bodies that otherwise do make basement membrane, the tissue is fully rescued and the formation of basement membrane is seen (S. Li et al. 2002; Murray and Edgar 2000). Collagen IV knockdown mice can survive to E10.5-11.5 if laminin is still deposited (Pöschl et al. 2004). If certain basement membrane components, such as laminin and collagen IV, are mutated or deleted it leads to early embryonic death due to massive defects in the circulatory system. When the basement membrane was inhibited from establishing the necessary thickness by mutating nidogen, the mouse lacked the ability to form a healthy vascular system (Candiello et al. 2007).

As collagen IV is dependent on laminin for assembly, perlecan is dependent on collagen IV. When collagen IV is knocked down, perlecan levels are reduced in assembly (Pastor-Pareja and Xu 2011). In other words, Pastor-Pareja et. al showed without collagen IV in the basement membrane they were unable to see the incorporation of the perlecan. Perlecan deficient mice are able to normally develop, but die at E10.5 from heart failure cause by unstable basement membrane in a mechanically high stress environment (Costell et al. 1999). Perlecan defects go beyond the basement membrane where tears in the cartilage can be seen (Costell et al. 1999).

For the fourth conserved component of the basement membrane, nidogen, its dependency on the other components has been questioned for many years. Two forms of nidogen in the murine basement membrane exist and upon the knockdown of one or both of the isoforms there is no difference as assayed by light and electron microscopy

in the murine adult kidney basement membrane (Gersdorff et al. 2007). In C. elegans nidogen is required for switching the axon from circumferential to longitudinal in migration. However, the basement membrane can still assemble in the absence of nidogen (Kim and Wadsworth 2000). Mouse studies have also concluded that nidogen mutated animals show no phenotypic difference during development, but nidogen is required for both renal and lung formation. Interestingly, mice with a mutation in the nidogen-binding region in laminin die shortly after birth due to insufficient kidney and lung development (Willem et al. 2002). Recently, a 2018 paper from the Martin-Bermudo lab, showed that nidogen is not essential for viability or organogenesis in flies, but is required for fertility. Furthermore, it is also required for the proper formation of the basement membrane in the adipose tissues and flight muscles. Without nidogen in the larval adipose tissue, the Laminin and Collagen IV networks will uncouple as nidogen is the linker which connects Laminin and Collagen IV (Dai et al. 2018). Moreover, Nidogen depends on laminin deposition for incorporation into the basement membrane (Dai et al. 2018; Ramos-Lewis and Page-McCaw 2018).

Cellular sources of the basement membrane components

The assembly of the basement membrane has been studied mostly in vitro with more recent findings occurring in vivo. In vitro studies show epithelial cells are able to secrete their own basement membrane and this basement membrane is assembled by cells. However, sometimes the basement membrane is secreted by cells far away (Hohenester and Yurchenco 2013). Epithelial, endothelial, and mesenchymal cells of the mouse embryo have been shown to produce varying levels and types of basement

membrane components as indicated by mRNA expression (Thomas and Dziadek 1993). The differing levels and patterns of gene expression for each basement membrane component have been shown to have an impact on the branching morphogenesis in embryonic mouse lungs (Thomas and Dziadek 1994). This shows the importance of the proper gene expression patterns for the basement membrane components. The paper also showed that collagen IV α1, laminin β1, and laminin β2 genes were expressed both in the mesenchyme and epithelium while nidogen was only expressed in the mesenchyme. Laminin α gene expression was restricted to epithelial-mesenchymal interface cells. The specific type depends on the region of interest (Thomas and Dziadek 1994). The production of nidogen in the mesenchyme has been shown to be important, as mesenchymal nidogen is able to bind to epithelial laminin during epithelial development (Ekblom et al. 1994). Blocking the nidogen binding site of laminin β2 using antibodies disrupted the epithelial development in embryonic mouse kidney and lung (Ekblom et al. 1994). In Drosophila studies, it has been shown collagen IV comes from blood cells (hemocyctes) during early embryogenesis (Lunstrum et al. 1988).

In a cell culture model, the neighboring cells secrete the basement membrane components. In the cell culture model, there are two possible sources for new basement membrane components, the media or the neighboring cells. In vivo, there are a multitude of other players with the ability to secrete and deposit new basement membrane. After laminin assembles into a heterotrimer it binds to the cell through integrin and other cell surface receptors. Collagen IV also goes through self-assembly then proceeds to bind to laminin through nidogen and heparan sulfates, such as perlecan and agrin (Hohenester and Yurchenco 2013). Although most of these findings

have been confirmed in vivo, it is now known that the basement membrane is not just secreted by neighboring cells in vivo.

The role of basement membrane components in tissue morphogenesis

Certain basement membrane components have been shown to be necessary for tissue-specific morphogenesis. Using a GFP-based RNAi method (iGFPi) to knock down GFP-trapped proteins, the Xu lab at Yale showed that collagen IV plays a role in the organ shape. Collagen IV is necessary for constricting the organ then for recruiting perlecan, which counteracts this force (Pastor-Pareja and Xu 2011). Laminin was shown to have an early role in the set-up of cell polarity in the C. elegans pharynx. None of the other basement membrane components were shown to play a role in the orientation of cell polarity, and this role was interestingly distinguishable from laminin's later basement membrane integrity role. Overgrowth of the plasma membrane of Drosophila adipocytes causes an over accumulation of the collagen IV protein (Zang et al. 2015). The fibrotic nature of this phenotype shows the importance in understanding the relationship between the cells and the basement membrane. Another study showed multiple cell-specific transcription factors regulate the expression of the Drosophila basement membrane gene, Nidogen (Zhu et al. 2012). So, not only do the basement membrane components play a role in the regulation of tissue and organ development, but the cells can also play a role in basement membrane transcription.

If the basement membrane components are not always secreted locally then what determines where a basement membrane is assembled? Not much is known about the specifics of where basement membrane is laid down; however, it is known

that integrins play an integral part in the formation and assembly of the basement membrane. Upon conditional ablation of B1 integrins in the skin of mice, there is severe failure of the basement membrane to assemble, which causes downstream effects such as hemidesmosome instability, lack of epidermal proliferation, and hair follicle formation failure (Raghavan et al. 2000). Dystroglycan is also thought to play a role in connecting the basement membrane to the muscles.

Furthermore, it has been shown secreted protein acidic and rich in cysteine (SPARC) can also be a key player in the assembly and formation of the basement membrane. SPARC-null mice show a phenotypic abnormality in their cell surface-basement membrane interface in their eye lenses. Filopodial projections from various eye cells reached into the basement membrane causing disruption. SPARC seems to be an important component in assembling the proper basement membrane components on this interface (Norose et al. 2000). A recent paper by Sally Horne Badovinac's lab shows the importance of SPARC in egg elongation and collagen IV regulation. Through SPARC over-expression the egg was not able to elongate properly by preventing the necessary rise in collagen IV levels throughout elongation (Isabella and Horne-Badovinac 2015b).

Cross-linking of collagen IV

After the deposition of the protomers into the basement region, the C-terminal NC1 domains cross-link via sulfilimine bonds to form a hexamer (Vanacore et al. 2009; L. I. Fessler and Fessler 1982). Collagen IV forms superstructures by one protomer (a trimer of α collagen IV chains) cross-linking with another protomer to form a hexamer

(Kalluri 2003; Yurchenco 2011). These hexamers are able to cross-link to other hexamers on the N-terminus side, 7S domain, to form tetramers and then go on to form superstructures. All of this cross-linking is thought to be imperative for the strength of the basement membrane. There is additional disulfide cross-linking occurring between the long collagenous domains to provide additional support to the collagen IV polymer scaffold (L. I. Fessler and Fessler 1982; SIEBOLD, DEUTZMANN, and KUHN 1988).

In 1992, Nelson et. al. discovered a novel protein combining peroxidase and extracellular matrix motifs, which they proposed could bind the collagen IV (Nelson, Fessler, Takagi, Blumberg, Keene, Olson, Parker, and Fessler 1994a). However, they did not know the function of the enzyme. In 2009, Roberto Vanacore discovered the NC1 covalent crosslink was a bond never seen before in nature, a sulfilimine bond. Then three years later, Gautam Bhave discovered the necessity of peroxidasin and a hypohalous acid in cross-linking of these then sulfilimine bonds.(Bhave et al. 2012). Finally, in collaboration with the Page-McCaw lab, McCall et. al. showed peroxidasin required bromine as its cofactor for crosslinking.

An insight to basement membrane repair

As with all biological systems, basement membrane will become damaged and will need to be repaired. As will be discussed in Chapter 2 of this thesis, the basement membrane distributes the forces experienced by muscle contraction and relaxation, and when the basement membrane is unable to distribute these forces then muscular dystrophy and skin blistering results (Nyström, Bornert, and Kühl 2017). Alport syndrome, Goodpasture's syndrome, and thin basement membrane diseases are more

examples of basement membrane diseases. Other diseases such as asthma, kidney failure, and diabetes have been shown to have damaged basement membranes, which may not be able to repair properly due to a faulty repair machinery (Flood-Page et al. 2003; Sugimoto, Mundel, Kieran, et al. 2006; Preil et al. 2015).

Will Ramos-Lewis, another member of the Page-McCaw lab, looked at the mechanistic repair of the varying basement membrane components in puncture wounds of Drosophila larvae. His data showed the mechanism of basement membrane repair are subtly different than those of embryonic assembly (Ramos-Lewis, LaFever, and Page-McCaw 2018). His western blot data raised questions on the turnover rates of the basement membrane as he was never able to deplete the hemolymph of the various basement membrane components without also affecting the protein levels in the basement membrane. It is known there is normal turnover of the basement membrane components and even the wild-type basement membrane proteins need to be replaced over the course of its lifetime. Basement membrane turnover occurs more rapidly in the gut than elsewhere in the body. Due to the gut being exposed to a vast array of damaging bacteria as it connects the outside world to the inner body, the gut basement membrane is more apt to be damaged. Even with the varying basement membrane diseases, very little is known about the mechanism of basement membrane repair.

As stated earlier in this chapter, there are four conserved components of the basement membrane across all phyla; laminin, collagen IV, perlecan, and nidogen. In chapter 2 of this thesis, we will show that two core basement membrane components, laminin, collagen IV, are necessary for the repair of the basement membrane in the gut

of the Drosophila. It does not seem there is a change in the level of cross-linking of collagen IV after damage or during the course of repair.

Much of the *de novo* basement-membrane assembly experiments have been done in cell culture, a system that cannot accurately answer questions about *in vivo* repair. The self-assembling nature of the basement membrane was first discovered *in vitro* with proteins purified from EHS sarcoma cell media culture (Matrigel) (Kleinman and Martin 2005). However, Matrigel cannot accurately recapitulate the multitude of players in an *in vivo* system. Some of these key players may be vital in understanding the repair mechanism of the basement membrane.

Why Drosophila for understanding repair?

Originally, the absence of basement membrane repair studies was due to the lack of a usable model system that allowed for manipulation of the varying components *in vivo.* However, the genetic advances of Drosophila have allowed for alteration of various proteins in both a spatial and temporal fashion. This latter part is critical for basement membrane protein knockdown as whole animal mutations are embryonically lethal and therefore, the proteins needs to be conditional mutated or knock-downed in a temporal fashion, after assembly has been completed.

Drosophila is a powerful model organism for the analyzing basement membrane dynamics. Fly basement membrane is homologous, yet simplified, compared to its vertebrate counterparts. For example, flies possess a single collagen IV heterotrimer encoded by 2 genes (*Cg25C* /*Col4*α*1* and *vkg*/*Col4*α*2*) while mice have 3 different collagen-IV heterotrimers assembled from 6 genes (*Col4*α*1, Col4*α*2, Col4*α*3, Col4*α*4,*

Col4α5, Col4α6). This pattern holds true for the other conserved proteins. Flies only form two laminin heterotrimers from 4 genes; while, mice form 15 laminin heterotrimers from 11 genes (Ramos-Lewis and Page-McCaw 2018). There is one nidogen protein in Drosophila and two in mice (Ramos-Lewis and Page-McCaw 2018). Finally, both Drosophila and mice only possess one perlecan protein (Ramos-Lewis and Page-McCaw 2018). For these core proteins, Drosophila have functional GFP-trapped proteins under the endogenous regulatory sequence (Ramos-Lewis and Page-McCaw 2018). This same pattern also holds true for the enzymes which modify the basement membrane. For the enzymes which cross-link Collagen IV, Peroxidasin and LOXL, there is one Peroxidasin in flies vs. 2 in mammals (Soudi et al. 2012), and 2 loxl proteins in flies vs. 4 in mammals (Csiszar 2001). For matrix metalloproteinases, the protease which cleaves the basement membrane protein components, flies have 2 matrix metalloproteinases in flies vs. 24 in mammals (Page-McCaw, Ewald, and Werb 2007).

	Basement membrane protein family	Mouse genes	*Drosophila* genes
Structural proteins	**Laminin**	**11 genes**	**4 genes**
	α-chain	*Lama1*	*Laminin A (LanA)*
		Lama2	*wing blister (wb)*
		Lama3	
		Lama4	
		Lama5	
	β-chain	*Lamb1*	*LanB1*
		Lamb2	
		Lamb3	
	γ-chain	*Lamc1*	*Laminin B2 (LanB2)*
		Lamc2	
		Lamc3	
	Collagen IV	**6 genes**	**2 genes**
	Collagen IV α1	*Col4a1*	*Collagen IV alpha 1 (Col4A1)*
	Collagen IV α2	*Col4a2*	*Viking (vkg)*
	Collagen IV α3	*Col4a3*	(not present)
	Collagen IV α4	*Col4a4*	(not present)
	Collagen IV α5	*Col4a5*	(not present)
	Collagen IV α6	*Col4a6*	(not present)
	Perlecan	**1 gene** *Hspg2*	**1 gene** *terribly reduced optic lobes (trol)*
	Nidogen	**2 genes** *Nid1* *Nid2*	**1 gene** *Nidogen/entactin (Ndg)*
Extracellular BM Modifying Enzymes	**Matrix Metalloproteinase**	**24 genes** *Mmp1a, Mmp1b, Mmp2, Mmp3, Mmp7, Mmp8, Mmp9, Mmp10, Mmp11, Mmp12, Mmp13, Mmp14, Mmp15, Mmp16, Mmp17, Mmp19, Mmp20, Mmp21, Mmp23, Mmp24, Mmp25, Mmp27, Mmp28, Mmp29*	**2 genes** *Matrix metalloproteinase 1 (Mmp1)* *Matrix metalloproteinase 2 (Mmp2)*
	Peroxidasin	**1 gene** *Pxdn*	**1 gene** *Peroxidasin (Pxn)*
	Lysyl Oxidase	**5 genes** *Lox* *Loxl1* *Loxl2* *Loxl3* *Loxl4*	**2 genes** *Lysyl oxidase-like 1 (Loxl1)* *Lysyl oxidase-like 2 (Loxl2)*

Table 1.1 Basement membrane components from Lewis-Ramos et. al. 2018 (Ramos-Lewis and Page-McCaw 2018)

Drosophila is also an excellent model organism to study damage and repair because of its sophisticated genetic tools. Utilizing a temperature sensitive system as well as tissue-specific upstream activation loci, the drosophila community can turn on and off almost any gene, in any specific cell or tissue, throughout the course of the animal's lifecycle. The community is also well-known for their generosity; they readily share their knowledge, flies, and reagents. Finally, there are a multitude of functional GFP-fusion proteins, which are expressed by the endogenous locus for all four of the major basement membrane proteins, which allows for easy visualization.

Why the gut as a model system to understand repair?

The intestine (gut) of the adult fruit fly is an excellent model system to study and understand damage. The gut of the Drosophila is a simplified complex system, which allows for easier analysis. The basement membrane in the gut underlies the epithelium layer and surrounds the circumferential muscles, which are responsible for peristalsis. A schematic representation of the gut is show below with the muscles in red and basement membrane in green. When the basement membrane is damaged, the surrounding muscles are sensitive to the mechanical changes experienced by the basement membrane causing the muscles to become dysmorphic as the basement membrane can no longer distribute the forces generated by the muscles (Andersen and Horne-Badovinac 2016), which is also seen in human muscular dystrophies (Kelemen-Valkony et al. 2012; Helbling-Leclerc et al. 1995). This simplified organization allows for easy imaging and analysis. The gut tissue is also an excellent model system as it is a large enough tissue that it allows for western blotting and protein analysis.

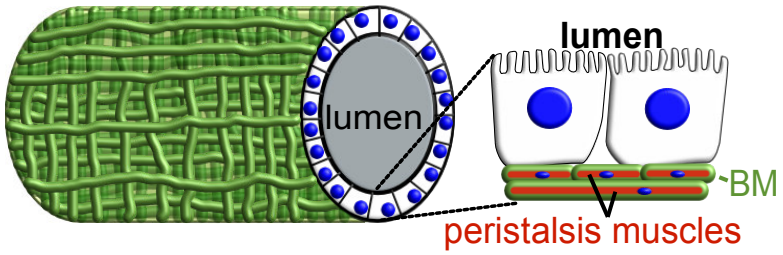

Figure 1.1- Schematic representation of the Drosophila gut.

An introduction to Dextran Sodium Sulfate

It is important to generate reproducible damage to the basement membrane of Drosophila in order to study repair. It is imperative the damage is able to repair itself and we can easily visualize and/or quantify the changes in damage and repair of the tissue. The Drosophila gut system is an ideal model to understand damage; however, we need a way to reproducibly damage it. For decades, Dextran Sodium Sulfate (DSS) has been fed to mice to induce ulcerative colitis, and most recently has made its way into being used in the fly community to induce damage. Specifically, the intestinal stem cell community, has used the DSS-feeding model to induce damage to the gut then analyze stem-cell regeneration. A paper from the Tony Ip's lab was looking for drugs to administrator to flies to induce intestinal stem cell divisions and tested dextran sodium sulfate. As a side note, they reported that DSS seemed to cause an unexplained disruption in the morphology of the basement membrane (Amcheslavsky, Jiang, and Ip 2009). Subsequent studies have utilized DSS feeding to induce damage in the fly gut gut (Amcheslavsky, Jiang, and Ip 2009; Ren et al. 2010; Karpowicz, Perez, and

Perrimon 2010; Cordero et al. 2012; Ren et al. 2013; Tian and Jiang 2014; You et al. 2014; Tian et al. 2015), but no one has further investigated the DSS effect on basement membrane.

The Page-McCaw lab became interested in using the DSS-damaging reagent when we noticed previous work out of our lab, where the loss of a basement membrane crosslinking enzyme, phenocopied the dextran sodium sulfate damage phenotype (McCall et al. 2014). Based on the similar phenotypes, we hypothesized that DSS was weakening the basement membrane. Therefore, we decided to feed the flies the chemical irritant, DSS. Chapter 2 of this thesis shows DSS causes the basement membranes of the gut to become morphologically thicker and mechanically weaker as well as causing dysmorphic muscle morphology. These phenotypes are easily quantified with muscle aspect ratio using epi-fluorescent microscopy as well as super-resolution microscopy. In collaboration with Nicholas Ferrell, a biomedical engineer in Medicine at Vanderbilt, a stress-strain analysis showing a quantifiable difference was performed and found a decrease in the mechanical stiffness of basement membrane damaged with dextran sodium sulfate.

Another important characteristic of a suitable damaging agent is one in which the tissue is able to recover from the damage. As shown in chapter 2, upon DSS damage, the basement membrane is remarkably able to recover within two days after DSS withdrawal. This is both a morphological and functional recovery. Therefore, DSS is a suitable reagent as it allows for highly reproducible damage and the repair occurs in a short-term frame. This thesis will use the DSS damage model, which we provide a

mechanism for, as a means to analysis basement membrane repair in the gut of the Drosophila.

Chapter 2

This chapter is an adaption from published work entitled-

DSS-induced damage to basement membranes is repaired by matrix replacement and crosslinking

Authors of the paper- Angela M. Howard, Kimberly S. LaFever, Aidan M. Fenix, Cherie' R. Scurrah, Ken S. Lau, Dylan T. Burnette, Gautam Bhave, Nicholas Ferrell, Andrea Page-McCaw

Abstract

Basement membranes are an ancient form of animal extracellular matrix. As important structural and functional components of tissues, basement membranes are subject to environmental damage and must be repaired while maintaining functions. Little is known about how basement membranes get repaired. This paucity stems from a lack of suitable in vivo models for analyzing repair. Here we show that Dextran Sodium Sulfate (DSS) directly damages the gut basement membrane when fed to adult Drosophila. DSS becomes incorporated into the basement membrane, promoting its expansion while decreasing its stiffness, which causes morphological changes to the underlying muscles. Remarkably, two days after withdrawal of DSS, the basement membrane is repaired by all measures. We used this new damage model to determine that repair requires collagen crosslinking and replacement of damaged components. Genetic and biochemical evidence indicate that crosslinking is required to stabilize the

newly incorporated repaired collagen IV rather than to stabilize the damaged collagen IV. These results suggest that basement membranes are surprisingly dynamic.

Introduction

Basement membranes are omnipresent extracellular structures in multicellular animals. They are strong thin sheets of extracellular matrix underlying epithelia, enveloping muscles and organs, and separating tissue layers. Basement membranes function as mechanical scaffolds to distribute cellular and tissue-level forces, and when they cannot distribute these forces, diseases such as muscular dystrophy and skin blistering result (Nyström, Bornert, and Kühl 2017). In addition to mechanical roles, basement membranes signal to cells and can tether other signaling molecules, directly and indirectly modulating cell differentiation, survival, migration, and polarity of epithelial cells (Kleinman and Martin 2005; S. Li et al. 2017; X. Wang et al. 2008; Bunt et al. 2010). Evolutionarily ancient structures, basement membranes are conserved from hydra to humans (Fidler et al. 2017). They are composed of four main components: laminin, collagen IV, perlecan, and nidogen. Super-resolution imaging of a glomerular basement membrane in vivo indicates it has a laminar structure with components spatially segregated into layers (Suleiman et al. 2013), a finding consistent with in vitro observations that laminin and collagen IV can polymerize independently to form sheet-like polymers (Yurchenco and Furthmayr 1984; Yurchenco et al. 1985; Yurchenco, Cheng, and Colognato 1992).

The mechanical strength of basement membranes comes mainly from collagen IV, which assembles non-covalently after undergoing a conformational change

mediated by high concentrations of extracellular chloride (Cummings et al. 2016). After extracellular assembly, the collagen IV network is reinforced by covalent crosslinking, the extent of which determines the stiffness of the basement membrane (Bhave, Colon, and Ferrell 2017). Crosslinking can occur at three distinct sites on a triple-helical collagen IV molecule: at the N-terminal 7S domain (Risteli et al. 1980; Langeveld et al. 1991), at lateral sites along the triple-helical domain (Yurchenco and Furthmayr 1984), and at the C-terminal NC1 domain (Vanacore et al. 2009). The best understood of these crosslinks is between NC1 domains, which are variably crosslinked head-to-head by sulfilimine bonds, covalent linkages catalyzed by the enzyme peroxidasin using bromide as a cofactor (Bhave et al. 2012; McCall et al. 2014). There are 2 possible sulfilimine crosslink sites within each NC1-NC1 dimer, and up to 6 per NC1 hexamer that joins two triple-helical structures. However, only about 2-4 of these 6 sites are occupied per hexamer on average (Bhave et al. 2012; McCall et al. 2014), and the sulfilimine occupancy ratio appears to be a tissue-specific property. Like basement membranes themselves, sulfilimine crosslinks and the peroxidasin enzyme are both conserved throughout the animal kingdom (Fidler, Vanacore, and Chetyrkin 2014).

Despite their fundamental importance, questions remain about how basement membranes are assembled, and even less is known about how they are repaired after damage. As with all biological systems, basement membranes routinely get damaged. Traumatic damage like skin wounds are one obvious context for basement membrane repair. Damage and repair are also endemic processes: for example, leukocytes migrate through basement membranes and the resulting lesions are repaired to maintain mechanical integrity (Huber and Weiss 1989). Damaged basement membrane

may also play a causative role in the progression of diseases such as asthma, kidney failure, and diabetes, in which altered basement membrane structures may be caused by faulty repair programs (Flood-Page et al. 2003; Sugimoto, Mundel, Sund, et al. 2006; Tsilibary 2003). Further, there are diseases of the basement membrane itself (e.g. Alport syndrome, Goodpasture's syndrome, thin basement membrane disease), and understanding repair is central to treating these conditions.

There is a paucity of information on basement membrane repair, stemming from a lack of models of basement membrane damage. Questions about de novo basement-membrane assembly have been addressed in vitro, in cell culture, and in embryos. For example, the self-assembling nature of basement-membrane components was originally discovered in vitro with proteins purified from EHS sarcomas (the origin of matrigel) (Yurchenco and Furthmayr 1984; Kleinman et al. 1986; Kleinman et al. 1982). Despite their power, these systems may not be suitable for analyzing repair because in vitro analysis removes cells from the architectural and mechanical environment of the tissue, both of which are likely important for matrix repair. More recently, biochemical studies on matrix assembly (Fox et al. 1991; Ries et al. 2001; J. Takagi et al. 2003; Hopf et al. 1999) have been complemented by genetic analysis of animals mutant for basement membrane proteins, and these analyses were critical in identifying an order of assembly: laminin first, collagen IV and nidogen each require laminin, and perlecan requires collagen IV (Pöschl et al. 2004; Urbano et al. 2009; Pastor-Pareja and Xu 2011; Ramos-Lewis, LaFever, and Page-McCaw 2018; Wolfstetter et al. 2019). Whole-animal mutants are embryonic lethal, however, and the analysis of repair requires conditional mutants that can be induced temporally, after assembly has been

completed. We recently published a study analyzing repair of basement membrane after an epidermal pinch wound in which the basement membrane was torn, generating a region devoid of basement membrane ~100 μm in diameter, and found that it repaired with a scar, incorporating the known basement membrane proteins according to an order of incorporation that is slightly different from the order of incorporation for assembly (Ramos-Lewis, LaFever, and Page-McCaw 2018). This assay mimics trauma wounds, with new matrix filling the breach as the cell layer migrates in; however, it is not suitable for biochemical analysis or genetic screening because the wounds are painstaking to administer and are variable and small in size. Thus, we sought a complementary assay for analyzing basement membrane repair.

Previously, we reported that when either peroxidasin or its cofactor bromide is limiting during Drosophila development, basement membranes become measurably expanded and the muscles they support become deformed (McCall et al. 2014). This phenotype was first evident around the larval midgut, suggesting that this tissue has a heightened requirement for sulfilimine crosslinking. This loss-of-crosslinking phenotype appeared surprisingly similar to published images of the deformation caused by feeding flies the intestinal irritant dextran sodium sulfate (DSS) (Amcheslavsky, Jiang, and Ip 2009), a polyanionic derivative of the polysaccharide dextran. Stemming from the similarity, this study investigates whether and how DSS damages the basement membrane, and whether and how crosslinking is important for basement membrane repair. In this report, we introduce a new DSS-based experimental model to probe basement membrane damage and repair, one which is reproducible and suited to

microscopy. Using this model, we determine that replacement and crosslinking are essential processes of basement membrane repair.

Results

DSS feeding phenocopies loss of basement membrane proteins in the midgut

We focused on DSS as a potential basement membrane damaging agent. DSS is a 36-50 kDa negatively charged derivative of the carbohydrate polymer dextran, and administering DSS to mice in drinking water has long been used to induce a condition like ulcerative colitis. Because of its use in damaging the mouse intestine, DSS has also been utilized in adult Drosophila to damage the fly gut epithelium (Amcheslavsky, Jiang, and Ip 2009; Ren et al. 2010; Karpowicz, Perez, and Perrimon 2010; Cordero et al. 2012; Ren et al. 2013; Tian and Jiang 2014; You et al. 2014; Tian et al. 2015). In the first report of treating flies with DSS (Amcheslavsky, Jiang, and Ip 2009), it was noted that DSS appeared to alter basement membrane around the gut. The basement membrane is a sheet-like extracellular matrix that gets its mechanical strength from covalent crosslinking of the collagen IV polymer (Bhave, Colon, and Ferrell 2017). The DSS-induced basement membrane phenotype reported by Amcheslavsky et al appeared similar to a phenotype we reported in larvae when we mutated or inhibited Peroxidasin (Pxn), a collagen IV crosslinking enzyme (McCall et al. 2014). Thus, it seemed possible that DSS was interfering with collagen IV function.

To examine these similar phenotypes, we compared the treatments of DSS-feeding and ubiquitous Peroxidasin knockdown (with TubP-Gal4) in the midguts of adult females, which are larger than the midguts of males. The Drosophila gut is comprised of an epithelial monolayer, exposed to the lumen on its apical side and abutting the basement membrane on its basal side. Several basement membranes are expected to

lie in close apposition outside the midgut. The epithelial basement membrane lies between the epithelial layer and the underlying visceral muscles responsible for peristalsis, which run circumferentially and longitudinally along the gut. Typically, muscles are wrapped in basement membrane (Yurchenco 2011). Further, basement membranes separate organs from the body cavity and hemolymph. Fig. 2.1A shows a schematic of these tissues and their associated basement membranes, based on our imaging in this study.

To visualize the basement membrane, we used viking (vkg)-GFP^{454}, which has a fully-functional GFP-trapped collagen IV α2 protein transcribed from the endogenous genomic locus. In these flies, collagen IV can be easily visualized by GFP fluorescence with standard epifluorescence microscopy (Fig. 2.1B). We fed flies 3% DSS in a 5% sucrose solution over the course of 2 days and confirmed the previous findings that the tissue appeared altered compared to controls fed only sucrose (Fig. 2.1A-C and Fig. 2.3). On closer inspection, we found that the obvious DSS-induced morphological changes were caused by the peristalsis muscles, which appeared as dark areas surrounded by basement membrane. In optical cross-sections along the long axis of the midgut after DSS treatment, the circumferential muscles appeared contracted inward, protruding toward the epithelia and lumen, giving a rounder appearance in cross-section that was also evident by phalloidin staining of actin (Fig. 2.1E-F'). A similar rounding of circumferential muscles was observed when Pxn was knocked down ubiquitously in adults (Fig. 2.1D). This rounded muscle phenotype was quantified by measuring the aspect ratio of the circumferential muscles in cross-section (Fig. 2.1D'), which was significantly different from controls (Fig. 2.1G). The altered

appearance of the basement membrane and contracted morphology of the muscles was also evident when we visualized the basement membrane components laminin (LanB1-GFP, Fig. 2.1 H,I) or perlecan (Trol-GFP, Fig. 2.1 J,K).

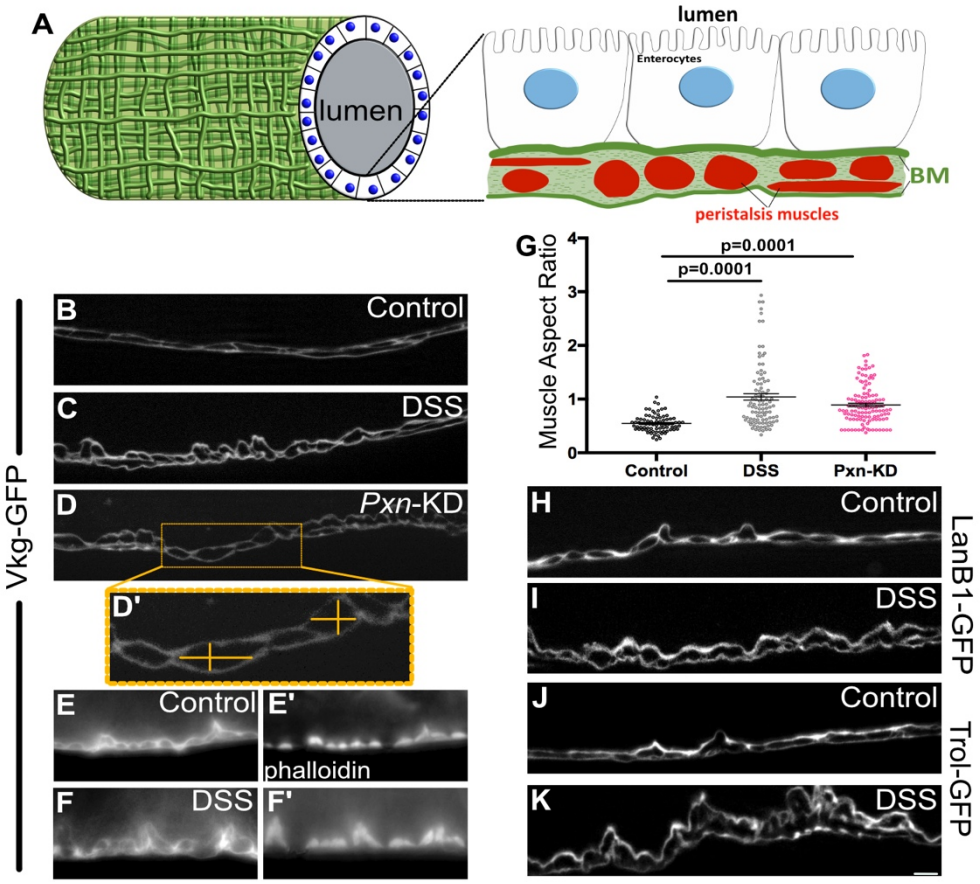

Fig. 2.1. DSS alters gut muscle morphology, similar to loss of Pxn.

(A) Schematic representation of the Drosophila gut based on imaging in this study. See also Figs. S1, S3. (B-D) A functional Vkg-GFP (Collagen IV α2) protein allows visualization of the basement membrane under the enterocytes and surrounding the muscles. (C) Morphology is disrupted in DSS-fed adult wild-type flies. (D) Morphology is similarly disrupted in flies with adult-onset knockdown of Pxn, a basement membrane cross linking enzyme, knocked down ubiquitously with TubP-Gal4. Muscle aspect ratio measurements are illustrated in D'. (E-F') Basement membrane labeled with Vkg-GFP (E,F) surrounds muscles, stained with phalloidin (E',F'). After DSS feeding, apparent displacement of basement membrane represents changes in muscle morphology (F,F'). (G) Muscle aspect ratio, measured as in D', changes in response to either DSS feeding or Pxn knockdown. 5-6 flies were analyzed for each condition. (H-I) A functional LanB1-GFP labels basement membrane under the enterocytes and surrounding the muscles. LanB1-GFP flies fed DSS recapitulate changes in muscle morphology visualized with Vkg-GFP. (J-K) A functional Trol-GFP labels basement membrane under the enterocytes and surrounding the muscles. Trol-GFP flies fed DSS recapitulate changes in muscle morphology visualized with Vkg-GFP and LanB1-GFP. B-F, H-K are optical cross sections, as illustrated in A. Scale bar= 5 μm.

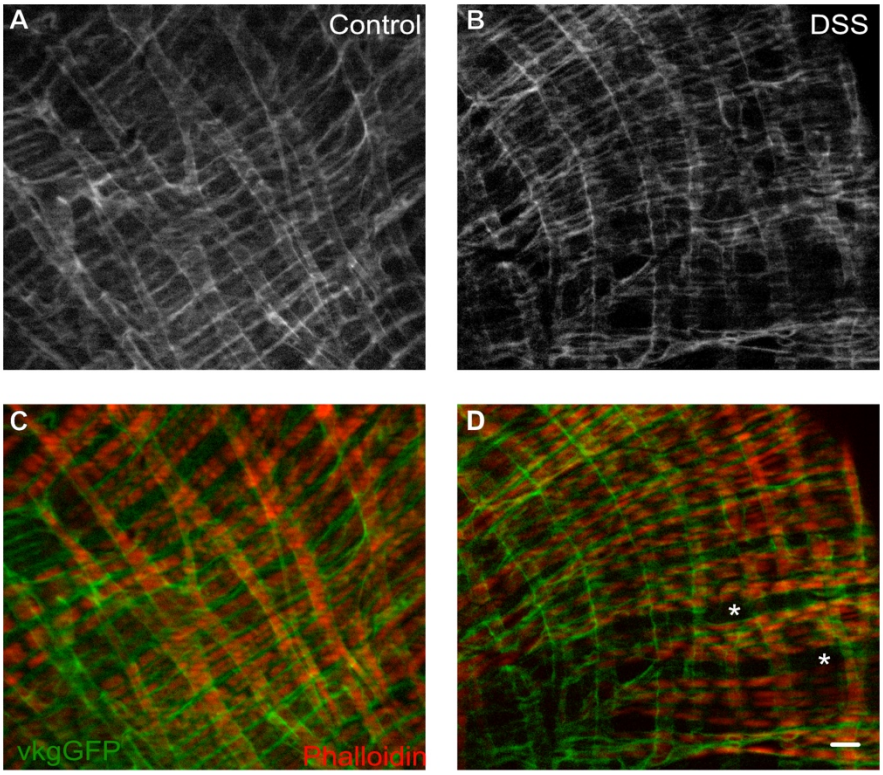

Fig. 2.2- Surface view of the gut basement membrane after DSS feeding.

(A) Tangential view of the gut basement membrane (Vkg-GFP) in control-fed flies. **(B)** Tangential view of gut basement membrane in DSS-fed flies. **(C-D)** Merged images of above showing the basement membrane (green) surrounding the muscles (phalloidin, red). Apparent "holes" in basement membrane (asterisks in D) represent areas where the muscles have separated. Scale bar= 10 μm.

As demonstrated by the Peroxidasin knockdown, defects in muscle morphology can result from the loss of basement membrane function. A mechanistic relationship between basement membrane function and muscle morphology and function has arisen from muscular dystrophy studies. Normally, muscle contraction force is resisted by the basement membrane, as the contraction force is transmitted by covalent linkages connecting the contractile machinery to the basement membrane (schematic in Fig. 2.3A). Muscular dystrophy disease genes encode proteins comprising components of these mechanical linkages, including the basement membrane protein laminin (Mercuri and Muntoni 2013). In muscular dystrophy patients, these linkages are disrupted so that muscle-generated contractile forces pull on the unsupported plasma membrane, resulting in membrane tears, calcium entry, muscle hypercontraction, and eventual muscle damage (Nyström, Bornert, and Kühl 2017; Vila et al. 2017). The visceral muscles in Drosophila are striated and multinucleate, more similar to mammalian skeletal muscle than mammalian visceral smooth muscles. Striations are caused by repeating sarcomeres, units of actomyosin contractile machinery, which have multi-protein covalent linkages extending from the Z-bands to the basement membrane (Maartens and Brown 2015). Previous work showed that the reduction of laminin in Drosophila ovarian muscles decreases sarcomere size, recapitulating a muscular dystrophy phenotype (Andersen and Horne-Badovinac 2016). As in ovarian muscles, Drosophila gut muscles decreased sarcomere size by about 10% upon reduction of laminin (LanB1-RNAi driven by TubP-Gal4, $Gal80^{ts}$; Fig. 2.3B-D). We reasoned that if DSS damaged muscles indirectly via the basement membrane, DSS should also decrease sarcomere size. In the DSS fed flies, an even more pronounced decrease in

sarcomere size was observed (~30%, Fig. 2.3F-G), although incomplete knockdown of laminin may have contributed to the bigger effect by DSS. The decrease in sarcomere size was not caused by active contraction in the DSS-treated guts: although treatment with relaxation buffer did somewhat increase sarcomere size of both DSS and control-fed flies, the DSS sarcomeres remained significantly shorter than controls (Fig. 2.4). These results are consistent with the interpretation that DSS damages the basement membrane of peristalsis muscles, leading to muscle damage and altered muscle morphology.

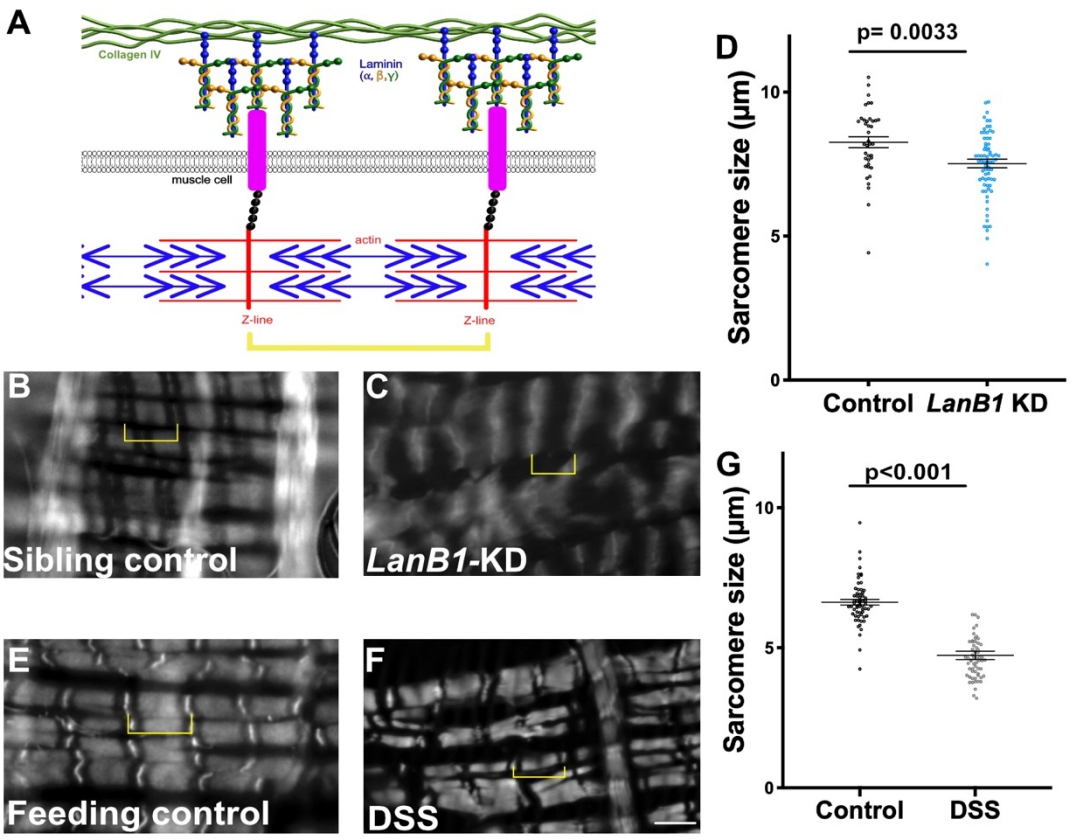

Fig. 2.3. DSS-induced muscle damage is similar to muscle damage from loss of basement membrane.

(A) Schematic representation of the linkage between the actomyosin contractile machinery and the basement membrane. The linkage between the basement membrane and the muscles can occur through integrins or dystroglycans. **(B-C, E-F)** Phalloidin staining revealed sarcomeres in longitudinal gut muscles. Yellow brackets indicate sarcomeres. Scale bar= 5 µm. **(D)** Knockdown of LanB1 ubiquitously with TubP-Gal4 reduced sarcomere size about 10% compared to control. Sarcomeres were measured in 5 flies for each condition. **(G)** Feeding flies DSS reduced sarcomere size about 30% compared to control. Sarcomeres were measured in 4 control and 6 DSS flies. See also Fig. S2 for sarcomere length in relaxing buffer.

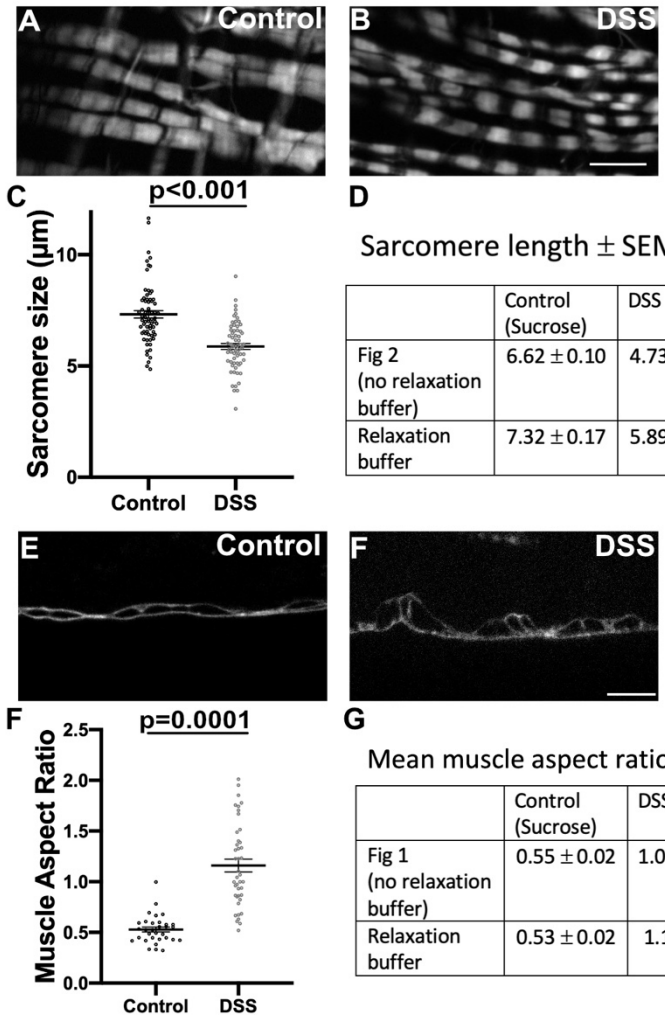

	Control (Sucrose)	DSS
Fig 2 (no relaxation buffer)	6.62 ± 0.10	4.73 ± 0.15
Relaxation buffer	7.32 ± 0.17	5.89 ± 0.14

	Control (Sucrose)	DSS
Fig 1 (no relaxation buffer)	0.55 ± 0.02	1.042 ± 0.06
Relaxation buffer	0.53 ± 0.02	1.16 ± 0.06

Fig. 2.4. DSS muscle damage is still evident when guts are treated with relaxing buffer.

Midguts from DSS-fed and control flies were dissected and incubated in relaxing buffer to allow muscle relaxation before analysis.

(A-B) Phalloidin staining to show sarcomeres in midgut longitudinal muscles dissected in relaxing buffer. **(C)** Sarcomere length is still significantly shorter in DSS fed flies than control-fed flies, indicating that muscles are damaged and not simply contracted by DSS. **(D)** Relaxing buffer did cause moderate lengthening of sarcomeres in both control and DSS fed flies when compared to sarcomere sizes from Fig. 2.

(E-F) Vkg-GFP outlines were used to calculate the cirumferential muscle aspect ratio of guts treated with relaxing buffer. (**G)** Muscle aspect ratio is still significantly greater in DSS fed flies than control fed flies, indicating that muscles are damaged and not simply contracted by DSS. (**H)** Relaxation buffer had little effect on the aspect ratio

Scale bars = 10 µm

DSS expands the basement membrane sheet

Basement membranes have traditionally been imaged by electron microscopy, so we used transmission electron microscopy (TEM) to image the gut in cross sections perpendicular to the long axis of the gut. In control samples, basement membrane was observed on the basal surface of the enterocytes and also on the outer surface of the muscles; between these layers and in the inter-muscle regions, the organization of the extracellular matrix was unclear (Fig. 2.5A,A', Fig. 2.6). After DSS feeding, the most obvious change to the tissue was in the peristalsis muscles, which were irregular and shredded (Fig. 2.5B, B' yellow arrows), consistent with our epifluorescence analysis. Importantly, the basement membrane itself appeared thicker after DSS feeding. Measuring the expansion of the basement membrane on the basal surface of the enterocytes (pseudo-colored green, Fig. 2.5A'-B'), the basement membrane was 140 ± 60 nm thick in controls, whereas after DSS treatment it was 330 ± 250 nm thick (Fig. 2.5C). Thus, by TEM basement membrane appeared over twice as expanded after DSS feeding.

We were concerned about possible dehydration artifacts associated with fixing samples for EM, and we were also unsure how to interpret the uncharacterized matrix between the apparent basement membrane and the muscles. Thus, we repeated our experiments using super-resolution Structured Illumination Microscopy (SIM), which gave ~2x increase in resolution compared to diffraction-limited techniques such as laser scanning confocal (Gustafsson et al. 2008) with two advantages over TEM: a standard formaldehyde-based immunohistochemistry fixation protocol was utilized; and the basement membrane was identified with a fluorescent Vkg-GFP (col4α2) rather than as

an unlabeled electron-dense structure. By SIM imaging, the control basement membrane was 260 ± 50 nm thick, whereas DSS treated basement membrane expanded to 390 ± 100 nm thick (Figure 2.5D-F). Thus, two independent fixation and visualization techniques determined that basement membranes expanded after DSS treatment.

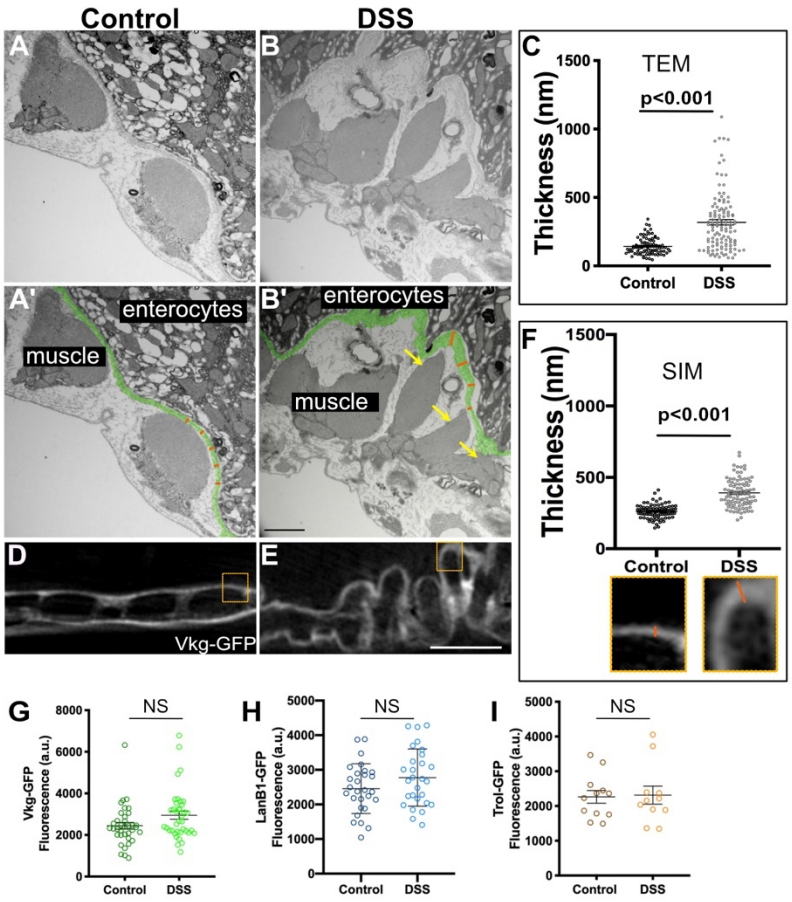

Fig. 2.5. DSS expands gut basement membrane without changing matrix protein levels.

(A-B) TEM images showing the peristalsis muscles and basement membrane of the midgut of a control or DSS-fed fly. **(A'-B')** Same images as A-B with labels. Basement membrane is pseudo-colored green. Orange lines illustrate how basement membrane thickness under the enterocytes was measured at regular intervals as shown in C; actual measurements extended across the entire micrograph although orange lines are confined to one region for illustration. Yellow arrows in B' indicate shredded muscle. Scale bar= 1 μm. **(C)** Quantification shows a significant increase in the thickness of the basement membrane after DSS feeding. **(D-E)** Structured Illumination Microscopy (SIM, superresolution) images of Vkg-GFP in the midgut basement membrane in control (D) or DSS fed (E) flies. Scale bar= 5 μm. **(F)** Quantification shows a significant increase in the thickness of the Vkg-GFP basement membrane after DSS feeding, measured in a blinded fashion like insets below X axis, corresponding to boxes in D,E. Measurements were made on 4 control and 5 DSS flies. **(G-I)** Basement membrane protein levels are not significantly different in control vs. DSS-fed midguts, as indicated by fluorescence levels of Vkg-GFP (G), LanB1-GFP (H) or Trol-GFP (I). Each dot represents one midgut.

Basement membrane expansion could indicate an increase in basement membrane proteins, resulting in a thicker structure; alternatively, it could indicate a fracturing or delaminating mechanical failure of the basement membrane sheet. To address whether increased basement membrane proteins were present after DSS feeding, we measured the total fluorescence of the GFP-labeled basement membrane proteins within the basement membrane around the gut. We imaged the fluorescence of Vkg-GFP (Fig. 2.5G), LanB1-GFP (Fig. 2.5H), and of Trol-GFP/perlecan (Fig. 2.5I), all functional GFP fusions expressed from endogenous regulatory sequences. For each, the total fluorescence levels were unchanged after DSS feeding. Independently, we found no difference in gut length or diameter after DSS feeding (Fig. 2.7). We conclude that the expansion in basement membrane is not caused by an increase in basement membrane deposition; rather, the basement membrane expansion suggests mechanical failure.

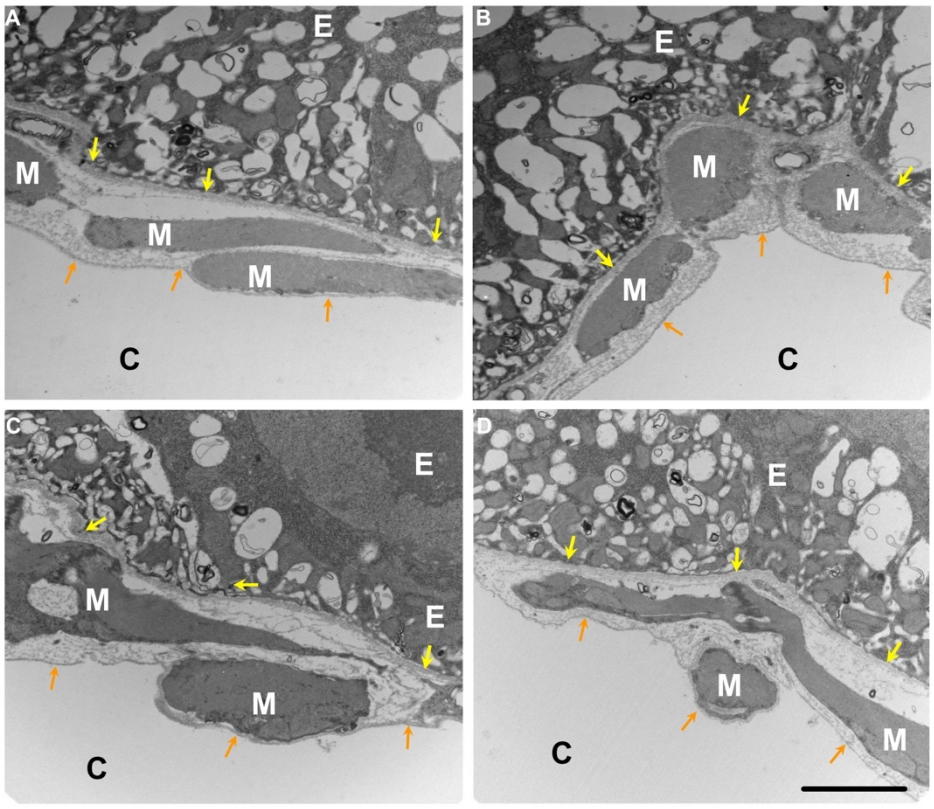

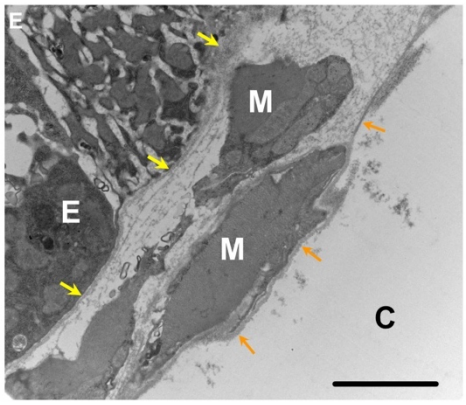

E- enterocyte epithelial layer.

C- body cavity.

M - muscle.

Scale bar = 2 μm

Fig. 2.6. The basement membranes of control midguts show a variety of morphologies.

(A-E) TEM images of control wild-type (*w*^{1118}) midguts, fed 48 h on a sucrose diet. The longitudinal and circumferential muscles are perpendicularly oriented to each other. In TEM images, the longitudinal muscles appear round in cross-section, whereas circumferential muscles appear long, because guts were cut in cross-section. In contrast, SIM and optical sections are taken along the long axis, so that the circumferential mucles appear round and longitudinal muscles appear long as shown in Fig. 1A. Either circumferential or longitudinal muscles can be found next to the body cavity (see also Figs. 3A and 5B), leading us to conclude that the longitudinal and circumferential muscles are in some kind of basket weave pattern, as depicted in Fig. 1A.

Sheet-like basement membranes are observed 1) underneath the epithelial enterocyte layer, indicated by yellow arrows, and 2) outside the muscles separating them from the body cavity, indicated by orange arrows. The structure of the material between these two layers is unclear, although SIM imaging indicates that the material between and around the muscles contains collagen IV even though it is not organized into a sheet (Figs. 3D and 7A).

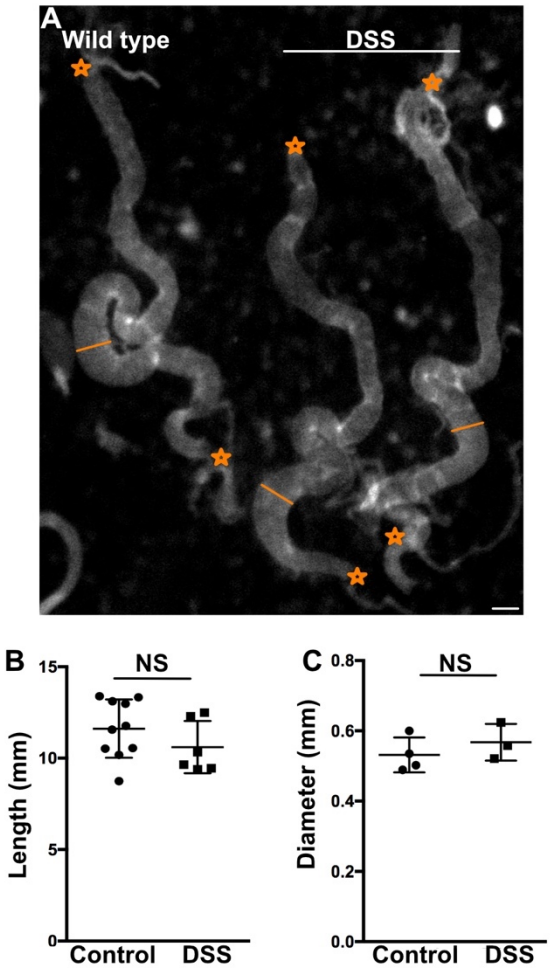

Fig. 2.7. DSS has no significant effect on the length or diameter of the gut.

(A) Brightfield image of guts dissected from control flies. The entire gut length is measured as the distance between the two stars, top and bottom. The diameter is measured as indicated by the orange line across the midgut. **(B-C)** Neither the length (B) or diameter (C) was significantly changed between animals fed DSS vs control food for 48 h. Scale bar = 500 μm

DSS localizes to basement membranes

To gain insight into how DSS expands the basement membrane, we fed fluorescently-labeled FITC-DSS to flies and visualized its localization in unfixed gut tissue after a 6-h chase (Fig. 2.8A-F). For controls, we fed flies unconjugated FITC (no DSS treatment), or we fed flies unconjugated FITC and unconjugated DSS, as separate molecules, to control for any stickiness of FITC to DSS-damaged tissues (Fig. 2.8A-C). Basement membrane was labeled with a functional protein-trapped Trol-RFP, rendering the basement membrane red. Labeled FITC-DSS localized reproducibly to the basement membrane of the damaged guts, whereas no fluorescence was observed in the basement membrane of either control (Fig. 2.8D-F). These results were obtained in unfixed tissue, as FITC-DSS washed out during the fixation procedure because it has no amine groups to fix it in place. The localization of FITC-DSS to the basement membrane indicates that DSS is transported from the gut lumen through the entero-cytes (cells that specialize in nutrient transport) to the adjacent basement membrane where it accumulates; indeed, punctae of FITC-DSS were observed within the epithelial layer (Fig. 2.9I). The basement membrane morphological expansion could be caused by negatively charged DSS creating osmotic pressure leading to swelling. This pathological swelling of basement membrane could cause mechanical weakening, as implied by the presence of dysmorphic muscles. Because DSS has been used extensively in mouse models, we performed a similar experiment, feeding FITC-DSS to mice and examining its intestinal localization. In mice, FITC-DSS localizes to punctae along the epithelial layer, co-localizing with intercellular junctions, and not to the

underlying basement membrane (Fig. 2.9), indicating that murine enterocytes do not transport DSS across the epithelial barrier as do Drosophila enterocytes.

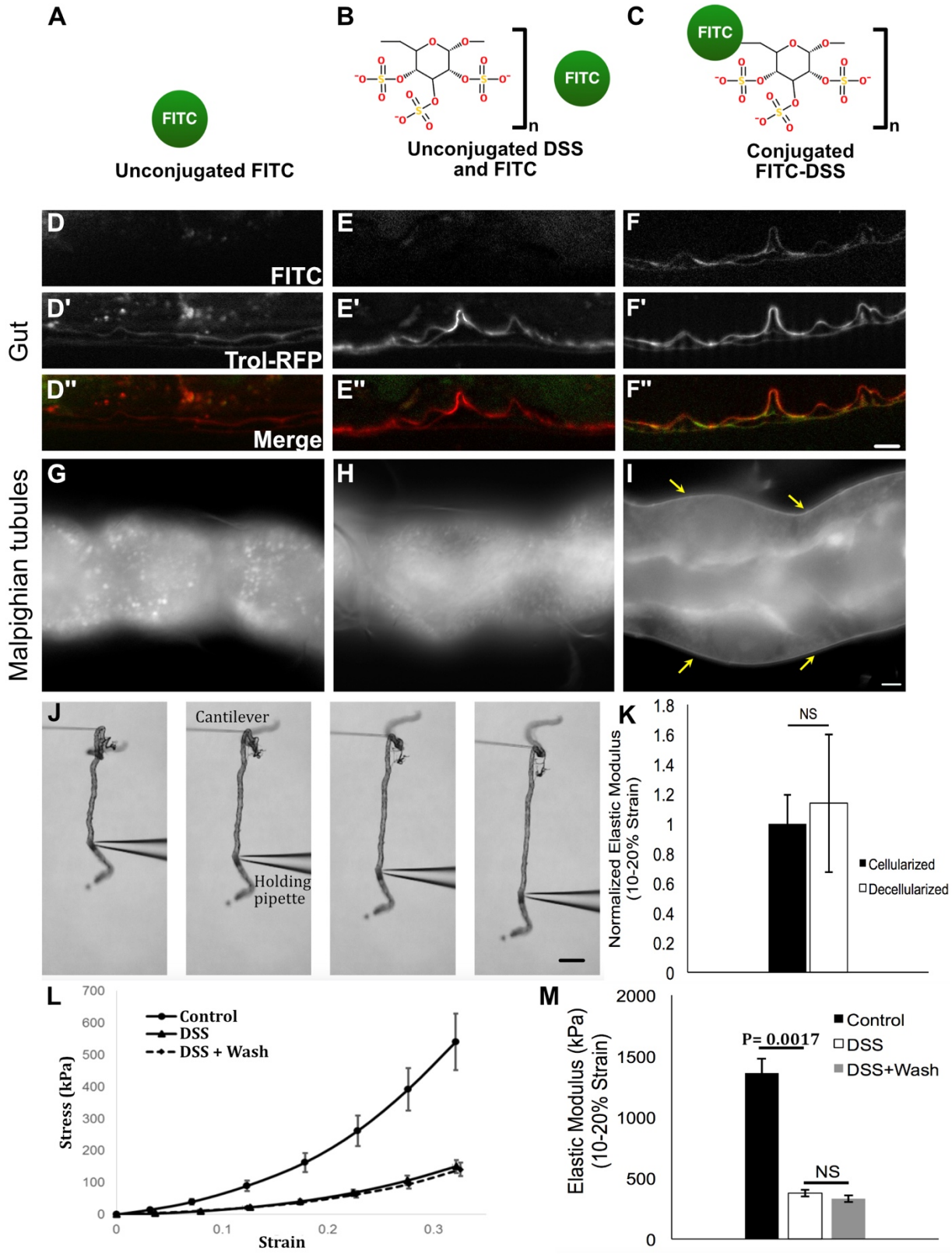
A
FITC
Unconjugated FITC
B
FITC
Unconjugated DSS and FITC
C
FITC
Conjugated FITC-DSS
Gut
Malpighian tubules
D
FITC
D'
Trol-RFP
D''
Merge
E
E'
E''
F
F'
F''
G
H
I
J
Cantilever
Holding pipette
K
Normalized Elastic Modulus (10-20% Strain)
NS
Cellularized
Decellularized
L
Control
DSS
DSS + Wash
Stress (kPa)
Strain
M
Elastic Modulus (kPa) (10-20% Strain)
P= 0.0017
NS
Control
DSS
DSS+Wash

Figure 2.8. DSS accumulates in basement membranes where it permanently decreases basement membrane stiffness.

(A-C) Feeding conditions for testing DSS localization. **(D-F)** After feeding, FITC-DSS specifically localizes to the basement membrane, labeled with Trol-RFP, in the midgut. **(G-I)** FITC-DSS specifically localizes to the basement membrane (arrows in I) of the Malpighian tubules after soaking *ex vivo*. **(J)** Assay for measuring tubule stress-strain response. The tubule is stretched between a cantilever and a holding pipette. Stress and strain are calculated from the bending of the cantilever and the changes in the tubule length. **(K)** Normalized stiffness for intact and detergent-decellularized tubules. There was no significant difference between cellularized and decellularized tubules, indicating that resistance to strain is imparted by the basement membrane. 5 cellularized and 3 decellularized tubules were analyzed. **(L)** Stress-strain curves for control, DSS treated, and DSS treated and washed tubules showing a downward shift in the stress-strain curves for DSS treated tubules. 5 flies were analyzed for each condition. **(M)** Elastic modulus for control and DSS treated tubules, calculated from the data in (L). DSS treatment significantly reduced basement membrane stiffness. No significant difference was detected between DSS treated tubules following removal of DSS (wash). Scale bar = 5 μm in (F",I), Bar = 200 μm in (J).

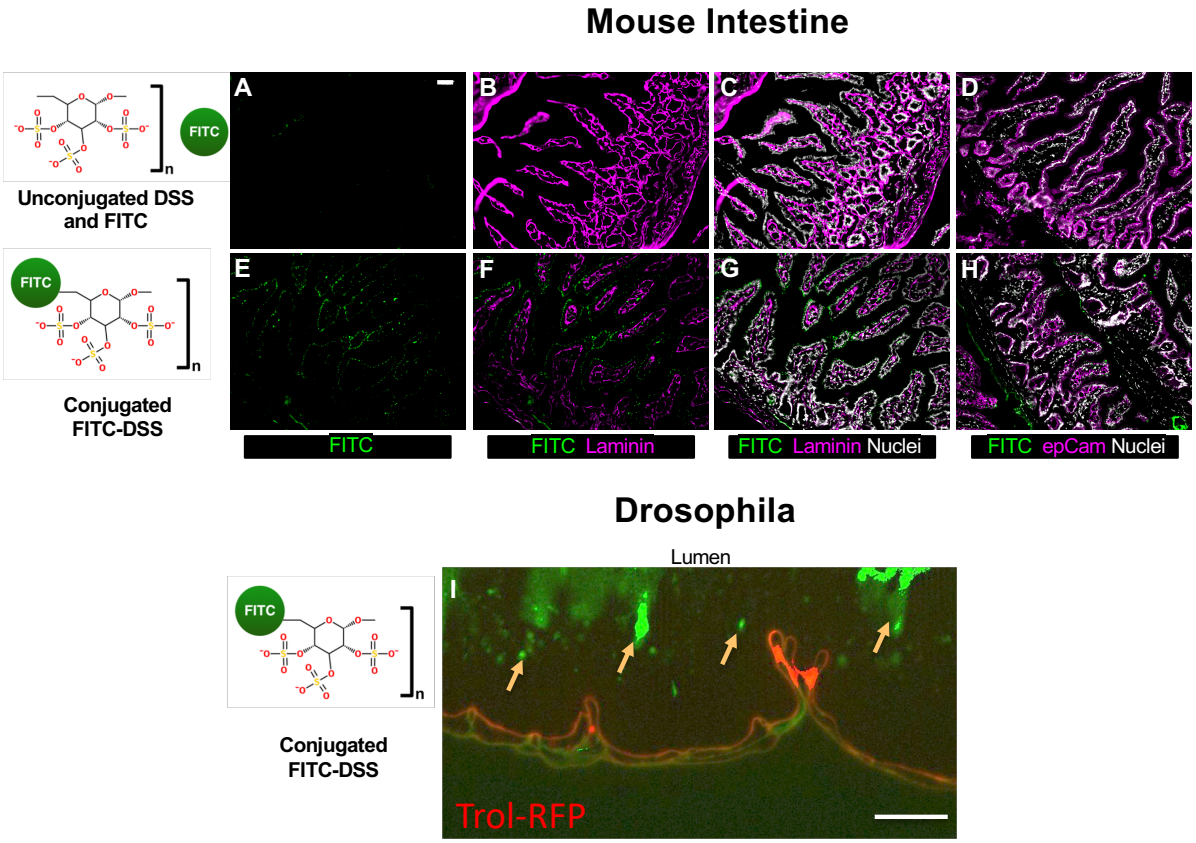

Fig. 2.9. In mice, DSS does not accumulate in intestinal basement membranes but rather at cellular junctions.
(A-D) Intestines from control mice administered DSS and unconjugated FITC. (A-C) represent the same sample stained for the basement membrane protein laminin, whereas (D) was stained for E-cadherin. No clear FITC signal is observed (A).
(E-H) Intestines from mice administered FITC-DSS. (E-G) represent the same sample stained for the basement membrane protein laminin, whereas (H) was stained for E-cadherin. FITC-DSS localized in punctae (E) that did not colocalize with basement membrane laminin. Rather, FITC-DSS localized near the epithelial plasma membrane, stained with E-Cadherin. Scale bar= 50 μm.
(I) Drosophila guts with FITC-DSS evident in the enterocytes, likely during transport. The lumen is intentionally omitted from the top of the image because it is significantly brighter. Scale bar = 10 μm.

DSS decreases the mechanical stiffness of basement membranes

We wanted to directly test the stiffness of the basement membrane after DSS treatment; however, the gut basement membrane cannot be separated from the peristalsis muscles, which would significantly alter tissue stiffness independently of the basement membrane. As an alternative, we analyzed the Malpighian tubules, part of the Drosophila excretory system. These simple tubules have only a tube-shaped epithelial monolayer surrounded on the outside by basement membrane, without muscle or exoskeleton. We did not expect DSS to diffuse to the Malpighian tubules at high levels after feeding in vivo because it gets trapped around the gut; instead, we treated the Malpighian tubules with DSS ex vivo by soaking them in a DSS solution for 20 min. As observed for guts after DSS feeding, conjugated FITC-DSS accumulates in the basement membrane surrounding the tubule, whereas unconjugated FITC does not, either in the presence or absence of DSS (Fig. 2.8G-I).

To measure the stiffness of the Malpighian tubule basement membrane directly ex vivo, we used a glass micro-cantilever system to measure the tensile stress-strain response. This technique is used to estimate the stiffness of the basement membrane, reported as the elastic modulus (Young's modulus). To evaluate the contribution of the basement membrane to tubule stiffness, we compared the elastic modulus of intact tubules to those that were decellularized by the addition of detergent after dissection. Decellularization did not significantly change the stiffness of the tissue (Fig. 2.8K), confirming that we were measuring the stiffness of the basement membrane. In contrast, the Malpighian tubule stiffness was significantly decreased after soaking in DSS (Fig. 2.8L,M), indicating that DSS disrupts the mechanical properties of the

basement membrane. We considered the possibility that basement membrane stiffness was altered by DSS only during the time that DSS resided in it, asking if the stiffness returned immediately upon DSS wash-out. To test this possibility, we used labeled FITC-DSS to determine conditions for rinsing out DSS after it became lodged in the basement membrane, and then tested Malpighian tubules soaked in and then rinsed of DSS. We found that the elastic modulus of the basement membrane was virtually unchanged after DSS removal (Fig. 2.8L,M). Thus, ex vivo DSS inflicts irreversible mechanical damage on the basement membrane.

One possibility for how DSS could access the basement membrane in vivo is by damaging the enterocyte barrier, thus exposing the basement membrane to the contents of the gut lumen including DSS. If this were the case, loss of gut epithelial barrier function would precede or be simultaneous with basement membrane damage. Epithelial barrier function can be evaluated using a blue food dye, which spreads throughout the body of the fly when the intestinal barrier is breached, termed a “smurf” phenotype (Fig. 2.10A). To investigate the function and loss of the intestinal epithelial barrier, we fed flies with blue dye for 6 days, with or without DSS, and scored the flies regularly for body color (Fig. 2.10B,C). Dead flies with blue bodies were excluded from the count, as barrier integrity is always lost on death; dead flies were much more prevalent with DSS feeding than without (Fig. 2.10D,E and Fig. 2.11). The majority of smurfy (blue) flies were observed after 5 days, with the first instance recorded after 3 days, well after the onset of basement membrane damage, which we always assayed after 2 days of DSS feeding when all samples show the effects. Therefore, DSS damages basement membranes directly, rather than after the loss of epithelial barrier.

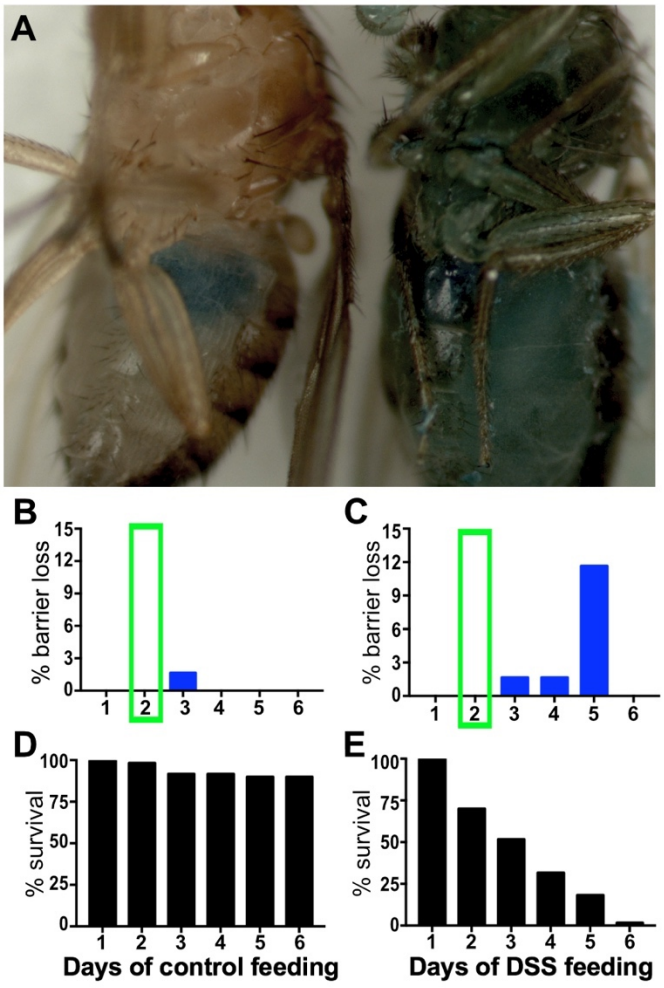

Fig. 2.10. Basement membrane damage precedes loss of epithelial barrier integrity.

(A) In control-fed fly (left), blue dye remained in the gut. In DSS-fed fly (right), the gut lost barrier integrity and blue dye escaped to the body. **(B-C)** Percentage of control (B) and DSS-fed (C) flies that lost barrier integrity. Green box highlights 2-day timepoint when basement membrane damage was observed by EM, SIM, and muscle morphology. **(D-E)** Survival of the same flies as in (B-C) over the course of 6 days on the liquid feeding regimen. 60 flies per condition.

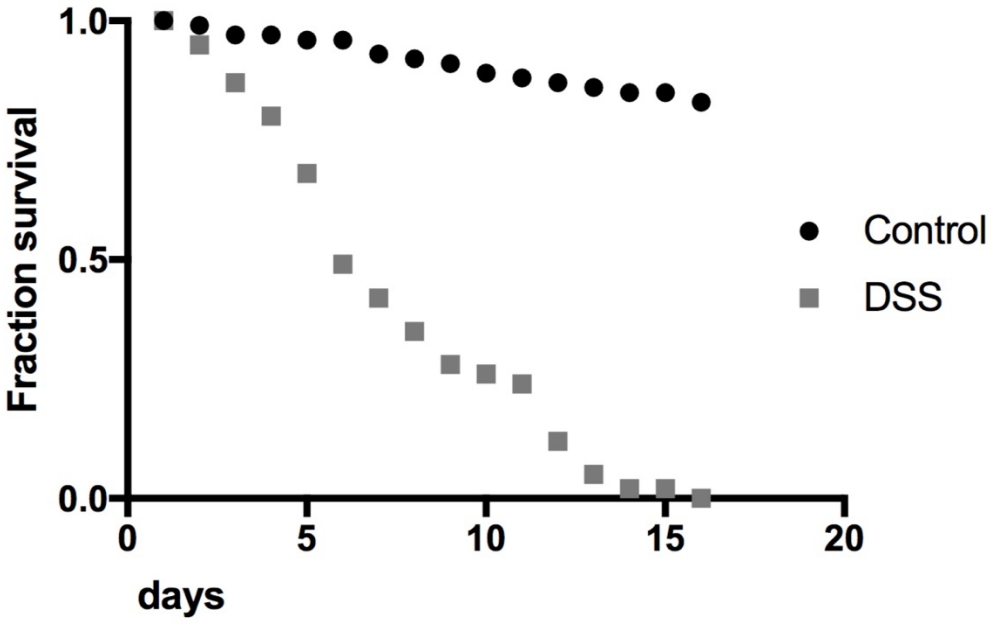

Fig. 2.11. Flies fed DSS have an increased mortality rate.

Flies continuously fed DSS for 16 days die rapidly compared to controls. These results are similar to those reported by Amcheslavsky et al (2009).

Basement membranes are repaired 48 h after DSS withdrawal

Taken together, the above data indicate that on feeding, DSS accumulates in the basement membrane of the gut and mechanically damages it, causing the gut muscles to become dysmorphic. We next asked if the basement membrane could be repaired after DSS damage was inflicted. The muscle aspect ratio was surveyed at various times after removing the flies from DSS to normal food. Although there was a short-lived reversal of muscle shape within 3 h, lasting recovery was accomplished more slowly, returning to normal 48 h after termination of DSS feeding (Fig. 2.12A). To confirm that the basement membrane itself had repaired, in addition to the muscles, we examined the basement membrane by TEM at 48 h after terminating DSS feeding and found that the basement membrane sheet had returned to its previous undamaged width (Fig. 2.12B-E). When analyzed by SIM as well as by TEM, the basement membrane of control flies returned to its normal width by 48 h after termination of DSS (Fig. 2.14G). 48 h after DSS termination, the levels of basement membrane proteins Vkg, LanB1, and Trol/perlecan were not significantly different than in undamaged midguts as measured by GFP-fusion protein fluorescence (Fig. 2.13). Thus, both muscle morphology and direct measurement indicated that basement membrane repaired within two days after DSS treatment.

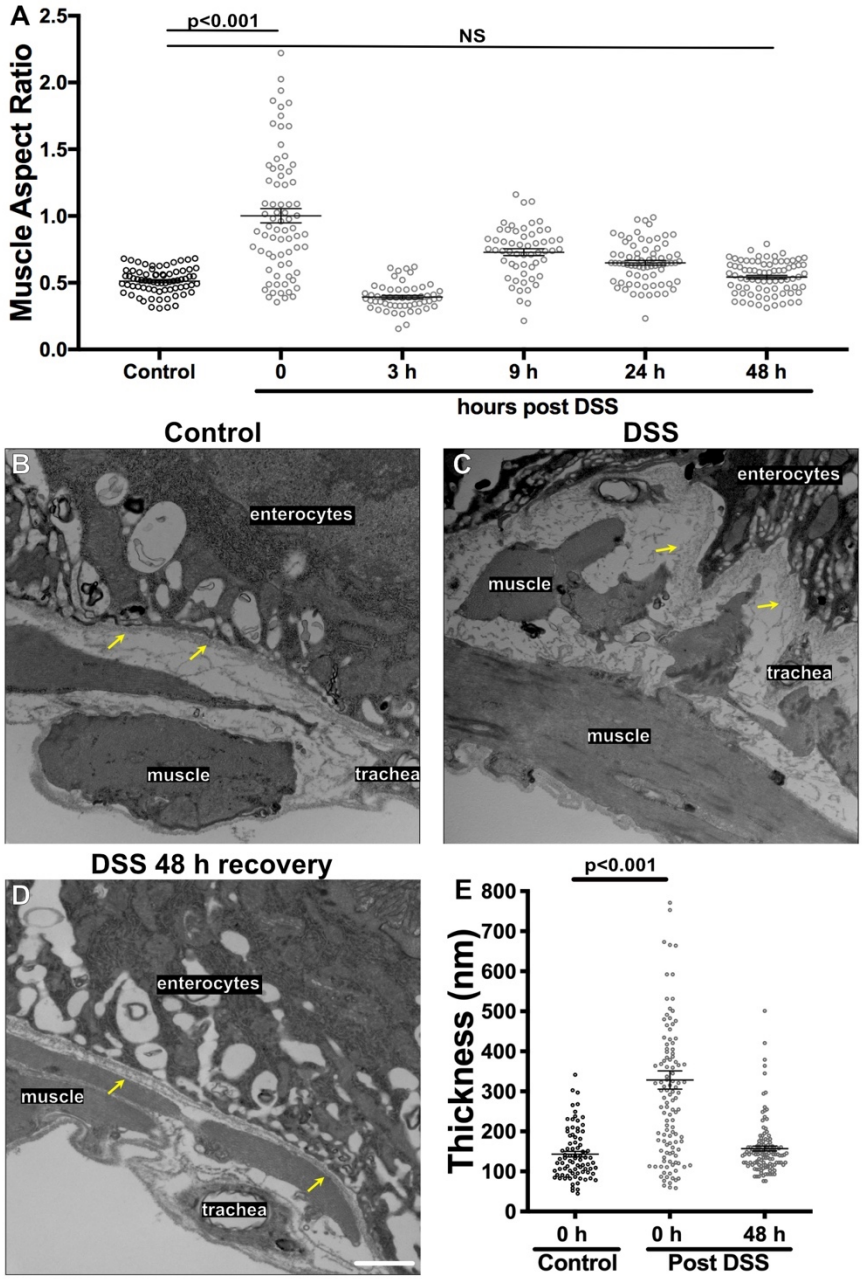

Fig. 2.12. Basement membrane is repaired 48 h after termination of DSS feeding.

(A) Muscle morphology was analyzed at the indicated times after withdrawing animals from DSS food to normal food. The muscle aspect ratio was restored at 48 h after terminating DSS feeding. 4-8 flies were analyzed for each time point. (B-D) TEM image of muscles and basement membrane of the midguts in a control-fed fly (A), DSS-fed fly (B), and a fly that recovered on normal food for 48 h after DSS feeding (C). Basement membranes are indicated with yellow arrows. Both muscle morphology and basement membrane thickness have been repaired by 48 h. (E) Quantification showing repair of basement membrane thickness 48 h after termination of DSS feeding, measured on TEM micrographs. Scale bar=1 μm.

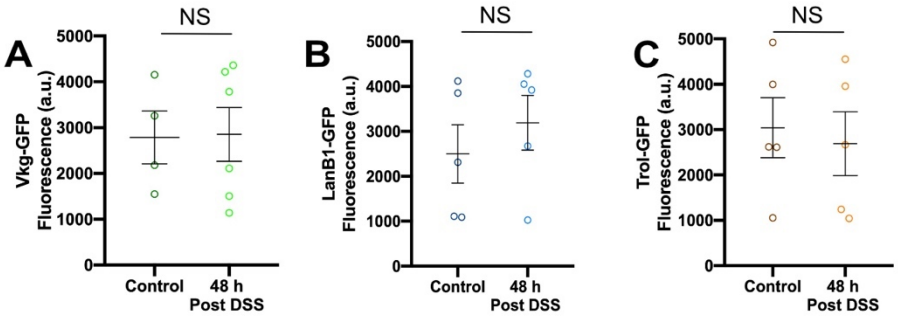

Fig. 2.13. Basement membrane protein levels were not significantly different after repair.

(A-C) Basement membrane protein levels were not significantly different in control vs. DSS-fed midguts allowed to recover for 48 h, as indicated by fluorescence levels of Vkg-GFP (A), LanB1-GFP (B) or Trol-GFP (C). Fluorescence was measured 48 h after removal from DSS to normal food; controls were sucrose-fed for 48 h then switched to normal food for 48 h to match experimental conditions. Each dot represents one gut.

Matrix replacement and collagen crosslinking are required for basement membrane repair

Having established the time course for repair, we analyzed biological requirements for repair. The role of collagen IV crosslinking in repair was investigated by knocking down the NC1-crosslinking enzyme Pxn ubiquitously in adults with TubP-Gal4, Gal80^{ts} for 7 days before feeding with DSS for two days, then removing from DSS to allow repair for two more days. When basement membrane morphology was analyzed by SIM, the basement membranes of Pxn-knockdown flies did not recover and remained expanded even 48 h after they were removed from DSS to normal food, in contrast to sibling controls, which repaired (Fig. 2.14A-G). We next analyzed muscle aspect ratio as a readout of basement membrane repair in these Pxn-knockdown flies. As noted in Fig. 2.1, even before DSS feeding, the Pxn-knockdown muscles have an increased aspect ratio; this ratio is exacerbated by DSS feeding, and it does not recover after removal of DSS (Fig. 2.14O); we confirmed the specificity of this phenotype with a second Pxn RNAi line (not shown). As an independent method of assessing the role of crosslinking, we fed flies phloroglucinol (PHG), an irreversible chemical inhibitor of Pxn (Bhave et al. 2012). PHG has two advantages over genetic knockdown: first, there is no pre-treatment because it is immediately effective, eliminating complications from long-term loss of Pxn before DSS feeding; second, it is likely to give a more penetrant phenotype than RNAi-based knockdown, which is usually incomplete. PHG was administered with the DSS or vehicle, and it caused a modest increase in muscle aspect ratio even without DSS during the course of the 4-day experiment (2 days treatment, 2 days recovery); when combined with DSS, the muscle aspect ratio became

severely increased, and this ratio did not recover even 48 h after DSS withdrawal when PHG was maintained in the food (Fig. 2.14H-N). We conclude crosslinking is required for repairing the basement membrane after DSS-induced mechanical damage.

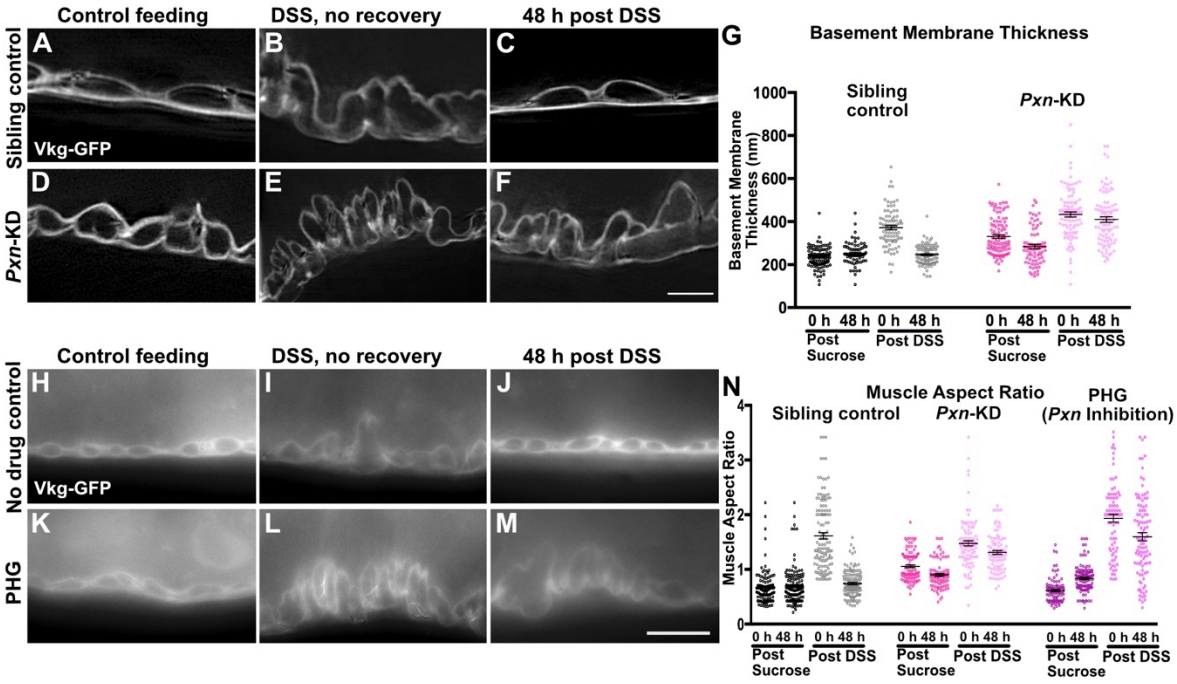

Fig. 2.14. Peroxidasin is required for basement membrane repair.

(A-F) SIM images of Vkg-GFP in the midgut basement membrane of control flies (A-C) or flies with Pxn knocked down in adults with TubP-Gal4, Gal80ts. Basement membrane was thicker upon DSS feeding (B,E) but 48 h after termination of DSS, basement membrane returned to its undamaged thickness in control flies (C) but not Pxn-KD flies (F). Repair was also deficient with a second Pxn RNAi line (not shown). Bar=5 μm. **(G)** Quantification of the basement membrane thickness in SIM micrographs. 5-7 flies were analyzed for each condition. (H-M) Epifluorescence images of Vkg-GFP outlining muscles in midguts of no-drug control flies (H-J) or flies fed the Pxn inhibitor PHG (K-M). Muscles become dysmorphic with DSS feeding (I,L), but 48 h after DSS withdrawal muscles return to their undamaged state in control flies (J) but not Pxn-inhibited flies (M). Bar=10 μm. **(N)** Quantification of the muscle aspect ratio. 4-6 flies were analyzed for each condition.

We considered two mechanisms by which collagen crosslinking could be required for repair. First, crosslinking might be increased to stabilize the pre-existing collagen within damaged basement membranes, akin to stapling broken fragments together. Theoretically, up to 6 sulfilimine crosslinks can bridge every NC1 hexamer, but an average of only 2-4 crosslinks per hexamer is detected in bulk fly and vertebrate tissues (Fig. 2.15A) (Bhave et al. 2012; McCall et al. 2014). Thus, it seemed possible to increase the crosslinking in response to damage within the basement membrane. Alternatively, crosslinking might be required after the incorporation of new collagen IV that replaced damaged proteins, to maintain the original extent of tissue crosslinking. We evaluated these models both genetically and biochemically. We reasoned that if we knocked down collagen IV with RNAi, collagen replacement would be reduced; simultaneously, we could feed flies PHG to inhibit Pxn. If crosslinking were required only for the replaced collagen in the basement membrane, then the phenotype would be no worse when both were inhibited together. In contrast, if crosslinking and collagen replacement were separate mechanisms of repairing basement membrane, then the phenotype would be worse when both were inhibited (see model in Fig. 2.15B). We found that the phenotype of inhibiting both processes was no worse than inhibiting each alone (Fig. 2.15C), arguing that Pxn is required for maintaining the extent of collagen IV crosslinking after collagen is replaced during repair. In a separate biochemical experiment, we measured the amount of crosslinking in isolated guts by examining NC1 dimer electrophoretic mobility, which changes with crosslinking status, allowing us to calculate the number of crosslinks per hexamer. We found no significant change before, during, or after DSS treatment, with about 3.7 crosslinks/hexamer in the gut on

average, arguing that collagen IV does not become hyper-crosslinked in response to basement membrane damage (Fig. 2.15D-E).

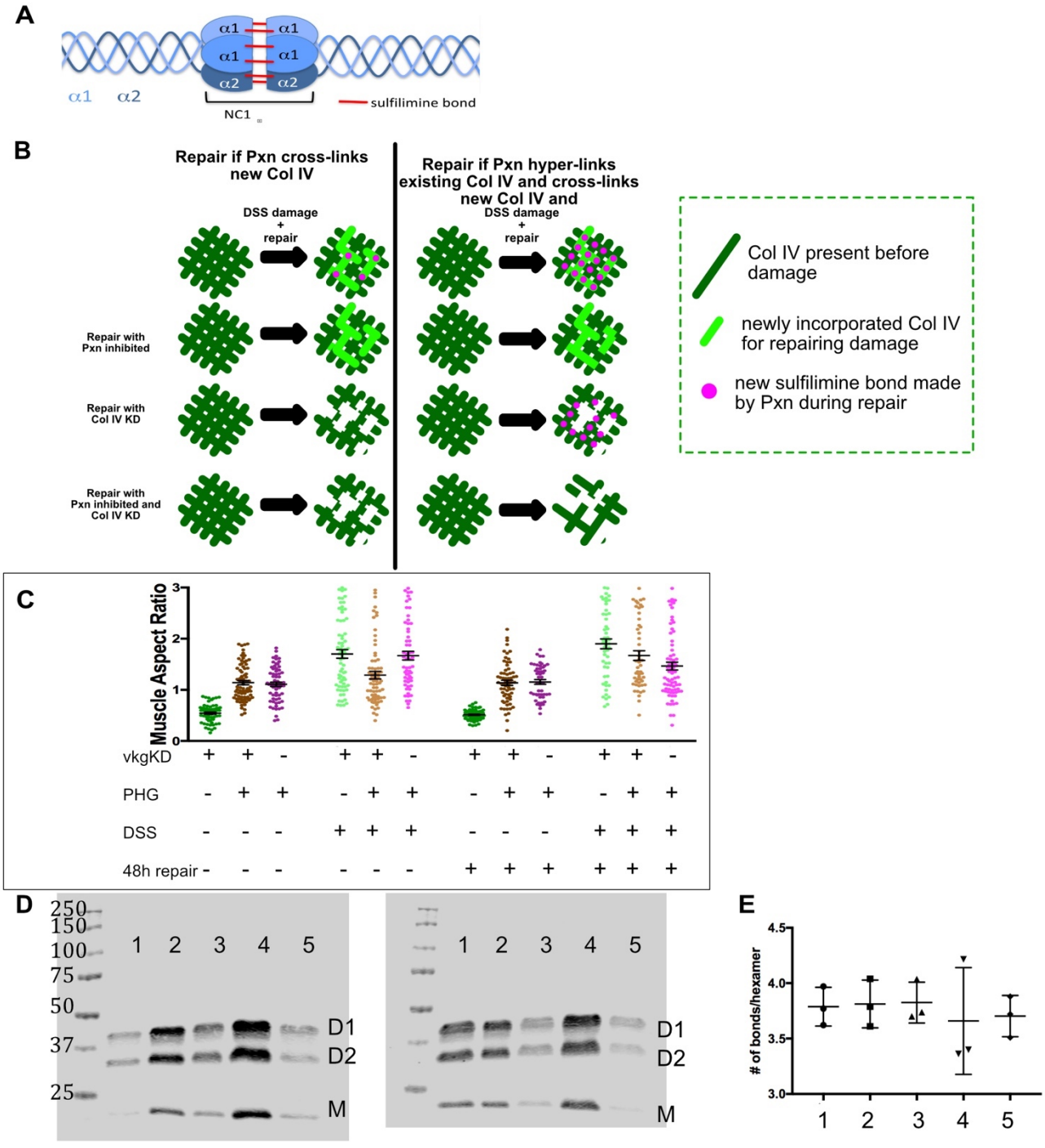
A
α1
α2
NC1
sulfilimine bond
B
Repair if Pxn cross-links new Col IV
Repair if Pxn hyper-links existing Col IV and cross-links new Col IV and
DSS damage + repair
Repair with Pxn inhibited
Repair with Col IV KD
Repair with Pxn inhibited and Col IV KD
Col IV present before damage
newly incorporated Col IV for repairing damage
new sulfilimine bond made by Pxn during repair
C
Muscle Aspect Ratio
vkgKD
PHG
DSS
48h repair
D
250
150
100
75
50
37
25
D1
D2
M
E
# of bonds/hexamer

Fig. 2.15. Peroxidasin does not hypercrosslink basement membrane during repair.

(A) Schematic showing 6 possible sulfilimine bonds per NC1 hexamer. **(B)** Models illustrate how loss of both collagen IV and Pxn are expected to affect repairing basement membrane: (left) Pxn is required only to crosslink the newly inserted collagen IV; (right) Pxn hypercrosslinks the basement membrane to stabilize it as part of the repair process. **(C)** Muscle aspect ratios after *vkg* knockdown (with *TubP-Gal4, Gal80ts*), Pxn inhbition by PHG, or both treatments, after control or DSS feeding, with or without a repair period of 48h after DSS withdrawal. Because the double treatment is not worse than the single treatments, we conclude that Pxn does not hypercrosslink collagen IV during repair. **(D)** 2 western blots of gut samples showing the Collagen IV NC1 domain, which has altered electrophoretic mobility depending on its crosslinked status: D1 is a dimer with one sulfilmine crosslink, D2 is dimer with two sulfilimine crosslinks, and M is monomer without crosslinks. Lanes: 1-normal food, 2-sucrose, 3-DSS no recovery, 4-DSS 48 h recovery, and 5-PHG. **(E)** The number of sulfilimine bonds calculated per hexamer of the 5 different condition types in 3 biological replicates. Sulfilimine crosslinking does not increase either after DSS treatment or repair.

These results indicate that an important mechanism of basement membrane repair is through direct replacement of the matrix components. We tested this model by knocking down two critical components of basement membrane, collagen IV (vkg) and laminin (LanB1), initiating knockdown ubiquitously after the animals reached adulthood. Under the knockdown conditions tested, no effect was observed before damage, but each was required for repairing the basement membrane after damage, as assayed by muscle aspect ratio (Fig. 2.16). Similar results were observed with second RNAi lines, ruling out off-target effects (not shown). Thus, basement membrane is repaired by replacement and crosslinking of the newly incorporated matrix.

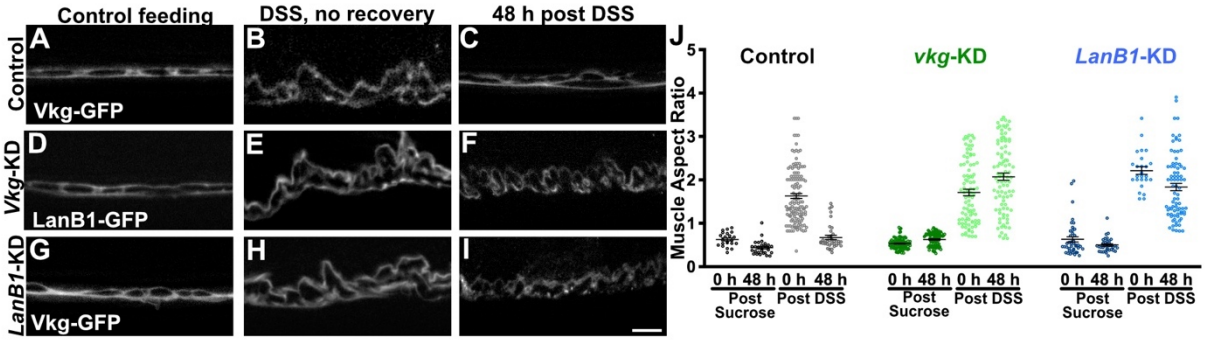

Fig. 2.16. Basement membrane repair requires new collagen IV and laminin.
(A-I) Epifluorescence microscopy images of Vkg-GFP (A-C, G-I) or LanB1-GFP. **(D-F)** showing the basement membrane and muscle morphology before, during, or after DSS feeding. When vkg or LanB1 is knocked down in adults with TubP-Gal4, Gal80ts, basement membranes do not repair as inferred from the muscle morphology (F,I). Scale bar= 10 um. **(J)** Quantification of the muscle aspect ratio. 4-6 flies were analyzed for all conditions, except 3 flies for the LanB1-KD 48h sucrose control. The repair-deficient phenotype was observed with second RNAi lines targeting vkg or LanB1 (not shown).

Discussion

DSS damages basement membranes

In this study, we determine that feeding DSS to flies damages the basement membrane around the midgut. Multiple assays were used to reach this conclusion. Specifically, FITC-DSS accumulates in the basement membrane around the midgut after feeding, and FITC-DSS binds to the basement membrane of Malpighian tubules upon soaking. The binding of DSS to basement membrane is relatively weak, as FITC-DSS washes out quickly when either tissue is incubated ex vivo. Upon DSS incorporation, the basement membrane expands as measured either by TEM of basement membrane electron density or by super-resolution microscopy of Vkg-GFP. Electron micrographs also show that after DSS incorporation the basement membrane becomes visibly damaged, appearing tattered and less dense. Despite these apparent structural changes, we have not detected changes in the protein composition of the basement membrane, as laminin, collagen IV and perlecan are still present, and the fluorescence levels of collagen IV, laminin, and perlecan GFP protein-traps are the same as in undamaged tissue. Basement membrane tensional stiffness is altered upon DSS incorporation into Malpighian tubules, which contain only epithelial cells surrounded by basement membrane, with no other components such as muscles or cuticle to alter their response to tension. The tensional stress-strain assay reveals that DSS irreversibly damages the basement membrane ex vivo, rather than temporarily changing stiffness during its incorporation, as the basement membrane does not recover its stiffness after the DSS is washed out. Finally, after removal of DSS from

food, repair of basement membrane damage occurs over 48 h in vivo. This repair process requires basement membrane proteins, including collagen IV, laminin, and the collagen IV crosslinking enzyme Pxn.

Although DSS clearly damages basement membrane, it is not possible to conclude that DSS damages no other tissue component. Interestingly, mouse enterocytes do not transport DSS across the epithelial barrier and DSS accumulates along extracellular junctions in the mouse intestinal lumen; although DSS is usually administered to mice for 7 days or longer (Chassaing et al. 2001), the level of tight junction protein ZO-1 begins to decrease after one day, with barrier permeability first observed at 3 days (Poritz et al. 2007), which is the same time as the earliest barrier permeability in flies. However, in flies the onset of basement membrane damage occurs before barrier permeability, so basement membrane damage is not secondary to barrier loss. Several lines of evidence support the conclusion that the substantial muscle damage induced by DSS feeding is secondary to basement membrane damage: similar muscle damage is recapitulated by Pxn knockdown; muscle morphology is not restored unless new basement membrane proteins can be incorporated; and basement membrane is damaged independently of muscles in the Malpighian tubules. We conclude that DSS causes direct damage to basement membranes, easily assayed by measuring muscle aspect ratio. Damage can also be measured by SIM, EM, or mechanical stiffness assays.

Basement membrane repairs within 48 hours by replacement and crosslinking

Importantly, upon termination of DSS feeding, the basement membrane around the gut was repaired within 48 h, as assayed by both width measurements and muscle morphology. With repair cleanly separated from damage, DSS represents an excellent system for analysis of basement membrane repair. Feeding adult flies DSS is easy and creates reproducible damage in the gut basement membrane, which can be scaled up for biochemical analysis (like Fig. 2.16) or genetic screening. The Drosophila gut itself is well suited to genetic analysis and microscopy, and unlike mechanical wounding, feeding DSS does not create cellular debris and/or clotting, which can be problematic for imaging. Further, Drosophila offers an excellent system for genetic analysis of basement membrane, as it has the same four basic protein components as mammals (collagen IV, laminin, perlecan, and nidogen) but there are far fewer genes encoding them (Ramos-Lewis and Page-McCaw 2018) and the enzymes that modify basement membrane are also conserved but fewer in number, with one peroxidasin to promote collagen IV crosslinking (Soudi et al. 2012) and two matrix metalloproteinases to cleave basement membrane proteins (Page-McCaw et al. 2003). We found some evidence for a fast-acting and temporary stabilization within 3h of withdrawing DSS, but this reversal was short-lived; repair was a slower process, leading to a gradual improvement over 48 h.

Using this system, we began an analysis of basement membrane repair. Production of new laminin and collagen IV are required for repair, indicating that the basement membrane is repaired through replacement of original matrix components, rather than by crosslinking damaged components or replacing with different proteins.

The crosslinking enzyme Pxn is also required. Because of the temporary improvement in aspect ratio observed at 3 h, we asked if NC1 sulfilimine crosslinking acted independently of protein replacement to stabilize basement membranes, but both biochemical and genetic analysis indicated that the role of Pxn is limited to crosslinking the newly incorporated replaced collagen IV.

Homeostasis of the gut and its basement membrane

The Drosophila gut is a widely used model of stem-cell mediated homeostasis and regeneration. In this self-renewing tissue, cellular repair appears to use the same mechanisms as homeostasis, in that enterocytes and entero-endocrine cells are regularly replaced during adult life. Interestingly, our results show that in the gut basement membrane, Pxn is required for both repair of damage and also for basement membrane maintenance. The maintenance requirement suggests that even without damage, there is turnover of either sulfilimine crosslinks or collagen IV during homeostasis, suggesting that the gut basement membrane may be a more dynamic matrix than previously suspected. Like for cellular homeostasis and repair, basement membrane repair may also utilize the same mechanisms as homeostasis.

Experimental Procedures

Fly husbandry. Drosophila melanogaster stocks were maintained at 25°C on standard cornmeal-molasses food unless otherwise indicated. See Supplementary Table 1 for a complete description of fly lines used. For the temperature sensitive RNAi experiments under $Gal80^{ts}$ control, crosses between Tub-Gal4, Tub-$Gal80^{ts}$ and UAS-$(gene)^{RNAi}$ were performed at 18°C and progeny were allowed to grow to adults at 18°C. 3-5 day old (mated) female flies were then transferred to 29°C for indicated times. For Pxn knockdown, adult females remained at 29°C for 14 d before dissection. To minimize basement membrane damage prior to DSS exposure in repair assays, Pxn knockdown or LanB1 knockdown adult females were transferred to 29° for 7 days prior to DSS/sucrose feeding, whereas vkg knockdown flies were transferred to 29°C for 11 days prior to DSS/sucrose feeding.

Table 2.1 - Drosophila lines used in this study.

Genotype	Source	Used for
w^{1118}	Todd Laverty, Janelia Farm	Figs. 2.2, 2.3, 2.4, 2.5, 2.6, 2.7, 2.8, 2.10, 2.11, 2.12
w; vkg-GFP^{454}	Yale Flytrap Project	Figs. 2.1, 2.2, 2.4, 2.5, 2.14, 2.13, 2.15, 2.16
w; LanB1-GFP	VDRC 318180	Figs. 2.1, 2.5, 2.13
trol-GFP^{1700} *w*	Flytrap line ZCL1973	Figs. 2.1, 2.5, 2.13
y trol-RFP w	Vincent Mirouse, French National Centre for Scientific Research	Figs. 2.8, 2.9
w; UAS-vkg^{RNAi}	VDRC 106812	Figs. 2.15, 2.16
w; UAS-vkg^{RNAi}	VDRC 41278	Not shown
w; *UAS-LanB1*^{RNAi}	VDRC 23121	Figs. 2.3, 2.16
w; *UAS-LanB1*^{RNAi}	VDRC 23119	Not shown
w; vkg-GFP^{454}*/CyO; UAS-Pxn*^{RNAi} */ TubP-Gal4, TubP-Gal80*^{ts}	This study; VDRC 15276	Figs. 2.1, 2.14
w UAS- Pxn^{RNAi}/FM7c	VDRC 15277	Not shown
w; *vkg-GFP*^{205}; *TubP-Gal4*, *TubP-Gal80*^{ts}*/SM6-TM6B*	Ramos-Lewis et. al. 2018	Fig. 2.16

w; *LanB1-GFP TubGal4 TubP-Gal80^{ts}/TM6B*	Ramos-Lewis et. al. 2018	Figs. 2.15, 2.16

DSS feeding regimen. As described in Amcheslavsky et. al. (Amcheslavsky, Jiang, and Ip 2009), a 2.5 cm x 3.75 cm piece of chromatography paper (Whatman cat. no 3030-861 Grade: 3 MM CHR) was placed in an empty vial. 500 µl of a 5% sucrose solution with or without 3% 36-50 kDa DSS (Dextran Sulfate Sodium Salt Colitis grade, MP biomedicals, CAS Number 9011-18-1, MW 36,0000-50,000;Solon, OH) was added directly to the chromatography paper in the vial. Anesthetized flies were carefully added to the vial so as to prevent them contacting the liquid media. Flies were transferred to a new vial with fresh media daily. Flies were fed according to this regimen for 48 h at 29°C. For recovery experiments, flies were allowed to recover for 48 h at 29°C on standard cornmeal molasses food. When indicated, 100 µM phloroglucinol was added to the DSS or sucrose solution before spotting onto the chromatography paper. For recovery in the presence of phloroglucinol, flies were transferred to molasses food (no cornmeal) containing 100 µM of phloroglucinol (Sigma-Aldrich 108736, St. Louis, MO) in solid media. Cornmeal was excluded to prevent the flies from eating around the phloroglucinol.

Gut dissections and preparation of posterior midguts: Adult females were placed in cold 1X PBS (137 mM NaCl, 2.7 mM KCl, 10 mM Na_2HPO_4, 1.8 mM KH_2PO_4) and were pinched with sharp #5 dissecting forceps (Dumont; Foster City, CA) between the abdomen and the thorax to separate the abdomen from the rest of the body. The

abdominal cuticle was peeled off, leaving the guts and Malpighian tubules. Dissecting guts this way prevents them from being torn or pulled. Guts were dissected and immediately transferred with a Pasteur pipette into a 4% paraformaldehyde (Ted Pella Inc. 18505; Redding, CA) /PBS fixative for 10 min at room temperature (RT), and washed 3 x 5 min with PBS. For SIM analysis and for knockdown-experiments in Fig. 2.16, guts were immunostained for GFP: blocked at 4°C overnight or RT for 2h in 5% BSA, 5% normal goal serum, 0.05% NaN_3, then incubated with rabbit anti-GFP (Torrey Pines, TP401) at 1:200 in above block for 12 h at 4°C or 2 h at RT, then washed 3 x 10 min at RT in PBS, and then incubated with FITC donkey anti-rabbit (Jackson ImmunoResearch 711-095-152) diluted 1:150 in block for 12 h @ 4°C or 2 h at RT, washed, and mounted. When indicated, AlexaFluor 647-conjugated Phalloidin (Life Technologies), diluted 1:20 in the above block, was added to 2° antibodies and incubated overnight at 4°. All samples were mounted in DAPI-containing mounting media (Vectashield, Vector Laboratories H1200). Analysis was confined to the posterior midgut, identified by its location anterior to the Malpighian tubules and posterior to the copper cell region, as depicted in the graphical abstract cartoon in Li et. al. (H. Li, Qi, and Jasper 2013). For gut dimensions, length was measured on intact guts from the crop to the posterior-most end of the gut; circumference was measured at the thickest part of the posterior midgut region.

Light microscopy. For standard epifluorescence imaging, single optical sections were captured using a Zeiss Apotome mounted to an Axio Imager M2 with a 63x/1.3 oil objective. Images were taken with an AxioCam MRm camera (Zeiss, Thornwood, NY),

X-Cite 120Q light source (Excelitas Technologies), and AxioVision 4.8 software (Zeiss). ImageJ (version 1.48v, National Institutes of Health, Bethesda, MD) 16-bit, grayscale, ZVI files were used for image analysis as well as for the images shown. For structured illumination microscopy (SIM), samples were mounted under a #1.0 coverglass (FisherBrand) and imaging and processing were performed on a GE Healthcare DeltaVision OMX equipped with a 60x Plan-apochromat N/1.42 NA oil objective lens and sCMOS camera.

For fluorescence intensity measurements of Vkg-GFP, LanB1-GFP, and Trol-GFP, samples to be compared were prepared on the same day and imaged at the same exposures. For each midgut, a representative field of the posterior midgut was imaged in a single optical cross section with a Nikon Apotome and a 63X objective. Within the field, a region of the midgut was selected for measurement based on its morphology, as only straight regions were analyzed. The ImageJ Measure tool was used to measure the total fluorescence intensity within a standard box (uniform length and area) that enclosed all the basement membrane of the enterocytes and muscles along a straight section of the midgut. An unpaired t-test was performed (GraphPad 7.0). As an independent method to verify the fluorescence intensity of Vkg-GFP, we imaged 3 dimensions of the entire posterior midgut region of 40 sucrose and 54 DSS-treated guts using a Nikon Spinning Disk microscope (Yokogawa CSU-X1 spinning disk head with Andor DU-897 EMCCD camera). After excluding regions that were out of focus, the maximum-intensity fluorescence projections were measured across the midgut, and data were compared with an unpaired t-test (GraphPad 7.0). Like the first method, this

second method of determining fluorescence intensity showed no difference between sucrose and DSS fed flies.

Transmission electron microscopy. Samples were processed for TEM and imaged in the Vanderbilt Cell Imaging Shared Resource-Research EM facility. Samples were dissected in and fixed with 2.5% glutaraldehyde in 0.1M cacodylate buffer, pH7.4 at RT for 1 h then left at 4°C for 10 days. The samples were washed 3 x 5 min in 0.1M cacodylate buffer, then incubated 1 h in 1% osmium tetroxide at RT, then washed with 0.1M cacodylate buffer (1% calcium chloride, 0.1 M sodium cacodylate, and pH adjusted to 7.4). Subsequently, the samples were dehydrated through a graded ethanol series: 30%, 50%, 75%, 85%, 95%, 100%, 100%, 100% each 15 min followed by a 1:1 solution of 100% ethanol and propylene oxide x 5 min. Samples were then infiltrated with 25% Epon 812 resin:75% PO for 35 min at RT. Next, they were infiltrated with 50% Epon 812 resin:50% PO for 1 h at RT then exchanged with new 50% Epon 812 resin:50% PO and incubated overnight at RT. Next day, the samples went through a 75%: 25% (resin: PO) exchange, then exchanged into pure epoxy resin for 3-4 h, then incubated with pure epoxy resin overnight. Next, the resin was exchanged with freshly made, pure epoxy resin and incubated for 3 h, then embedded in epoxy resin and polymerized at 60°C for 48 h. For sectioning and imaging, 70-80 nm ultra-thin sections were then cut from the block and collected on 300-mesh copper grids. The copper grids were post-section stained at RT with 2% Uranyl acetate (aqueous) for 15 min and then with Reynold's lead citrate for 10 min. Samples were subsequently imaged on the Philips/FEI Tecnai T12 electron microscope at 6500, 11000, 15000, 21000, and 30000x.

Basement membrane damage assays.

Measurements of basement membrane thickness. Transmission electron microscopy (TEM) images of the basement membrane underlying either the gut epithelial layer or surrounding the Malpighian tubules were acquired at 30000X zoom and analyzed in ImageJ. Measurements of basement membrane thickness were taken at regular intervals across the field of view from at least 10 images per experimental condition only where the basement membrane was clearly defined. A t-test was performed to compare DSS-fed versus sucrose-fed flies, using GraphPad Prism version 7.0 for Mac (GraphPad Software, San Diego California USA). Alternatively, SIM was used to measure basement membrane thickness as labeled by vkg-GFP fluorescence. A rotation student, unfamiliar with the experiment and blinded to sample identity, chose the locations and made the measurements. GraphPad Prism version 7.0 for Mac was used to perform statistical analysis on the sample set.

Sarcomere Measurements. The sarcomere size was measured in gut muscles stained with phalloidin by drawing a line in ImageJ (version 1.48v, National Institutes of Health, Bethesda, MD) from one phalloidin stained actin region to the next phalloidin stained actin region. When indicated, guts were dissected in relaxation buffer (20 mM sodium phosophate, 5 mM $MgCl_2$, 5 mM EGTA, 5 mM ATP solution, 5 mM DTT, 10 mM 100X Halt Protease Inhibitor) and allowed to incubate for 30 min before further processing (Xiao, Schöck, and González-Morales 2017).

Measurement of the Muscle Aspect Ratio: To quantify muscle morphology, the aspect ratio (height/width) of the muscles surrounded by basement membrane was determined from the basement membrane staining (Vkg-GFP or LanB1-GFP) surrounding the muscle. Height was measured at the tallest part of the muscle, and a line perpendicular to the height line was measured as the width, as shown in Fig. 2.1D'. Aspect ratio was calculated as height/width.

Measurement of Malpighian tubule basement membrane stiffness. Malpighian tubule basement membrane stiffness was measured in a similar manner to that described previously (Bhave, Colon, and Ferrell 2017). Briefly, measurement cantilevers were fabricated from pulled hollow glass capillary tubes and cantilever spring constants were measured in a manner similar to Shimamoto et al. (Shimamoto and Kapoor 2012). Malpighian tubules were attached to the measurement cantilever and a holding pipette (10 μm inner diameter), as shown in Fig. 2.4J, by applying vacuum. Both the measurement cantilever and holding pipettes were attached to micromanipulators. Imaging was performed on an inverted microscope (VWR) at 4X magnification with an attached digital camera for image acquisition. The holding pipette was translated in 40 μm increments to stretch the tubule and deflect the measurement cantilever. Images acquired at each deflection increment were used to calculate the deflection of the measurement cantilever and the displacement of the holding pipette. The change in the length of the tubule (Δl) was calculated as the difference between the distance traveled by the holding pipette and the deflection of the measurement cantilever (d_m). Initial length of the tubule was measured from an image acquired prior to translating the

holding pipettes. After the experiment was complete, tubules were observed to return to their original length, indicating that only elastic strain had been recorded.

Stress and strain were calculated according to equations:

$$\alpha = \frac{k_m d_m}{A} \quad (1)$$

$$\epsilon = \frac{\Delta l}{l_o} \quad (2)$$

where α is the stress, A is the cross sectional area of the tubular basement membrane, ε is strain, and l_o is the initial tubule length (Bhave, Colon, and Ferrell 2017; Shimamoto and Kapoor 2012). Area was calculated from the diameter of the tubule, averaged from six different measurements along its length, and the average width of the basement membrane as measured from TEM imaging.

FITC-DSS treatments. For feeding experiments, 3-5 day old female flies were fed for 48 h on 5% sucrose/3% DSS, with the DSS prepared as follows: FITC-DSS (Sigma Aldrich, cat. No. 78331-1G; St. Louis, MO) diluted 1:10 with regular DSS; DSS and unconjugated FITC in the same molar ratio as in the first condition (0.86 mg FITC and 300 mg DSS in 10 ml water); FITC alone at a matched molar concentration. After feeding, flies were placed on normal cornmeal-molasses food for 6 h as a chase, then guts were dissected in PBS and immediately mounted in Grace's Insect Media (BioWhittaker 04649F; Radnor, PA) for imaging without fixation.

For Malpighian tubule soaking experiments, tubules were dissected from 3-5 day old female flies in PBS and immediately transferred to PBS containing one of the

following: either FITC-DSS diluted 1:10 with regular DSS; DSS and unconjugated FITC in the same molar ratio as in the first condition (0.86 mg FITC and 300 mg DSS); or FITC alone at a matched molar concentration. Tubules were soaked for 20 min, then washed 3 x 2 min each with PBS, and mounted and imaged without fixing in PBS. To wash out the FITC-DSS or control FITC after soaking as above, tubules were washed 5 x 5 min washes in 1x PBS, which was determined by visual inspection under epifluorescence microscopy as sufficient to remove the fluorescence signal.

For mouse DSS experiments, mouse animal experiments were performed under protocols approved by the Vanderbilt University Animal Care and Use Committee and in accordance with NIH guidelines. C57BL6/J mice (Jackson Laboratory; Bar Harbor, ME) were administered a 2.5% Dextran Sulfate Sodium (DSS) solution in the drinking water consisting of 10% FITC-conjugated DSS/90% unconjugated DSS and were sacrificed 24 h later. Control mice received 10/90 mix of FITC+DSS mix (unconjugated)/90% unconjugated DSS. Upon sacrifice, intestinal tissues were removed, washed with 4% PFA, and spread longitudinally onto Whatman paper. Tissues were swiss-rolled, embedded in optimal cutting temperature medium (OCT), and frozen immediately at -80°C. For microscopy, tissues were sectioned at 5 μm thick onto glass slides. Slides were washed 1X in PBS and incubated at RT overnight in primary abs (1:100) EpCam (G88; Santa Cruz) and Laminin (Sigma), followed by 3 washes in PBS, and 1-h incubation in secondary abs (1:500) and Hoechst (1:100). Slides were mounted in Prolong Gold and viewed using fluorescent microscopy.

Gut barrier assay. 60 w^{1118} flies were fed with DSS or sucrose as above but also including 0.5% erioglaucine disodium salt (Sigma-Aldrich 861146, aka Brilliant Blue). The flies were examined 3 times daily (8 am, 2 pm, 8 pm) to assess barrier integrity (appearing blue or “smurfy” when barrier integrity is lost). The flies were deemed smurfy only if their bodies were blue and they were alive. Every smurfy fly was dead by the next time point.

Western blotting. Each sample contained roughly 200 w^{1118} adult fly guts, dissected in Grace’s Insect Media. Guts were transferred in 25-gut cohorts into a 2-ml pre-tared tube on ice, repeated until all samples were collected. Media was removed and samples were weighed, as 200 mg was a minimum starting mass. Samples were snap-frozen with LN_2. Using a cold mortar and pestle, frozen guts were ground into a fine powder, which was weighed then refrozen in LN_2. Samples were resuspended in deoxycholate solubilization buffer (1% sodium deoxycholate, 10 mM Tris 7.4, 1 mM EDTA) with 100X protease inhibitors (Thermo Scientific 78430; Waltham, MA) and 50 μM phloroglucinol, at a concentration of 5μl buffer per mg of powdered guts. Samples were sonicated (1 s pulse separated by 1 s pause for a total of 20 s) then incubated for 15 min on ice. To enrich for collagen IV, samples were spun in a microfuge at 16.1Xg for 30 min at 4°C, the pellet was washed (1 ml/200 mg sample) with chilled high salt wash (1 M NaCl, 50 mM Tris 7.4, 100 μM phloroglucinol), vortexed and incubated on ice for 15 min, then spun at 4°C for 30 min. The pellets were then washed (1 ml/200 mg sample) in a hypotonic wash (10 mM Tris 7.4, 50 μM phloroglucinol), tubes were inverted to rinse pellet, and then spun for 5 min at 4°C. Bacterial collagenase (1 mg/ml bacterial

collagenase CLSPA, [Worthington LS005273], 5 mM $CaCl_2$, 10 mM Tris 7.4, 0.1 mM phloroglucinol, 10 mM 100X Halt Protease Inhibitor) was added to the pellet at a concentration of 1 ml/200 mg sample, and the tube was inverted multiple times before being wrapped in foil and incubated for 24 h in a 37°C water bath. Precipitate was removed by spinning down at 4°C for 30 min, and the supernatant containing the collagen IV NC1 domains was immediately collected and filtered through a 0.2 μm pore mini-syringe filter. Using a Thermo Scientific Nano Drop 1000 spectrophotometer, the protein amount was determined, then samples were lyophilized and re-suspended in water at the standardized concentration of 10 mg/ml. 200 ng of sample was run per lane. Samples were resuspended in non-reducing 6x sample buffer, heated for 5 min at 95°C, and loaded onto a Bio-Rad non-reducing 10% gel (Mini-protean TGX 456-1034; Hercules, CA), and run at 100 volts. After removal from the apparatus and before transfer, the gel was reduced in 1X transfer buffer with 2% β-mercapthoethanol (Fisher Scientific 60-24-2) for 1 h at RT. A rabbit anti-NC1 primary antibody(McCall et al. 2014) (1:500) and a 680 anti-rabbit secondary antibody (1:8000, Li-Cor 926-32223) were used for imaging on an Odyssey CLx Li-cor.

Chapter 3

Peroxidasin is essential for normal egg development

Introduction to egg aspect ratio

For a long time, basement membrane has been thought of as a static sheet-like structure. However, recent studies have shown the dynamic nature of the basement membrane from egg formation to embryogenesis, even in restructuring during cancer (Isabella and Horne-Badovinac 2015b; Miner and Yurchenco 2004; Morrissey and Sherwood 2015; Fata, Werb, and Bissell 2004). In a 2011 paper, the Bilder lab showed Collagen IV acts as a molecular corset controlling the shape of the egg by constricting the center, leading to the growth in the anterior-posterior axis (Haigo and Bilder 2011). The molecular corset is comprised of actin bundles and fibril-like basement membrane proteins aligned perpendicularly to the axis of elongation (Cetera and Horne-Badovinac 2015; Horne-Badovinac 2014). In a dynamic process, the elongation of the egg occurs simultaneously with the migration of the follicle cells as well as the deposition and necessary alignment of the basement membrane fibrils (Cetera and Horne-Badovinac 2015; Haigo and Bilder 2011). Specifically between developmental stage 5 and 8, the Collagen IV levels double in the egg basement membrane (Haigo and Bilder 2011). In addition, when basement components or cell-matrix adhesion are defective during this developmental time frame, the egg elongation process is inhibited (Bateman et al. 2001; Haigo and Bilder 2011; Lerner et al. 2013; Lewellyn, Cetera, and Horne-Badovinac 2013; Isabella and Horne-Badovinac 2015a; Isabella and Horne-Badovinac 2015b).

Many labs used the Drosophila egg chamber and egg aspect ratio as a system to probe basement membrane's role in remodeling during morphogenesis (Isabella and Horne-Badovinac 2015b; Isabella and Horne-Badovinac 2015a; Daley and Yamada 2013; Horne-Badovinac 2014; Cetera and Horne-Badovinac 2015). During the maturation of the egg chamber, the shape of the egg morphs from spherical into a cylindrical form. The shape changes correlate with the increase in Collagen IV as well as a decrease in SPARC, a Collagen IV binding protein that acts as a negative regulator of egg chamber elongation (Andersen and Horne-Badovinac 2016).

Basement membrane plays a key, but indirect role in the growth of the egg chamber volume, which in turn is important for egg elongation. This indirect role comes from another player in the egg chamber development story, the peristalsis muscle sheath; this muscle sheath relaxes and contracts to aid in the egg chambers movement toward the oviduct for laying. Andersen et. al. recently showed another important function of muscle sheath contraction is to aid in vitellogenesis, pumping nutrients in the developing eggs. Altering the muscle sheath properties to hypocontract led to the reduction in the egg chambers growth and prevented proper egg length elongation. If the muscles hypercontracted, it produced elongated eggs (Andersen and Horne-Badovinac 2016). Some of these muscle changes were performed by altering the basement membrane.

As previously discussed in Chapter 1 and 2, the basement membrane surrounding the muscles plays an integral part in muscle function, including maintaining

muscle integrity, myogenesis as well as affecting muscle regeneration (Michele and Campbell 2003; Mayer 2003; Helbling-Leclerc et al. 1995; H. Xu et al. 1994; Blake et al. 2002; Jöbsis et al. 1996). All muscle cells are surrounded by basement membrane, which are linked through the integrin and dystroglycan pathways (Sanes 2003), allowing the basement membranes to distribute the actomyosin contractile forces across the entire muscle surface and preventing the muscles from shredding (Durbeej 2015). Therefore, it is logical that when laminin or integrins are knocked down during egg chamber development, muscle function was impaired and Andersen et. al. observed smaller egg chambers and shorter egg elongation (Andersen and Horne-Badovinac 2016). These results show the importance of the basement membrane-muscle sheath interactions during development.

The major protein in the basement membrane is Collagen IV and as stated above between developmental stage 5 and 8, the Collagen IV levels double in the egg's basement membrane (Haigo and Bilder 2011). In addition, basement membrane's mechanical strength comes from collagen IV as there are multiple types of crosslinking between the Collagen IV trimers, see chapter 1 (Bhave, Colon, and Ferrell 2017; Vanacore et al. 2009). Egg elongation occurs as basement membrane acts as a corset tightening around the egg chamber aiding in the growth anterior and posteriorly. Therefore, the egg is an ideal system to ask questions regarding the mechanism of Collagen IV crosslinking with egg elongation as the read out. McCall et. al. used this method to demonstrate that bromine was an undiscovered essential element (McCall et al. 2014) necessary for crosslinking the NC1 heads of Collagen IV. Peroxidasin requires bromine as a cofactor for crosslinking the NC1 heads of Collagen IV. McCall et. al.

showed when Peroxidasin, a necessary enzyme for Collagen IV cross-linking, was either inhibited or mutated, the egg chamber remained more spherical in shape and was unable to elongate properly (McCall et al. 2014); they were also smaller. Flies fed bromine depleted food could not survive. However, prior to their death, it was noted the females laid rounder eggs of decreased volume, which was assessed by measuring the egg aspect ratio (Fig 3.1A). The decrease in oocyte egg chamber volume upon peroxidasin inhibition or bromine depletion, shows the critical role the sulfilimine bond plays in the basement membrane function. This also supports the symbiotic interplay between the muscles and basement membrane. When the mothers were fed limiting concentrations of bromine, there was a dose-dependent response on the egg aspect ratio as seen from the cartoon (Fig 3.1B). However, when more bromide was added to the mother's food, the eggs tended to elongate more than control fed flies (McCall et al. 2014). (Fig 3.1B).

The cartoon schematic (Fig 3.1A) depicts the egg as it progresses from a spherical shape into its elongated form. The black lines represent the deposition of Collagen IV throughout the development of the egg. The changes in shape were reported as an aspect ratio, which is the length over diameter of the egg, also shown below.

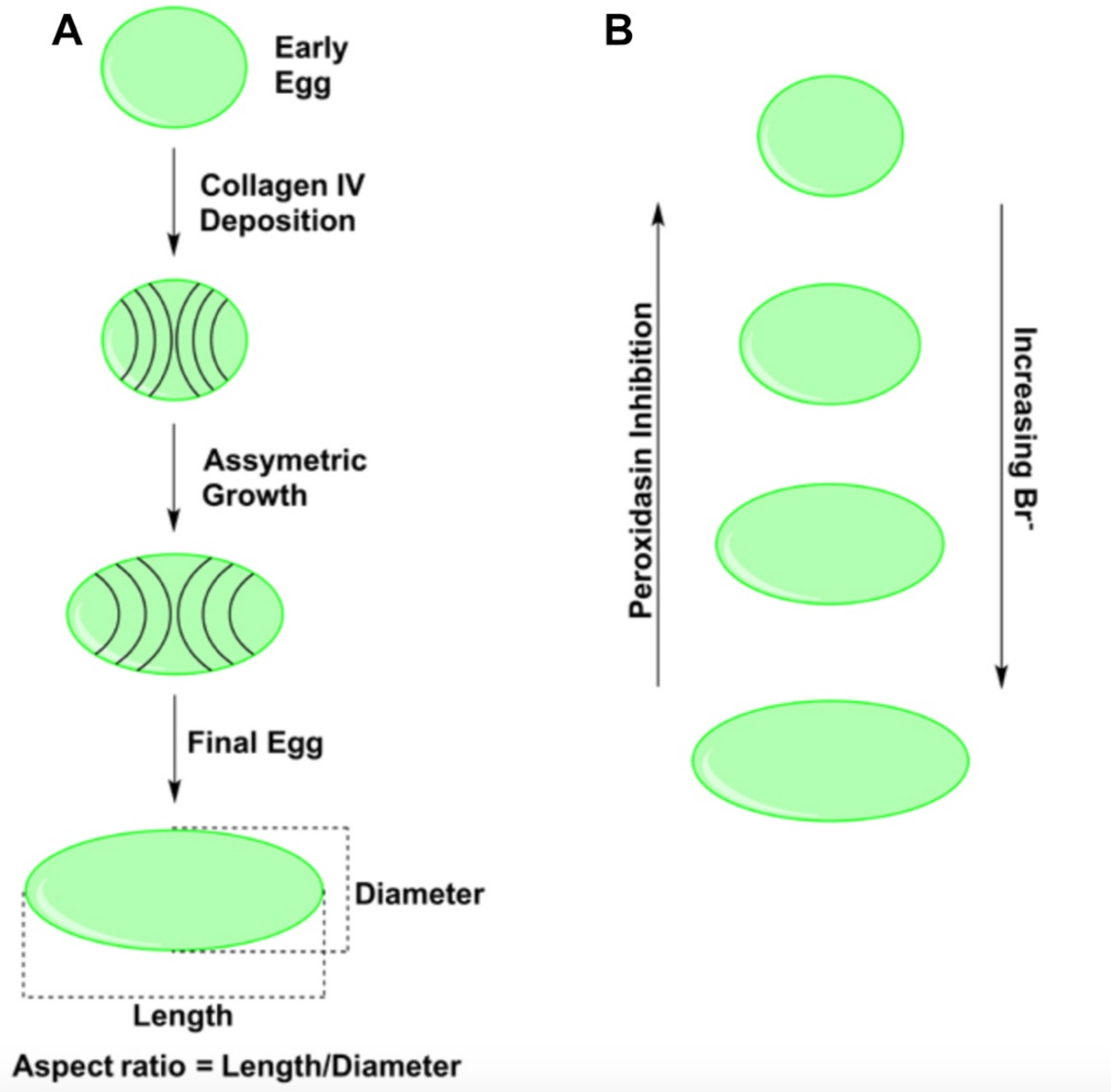

Adapted from Rouzer et. al. 2014

Fig 3.1- Cartoon Schematic of Drosophila Egg Development

(A) A cartoon schematic of the molecular corset forming in the center of the egg chamber to form the elongated eggs. The bottom egg depicts how the aspect ratio was measured and determined. **(B)** A cartoon schematic showing how the inhibition of peroxidasin or differing levels of bromine affect the egg elongation.

Results

Based on this work as well as other over-expression experiments, we asked if the egg aspect ratio would increase if peroxidasin was over-expressed. From work described above, when more bromine was added to the mother's food, the eggs elongated and as bromine is the essential cofactor for peroxidasin, we hypothesized that if peroxidasin was overexpressed, we would see the same egg elongation. We did not see the addition of bromide in our food led to a significant increase in egg elongation. Four peroxidasin over-expression lines (3-42, 2-25, 1-4, 1-37) crossed to Actin-Gal4 were allowed to lay eggs over the course of 5 days, were used to assess if peroxidasin can led to an egg elongation. Using this egg aspect ratio, we observed an increase in the egg aspect ratio when peroxidasin is over-expressed (Fig. 3.2B). However, the mean difference of the varying egg aspect ratio day to day was so close that the significance was questionable in some of the biological replicate experiments. Therefore, we asked if bromine was the limiting reagent by adding 100 μM of bromine to the fly food concurrent with the peroxidasin overexpression, and asking if we would observe a more significant difference between the conditions. The presence of elevated bromine simultaneously with peroxidasin overexpression leads to an increase in the significant difference between the control and the experimental condition (Fig. 3.2C). The remainder of the experiments were performed with additional bromine in the food (Fig 3.2D). From these experiments, we verify peroxidasin and bromide work in conjugation with one another to either aid in the formation of the molecular corset or in the muscle sheath contraction and relaxation.

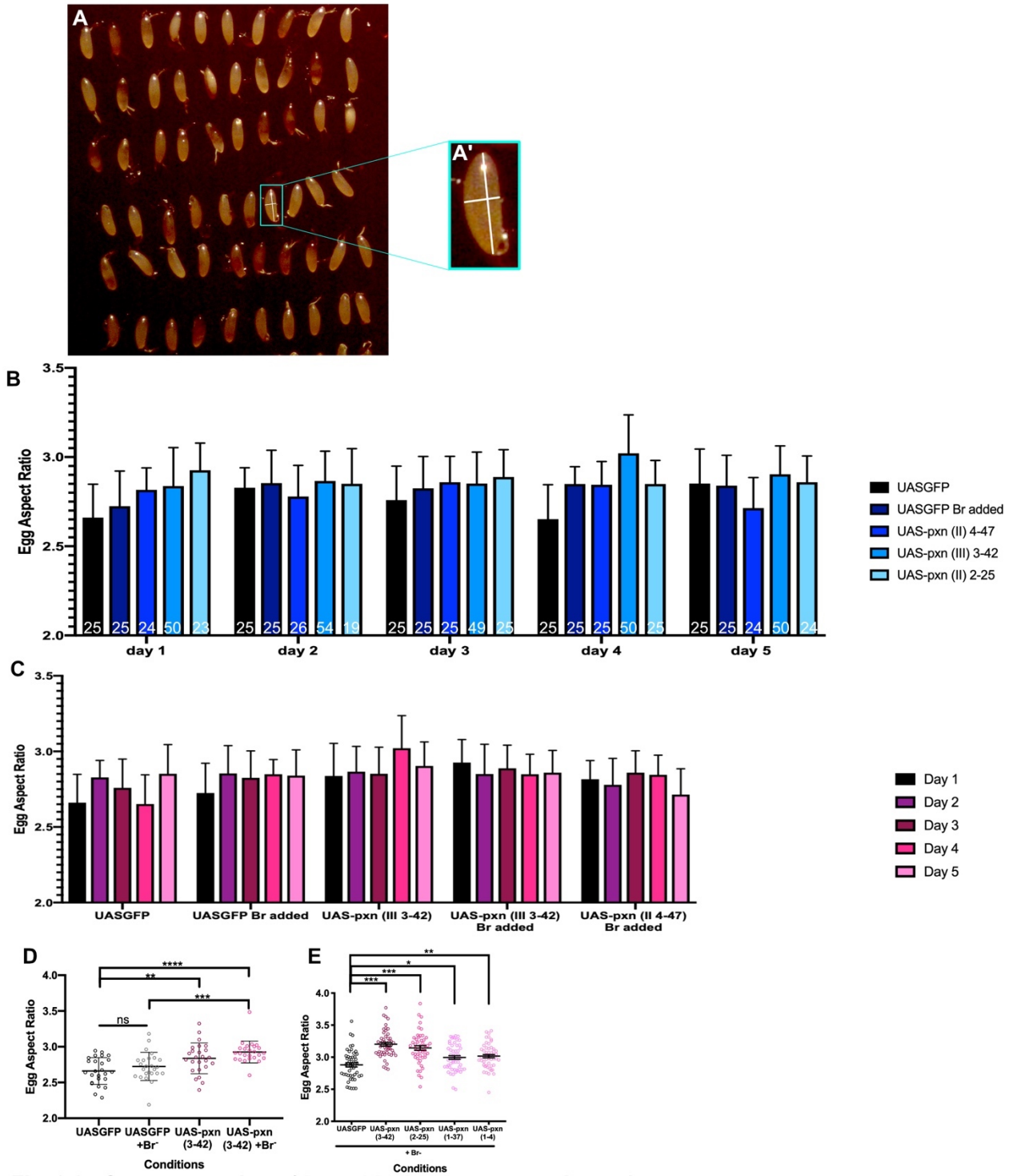

Fig. 3.2. Over-expression of Peroxidasin causes egg elongation
(A) Brightfield image of eggs laid from a control fly after 1 day at 29 C. Blue box shows (A') Egg aspect ratio measurements illustrated. **(B)** Quantification of the egg aspect ratio over the course of 5 days at 29 C. N values are each independent eggs. **(C)** The quantification of the egg aspect ratio in B rearranged by genotype. **(D)** A representative quantification of egg aspect ratio after 1 day recapitulating the results in B/C. **(E)** A representative quantification of the egg aspect ratio of over-expression flies with bromine added to the food. An ANOVA test was used to determine statistical significance among all data sets, followed by unpaired t-tests coupled with a Bonferroni correction to determine significance between specific data sets.

Methods:

Egg Aspect Ratio Measurements: Actin-Gal4/TM6B flies were crossed to either a UAS-GFP (control fly) or to one of the four UAS-peroxidasin over expression flies. Flies were placed in an egg laying cage with a grape plate attached at the bottom. 100 μM concentration in food (from 100 mM NaBr aqueous solution) of bromine was added to the food for the bromide experiments. The flies were placed at 29 °C and the eggs were collected every 24 hours for a maximum of 5 days. The eggs were then imaged daily with a Zeiss Axiocam on a dissecting microscope. Using ImageJ (version 1.48v, National Institutes of Health, Bethesda, MD), the egg diameter and anterior to posterior axis length was measure. Then the aspect ratio was calculated by dividing the axis length by the diameter. An ANOVA test was used to determine statistical significance among all data sets, followed by unpaired t-tests coupled with a Bonferroni correction to determine significance between specific data sets.

The UAS-pxn flies were created by Kimi LaFever and rotation student, Stephanie Moore. The wild- type cDNA was cloned into the vector pBID-UASC-G, made by the McCabe lab at Columbia, with 10 copies of the UAS sequences. This is a phiC31 compatible vector, and so it was integrated at one of two specific landing sites. These are attP40 at 25C (2nd chromosome) or VK00033 at 65B (3L 3rd chromosome).

Chapter 4

Where My Work Has Been and Where My Work is Going- Summary and Future Directions of My Dissertation

Summary

This thesis worked on understanding basement membrane repair and homeostasis. The basement membrane was identified and characterized using electron microscopy, as electron microscopy offers the resolution necessary to distinguish a structure only 0.2 nm thick (Furuya 2008). Electron microscopy can detect damage to the basement membrane, which is seen in chapter 2. However, electron microscopy is very costly in both time and money and it was preferential for us to develop a non-electron microscopy assay to quantify both the damage and repair we see. We developed an assay using fluorescent microscopy to assess both damage and repair. Electron microscopy and light microscopy have both definitively shown us that dextran sodium sulfate damages the basement membrane, visualized by various basement membrane GFP fluorescence. A similar phenotype has previously been seen in peroxidasin mutant fly guts (Bhave et al. 2012). Because muscle damage was evident in our dextran sodium sulfate treated flies, we measured the aspect ratio across the circumferential muscles. This is a measurement of muscle damage, which we interpret as a secondary effect to the basement membrane damage, but does not directly measure basement membrane. Furthermore, we have reason to believe that the muscle

damage we observe is an effect of basement membrane damage (ARAHATA et al. 1993; Campbell 1995). The muscle aspect ratio measurements correlated well with our visual inspection of basement membrane damage via electron and wide field microscopy.

As stated above and discussed in chapter 2, we see dramatic damage to the peristalsis muscles upon dextran sodium sulfate damage. These muscles, like striated muscles in vertebrates, are ensheathed in basement membrane. In vertebrates, the basement membrane is an integral component of the force-distribution system mediated by dystrophin-dystroglycan. The loss of this system leads to the shredding of the muscles in a muscular-dystrophy phenotype (MD) as the muscle uses this pathway to bridge the muscle f-actin to the basement membrane's laminin (Arahata, Ishii, and Hayashi 1995; Campbell 1995; Parsons et al. 2002; Ross 2002).The basement membrane allows the copious amount of stress experienced by the muscles during contraction to be spread across it through this bridge, easing the amount of stress experienced. When the muscles are not able to spread the strain forces across the basement membrane, natural muscle contractions tear them apart (Campbell 1995; Parsons et al. 2002). Sally Horne-Badovinac's lab reported that the knock down of the basement membrane component laminin leads to not only damage of the basement membrane, but also notable muscle damage in similar peristalsis muscles (Andersen and Horne-Badovinac 2016). Knocking down other components in this pathway; including dystroglycans, sarcoglycans, dystrophins, integrins, laminin or collagen IV led to the same phenotypic muscular dystrophy phenotype (ARAHATA et al. 1993; Sanes 2003; Michele and Campbell 2003; Mayer 2003; Helbling-Leclerc et al. 1995; H. Xu et

al. 1994; Blake et al. 2002; Jöbsis et al. 1996). Therefore, we understand our muscle defects to be a readout of the loss of basement membrane integrity. The muscle aspect ratio is therefore a viable readout for muscle damage and repair.

To examine the kinetics of basement membrane damage and recovery, flies were fed dextran sodium sulfate for 2 days then allowed 48 hours of recovery. Flies were dissected either with or without the recovery period, and images of the midgut basement membrane were taken by optical sectioning. Based on the muscle aspect ratio assay, we quantify the damage to the basement membrane after 2 days of dextran sodium sulfate feeding. It also appears our basement membrane and muscles are able to repair within 48 hours of recovery.

We have well-established tools to affect the loss of function and gain of function of the NC1 cross-linking in the Drosophila collagen IV superstructure. NC1 domain heads of collagen IV are crosslinked by sulfilimine bonds between methionine and lysine on opposing NC1 domains (Vanacore et al. 2009). Sulfilimine bonds are formed by the peroxidasin enzyme, which uses hydrogen peroxide as a co-enzyme as well as a hypohalous acid as a co-factor for this redox reaction (Bhave et al. 2012; Nelson, Fessler, Takagi, Blumberg, Keene, Olson, Parker, and Fessler 1994a). McCall et. al. (2014) discovered bromine is the halide necessary for this cross-linkage (McCall et al. 2014). Manipulating peroxidasin and bromide, the NC1 crosslinking status of basement membrane was altered in vivo. Further, peroxidasin loss of function was achieved either by chemical inhibition with phloroglucinol or RNAi knock-down. The peroxidasin knockdown phenotype is lethal in flies while only showing a slight eye cataract phenotype in mice, perhaps owing to genetic redundancy of two peroxidasin homologs

in mice (Yan et al. 2014). Our possession of both loss of function and gain of function tools give us powerful tools to manipulate and analyze the role of basement membrane crosslinking in homeostasis and repair. These techniques are well worked out in Drosophila.

The NC1 hexamer that links the Collagen IV trimers has 6 possible binding sites for crosslinking the sulfilimine bonds. As assayed by biochemical analysis in flies and mice, an average of 2-4 of those sites are crosslinked per NC1 hexamer in the basement membrane (McCall et al. 2014; Bhave et al. 2012). The fact that not all the NC1 sites are crosslinked leads to a number of exciting possibilities. One of these interesting questions is if the extra unused NC1 sites are able to be utilized and crosslinked during repair to give the basement membrane additional mechanical strength.

To determine the function cross-linking plays in the recovery of the basement membrane after a lesion, we inhibited the NC1 crosslinking. We did this by inhibiting peroxidasin, which is required for sulfilimine bond formation, by expressing a peroxidasin RNAi or using phloroglucinol to inhibit its enzymatic porphyrin ring, rendering it inactive. Both methods are conditional and can be turned on after development has concluded, which is what we did. After inhibiting new sulfilimine bond formation, I damaged the basement membrane by feeding the *Drosophila* dextran sodium sulfate for 48 hours as discussed above and in chapter 2 then used a muscle aspect ratio assay, I was able to assess damage and repair. Using both a chemical inhibition and a temporal RNAi knockdown line of peroxidasin, we observe first basement membrane damage and then lethality after 2 weeks when lacking the ability

to cross-link at the NC1 head. This led us to expect sulfilimine cross-linking plays a critical role in the homeostasis of the basement membrane. In addition, upon chemical inhibition of peroxidasin and damage with dextran sodium sulfate, the basement membrane was unable to heal as observed by epifluorescent microscopy and measured by muscle aspect ratio. We then thought that peroxidasin may be necessary to cross-link pre-existing collagen IV or cross-link new collagen molecules if there is deposition of new collagen IV. Without the cross-linking of the NC1 heads the collagen IV would be unable to reinforce the super-polymer necessary for basement membrane function. Extracellular chloride ions are necessary in causing a conformational switch within the collagen IV NC1 head, which is essential for the assembly of collagen IV (Cummings et al. 2016). By performing a western blot on flies fed dextran sodium sulfate, we saw there were not changes in the number of sulfilimine bonds. This leads us to conclude, peroxidasin does not over-crosslink the basement membrane to compensate for the damage. However, the western blots (Fig. 2.16) show there is a lot of variability in the number of crosslinks from one blot to the next. In addition, there are no loading controls possible for this experiment as there are only the sulfilimine bonds left. Therefore, we are unable to normalize each lane and as seen in Fig 2.16, the protein levels vary in each western blot. We ran 3 biological replicates to try to alleviate these problems. Further, the whole gut basement membrane is not damaged and repaired- so the signal maybe lost in the noise.

Over-expression of the peroxidasin gene was driven in flies, who were mated and allowed to lay eggs. As previously described, collagen IV possesses 3 different types of cross-linking: 1. C-terminus NC1 heads 2. N-terminus 7s domain and 3.

Disulfide cross-linking across the triple helical domain. Previous work has shown that inhibiting the peroxidasin enzyme or depleting the fly's food of the necessary bromide co-factor causes the *Drosophila* egg to become rounder (McCall et al. 2014). Collagen IV is known to act as a corset around the fly egg, squeezing it into an elongated shape. However, upon inhibition of peroxidasin or lack of bromide, the collagen IV corset is very weak as there are no sulfilimine bonds, thus the egg is able to grow both in diameter and length leading a rounder egg. In our data, we saw an elongation of eggs when we over-expressed peroxidasin. These data suggest the levels of cross-linking can be affected with both inhibitory means as well as over-expression.

One of the key functions of the basement membrane is to establish and maintain tissue stability (Candiello et al. 2007; Pöschl et al. 2004; Aumailley and Gayraud 1998; Halfter et al. 2013). If certain basement membrane components, such as laminin and collagen IV, are mutated or deleted it will lead to early embryonic death due to massive defects in the circulatory system (Candiello et al. 2007). By using atomic force microscopy to measure the biomechanical properties of the Inner Limiting Membrane, which is the retinal basement membrane, it was revealed that the thicker newly deposited basement membrane possessed more mechanical strength than the thinner and older basement membrane (Candiello et al. 2007). When the basement membrane was inhibited from establishing the necessary thickness, the mouse lacked the ability to form a healthy vascular system. Inner limiting membrane was used as opposed to basement membrane in other locations due to its easy access and lack of adjacent interstitial connective tissue as opposed to any other basement in the mouse.

Moreover, Collagen IV has also been shown to be a vital component in the stiffness of the basement membrane (Candiello et al. 2007). Mechanical strength is believed to be conferred by cross-linking the collagen IV network. Cells growing on artificial matrices have the capacity to respond to the mechanical properties, such as stiffness, of their matrix (Reilly and Engler 2010; Aumailley and Gayraud 1998; Engler et al. 2006; Halfter et al. 2013). The matrix stiffness has also been shown to play a role in the progression of tumor growth in vivo (Butcher, Alliston, and Weaver 2009). Therefore, the biomechanical property of stiffness is very important. Previous research has shown the necessity of collagen IV in providing mechanical strength (Candiello et al. 2007). It is expected that the collagen IV scaffold obtains its mechanical strength and stiffness from its crosslinking. Furthermore, Gautam Bhave and Nick Ferrell showed a decrease in mechanical stiffness in mice kidney tubular basement membrane upon peroxidasin knockdown (Bhave, Colon, and Ferrell 2017). Using the dextran sodium sulfate damaging model, I went on to test the role of mechanical strength in the Malphigan tubules of flies.

Our hypothesis is that the dextran sodium sulfate damaging model was having a direct impact on collagen IV and therefore, it is logical to hypothesize that it had an effect on the mechanical strength of the basement membrane. The reason that we hypothesized there was a direct impact on collagen IV is because the dextran sodium sulfate damage recapitulated the damage seen when peroxidasin, the collagen IV crosslinking enzyme, was knocked down. Using two microneedles, the micromechanical properties of the basement membrane were tested. The manipulating needle was used to pull or apply force to our basement membrane sample and is

attached to the piezo actuator, and the stiffness of the tissue was measured by the deflection of a flexible force-sensing needle (Shimamoto and Kapoor 2012). The force is strong enough to pull the tissue tight without irreversible damage when the force-sensing needle moves. Multiplying the precaliberated stiffness by the tip's deflection, the force on the tip was estimated. To measure the overall elastic properties of the tissue, the relationship between how much force is applied and the deformation of the tissue is calculated over a time range (Shimamoto and Kapoor 2012). For these experiments, I used Malphigan tubules as opposed to the gut. Malphigan tubules, the excretory system of insects, are slender one-cell layer tubes that branch out where the midgut turns into the hindgut. They consist of only basement membrane and a single cell layer, without any complicating muscles or exoskeleton.

Although it was reasonable for us to expect the sole provider of the mechanical strength comes from the basement membrane, we decided to test this hypothesis. By lysing the cells, we removed the cellular layer, leaving only basement membrane in the tubules. From our collaborator Gautam Bhave's work in mice, we saw there is no difference between denuded basement membrane and intact tissue (Bhave, Colon, and Ferrell 2017). Working in collaboration with Nick Ferrell, we measured that Malpighian tubules damaged by dextran sodium sulfate have less mechanical stiffness than controls. This shows that dextran sodium sulfate not only affects the morphology of the basement membrane, but also a functional property.

The importance of mechanical strength in cell substrates has come into focus in the last few years with in vitro and cell culture models suggesting it has an important role in cell differentiation and maintenance as well as cancer progression. Therefore,

where the basement membrane obtains its mechanical strength in vivo is an important question. These initial experiments really set the stage for future interesting questions on the effects of basement membrane stiffness. If basement membrane stiffness is so central to tissue function, and it varies between tissues, it would stand to reason that stiffness is tightly regulated. Although, we show that peroxidasin cross-linking is not increased upon dextran sodium sulfate damage, other components may play a role. It seems possible that other enzyme regulates cross-linking. We can test candidate enzymes such as Mmp2, Mmp1, and methionine reductases to fit this role as well as screen for other possible unknown regulatory enzymes. I predict the matrix metalloproteinase proteins would enzymatically break down the basement membrane, therefore a loss of function mutant would lead to increase of the mechanical stiffness. We would be unable to do a matrix metalloproteinase overexpression as they would die. In contrast, if we overexpress the crosslinking enzymes Loxl1 or Loxl2, which cross links the n-terminus of Collagen IV, the basement membrane may increase the mechanical strength of the basement membrane.

We have shown in this thesis that the basement membrane is a dynamic system. Some previous work led us to believe this would be true as they showed the basement membrane was able to grow, shrink, turn over, repair, and move to assist in tissue attachment as needed (Morrissey et al. 2014; Avery and Horvitz 1989; Haigo and Bilder 2011; Pastor-Pareja and Xu 2011; Ihara et al. 2011). Basement membrane is highly conserved and is comprised of approximately the same four components (laminin, collagen IV, nidogen/enactin, & perlecan). However, even though it has the same core group of components, basement membrane in different tissues confers its own varying

mechanical strength as well as possesses its own unique component composition (Khoshnoodi, Pedchenko, and Hudson 2008; Fidler, Vanacore, and Chetyrkin 2014). Basement membrane is assembled by cells, but not always secreted by the next-door neighbor cell (Hohenester and Yurchenco 2013). However, very little is understood about basement membrane dynamics (Sherwood 2015). We hypothesized that the basement membrane's dynamics are the output of opposing assembly and degradation process. Further, we hypothesized that these mechanisms underlying basement membrane dynamics are recapitulated during homeostasis and the repair process. Our hypothesis is based on previous work showing that the crosslinking enzyme peroxidasin is required for the maintenance of the gut basement membrane (Bhave et al. 2012; McCall et al. 2014).

Over the last 5 years, we have determined that there are no changes in the protein levels of three of the major basement membrane components after dextran sodium sulfate treatment; Collagen IV, Laminin, and Perlecan (TROL). Therefore, the thickening of the basement membrane is not due to an increase in these protein levels. The length or the diameter of the gut is not affected by dextran sodium sulfate damage. We expect the endocytosis of the dextran sodium sulfate molecules through the cells which are then deposited in the basement membrane. Then these molecules will reside within the basement membrane drawing in water and pushing apart the basement membrane components. When flies are fed dextran sodium sulfate tagged with FITC, we see the localization of the FITC-fluorescence correlating with the basement membrane. We have yet to show if water molecules flood in to neutralize the highly negatively charged dextran sodium sulfate.

A different possibility for how dextran sodium sulfate molecules are able to obtain access to the basement membrane is through epithelial barrier loss allowing for direct access from the gut lumen through to the basement membrane. In such given circumstances, all of the luminal material would be able to penetrate through to the basement membrane and into the hemolymph. To test this theory, we used a well-known “smurf” assay, where blue dye is added to the food, which allows for the visualization of epithelial barrier loss. If the epithelial barrier loses its functionality then the blue dye will spread through the fly’s open hemolymph system and turn into a “smurfy” fly. As seen in chapter 2, our flies lost epithelial barrier function after 3 days while the dextran sodium sulfate had become lodged in the basement membrane causing damage by day 2. This eliminates this hypothetical scenario from being true. This experiment definitively shows us that basement membrane damage occurs prior to the epithelial barrier loss.

Because of all the original work done in mouse, we decided to pursue the question of where the dextran sodium sulfate molecules reside in the mouse gut. We performed a similar experiment, feeding FITC-dextran sodium sulfate to mice and examining its intestinal localization. In mice, FITC-dextran sodium sulfate localizes to punctae in the epithelial layer consistent with intercellular junctions, and not to the underlying basement membrane (see Chapter 2), indicating that murine enterocytes do not transport dextran sodium sulfate across the epithelial barrier as do Drosophila enterocytes.

The difficulty in obtaining intact basement membrane, void of adjacent cells and interstitial connective tissue, is one of the reasons why not a lot is known about the

biomechanical properties of the basement membrane (Candiello et al. 2007). *Drosophila melanogaster* is an ideal model organism to study the basement membrane, as it allows easy access to the basement membrane and is genetically amenable, facilitating powerful in vivo studies. Although the four main components of basement membrane are conserved in flies, there is significantly less redundancy in the fly than in mammals. In both mammals and flies, the gut has the most dynamic basement membranes and the Drosophila midgut has been intensively investigated for its ability to self-renew from a stem cell population (Amcheslavsky, Jiang, and Ip 2009; Reilly and Engler 2010; Tian and Jiang 2014). The fly gut is composed of a single layer of epithelial cells on top of a sheet of basement membrane. Underneath the epithelial basement membrane is circumferential and longitudinal muscles necessary for peristalsis, also sheathed in basement membrane. This is why we choose this system to start to study how the intestinal stem cells are affected by damage.

This thesis was conceptually innovative, as it allowed us to start analyzing basement membrane components and cross-linking roles in the dynamics and repair of the basement membrane. For many years the prevailing model has been that the basement membrane is assembled and then the structure was made permanent by the formation of the cross-links (Yurchenco 2011). In this view, cross-linking is an indicator of the static nature of the basement membrane. However, we show that the basement membrane as a more dynamic system with cross-linking being a vital part of this. With all that said, there is still a lot of interesting questions that can be asked about this system and damage model. For the next few pages, I will delve into future directions of this project.

Future Directions

How is basement membrane repair initiated?

Is repair of the basement membrane passive or active?

Dextran sodium sulfate damages the basement membrane, which in turn needs basement membrane components to be able to repair as seen in Chapter 2. This leads to the question of how is the basement membrane repaired mechanistically. One possibility is the idea that it is a passive event and the machinery is always there and working. This would imply there is a constant turnover of basement membrane components, which in turn would give us valuable information in regards to homeostasis and assembly in addition to repair. Another option is a repair response that is triggered by the damage that initiates repair. To test a repair response mechanism, we can look for upregulation of known repair response components such as Peroxidasin and/or H_2O_2 after dextran sodium sullfate damage.

Using two different fly lines, we would start by analyzing the location of both the peroxidasin protein as well as its transcriptional expression in the Drosophila adult. *Perxodasin* is expressed in the hemocytes of fly embryos, where the peroxidasin protein is then deposited into the basement membrane (Nelson, Fessler, Takagi, Blumberg, Keene, Olson, Parker, and Fessler 1994a). It is currently not known where *Peroxidasin* is expressed in the adult fly. Using a *Peroxidasin* transcriptional reporter line, *Pxn-Gal4, UAS-GFP*, (Stramer et al. 2005), in our preliminary data (Appendix E), we saw an upregulation of the GFP in the intestine. Before we start on the quest of determining where the source of this upregulation of peroxidasin transcription comes from, we

should confirm these results using qPCR. Then we should start by looking at the main tissues in the intestine. We can look for the source of *Peroxidasin* in a multitude of intestinal tissues including gut epithelium (enterocytes, enteroendocrine cells, enteroblasts, and stem cells), gut muscles, hemocytes, and fat body. A Peroxidasin transcriptional reporter was upregulated in intestinal epithelial cells upon feeding dextran sodium sulfate feeding, consistent with a role for Peroxidasin in repair. We will start by comparing the GFP levels of flies fed dextran sodium sulfate compared to sucrose control fed flies. To determine if a gut cell type is transcribing *Peroxidasin,* the tissue will be stained with the varying gut cell markers, and we will then look for co-localization with the GFP *peroxidasin* transcriptional reporter. Each of the cells has a specific antibody we can stain with; for intestinal stem cells we can stain for Delta, for enteroblast cells we can stain for Suppressor of hairless, for enterocytes we can stain for Pdm1, and for enterocytes we can stain for Prospero. For the gut muscle cells we can co-stain with SiR-Actin, and to determine if the hemocytes are transcribing peroxidasin, we can use the anti-Lozenge antibody (Evans, Liu, and Banerjee 2014). The fat body is such a unique structure that we would be able to determine if it were fat cells by morphology. If *Peroxidasin* transcriptional levels are upregulated in response to dextran sodium sulfate damage, we can then look at Peroxidasin protein localization using recently reported Peroxidasin-GFP protein trap (Nagarkar-Jaiswal et al. 2015). In addition, our lab is in possession of a Peroxidasin antibody (Nelson, Fessler, Takagi, Blumberg, Keene, Olson, Parker, and Fessler 1994b), which we can use to look at peroxidasin localization. For future experiments, the Page-McCaw Lab may want to invest time into making more of the antibody.

H_2O_2 has been shown to be required in other wounding models (Razzell et al. 2013; Niethammer et al. 2009) as well as a cofactor for Peroxidasin to crosslink the sulfilimine bonds of Collagen IV (Bhave et al. 2012). One repair mechanism possibility is Peroxidasin transcription/protein levels remain the same while H_2O_2 levels increase to drive the crosslinking of the new Collagen IV. Interestingly enough, H_2O_2 is known to be elevated in uninjured Drosophila guts compared to other tissues (Albrecht et al. 2011), and basement membrane is known to turn over rapidly in the gut of the mouse (Walker 1972). Genetically encoded fluorescent H_2O_2 sensor flies can be used to assess the H_2O_2 levels (Albrecht et al. 2011). These flies use redox probes to measure the levels of hydrogen peroxidasin in either the cytosol or in the mitochondrial matrix. Upon dextran sodium sulfate feeding, if hydrogen peroxide levels increase, the lab can ask if H_2O_2 is truly necessary for basement membrane repair by using a catalase, an enzyme that breaks down hydrogen peroxide into oxygen and water, to drive the reduction of H_2O_2 (S. Wang et al. 2015). Another route they can take if there are increased H_2O_2 levels is to look at Duox, an enzyme known to be responsible for increased H_2O_2 production. In other wounding models, Duox has been shown necessary to produce the H_2O_2 necessary for repair (Niethammer et al. 2009; Razzell et al. 2013). If we see no increases then we would term this a passive mechanistic repair.

To test if the basement membrane goes through a passive mechanistic repair turnover can be investigated. Although FRAP is the first place most scientists' minds go to when they want to assess turnover rates, we do not have the accessibility of the tissue in vivo. Therefore, the Page-McCaw Laboratory would need to utilize the outstanding genetic tools in the Drosophila to utilize a temporal knockdown strategy.

They could use the temperature sensitive fly, tubGal4/tubGal80^{ts}, coupled with UAS-GFP^{RNAi} to turn on and off the knockdown of genes tagged with GFP. These flies would be heterozygous for one of the major basement membrane components (vkg-GFP, LanB1-GFP, or Trol-GFP) to knockdown these proteins in a temperature sensitive manner. These flies would be raised at 18 C, which does not allow Gal4 activity, the GFP-RNAi is turned off, so the basement membrane would fluoresce green. The flies would then be transferred to 29 C, where the GFP-RNAi would be turned on, preventing the new synthesis of any basement membrane components GFP tagged but preserving the synthesis of the untagged (wild-type) allele. We would then ask how long it takes before the GFP disappears in the gut of the Drosophila. This would tell us the degradation rate of the major basement membrane components in the gut. The converse experiment can also be done to assess assembly of the basement membrane gut proteins. These flies would be raised at 29 C, where the GFP tagged proteins would not be synthesized nor deposited in the basement membrane, making the basement membrane not fluoresce bright green. Because the GFP-tagged protein is heterozygous, in either experimental design, when you knockdown the GFP tagged version of the protein, there is still the endogenous protein without a GFP tag. For this second experiment, we would be asking how long before the gut basement membrane in the fly turns bright green. Our control fly would be one raised at 29 C for its entire life to be able to compare levels of GFP. These results for control flies would be compared to assembly and disassembly rates for dextran sodium sulfate fed flies, to see if the turnover rates changed. If not, we could conclude that repair and homeostasis have similar mechanisms.

What role do cells play in responding to dextran sodium sulfate damage to the basement membrane?

Throughout the course of this thesis work, a multitude of questions surrounding cell behavior have been asked by both the audience members of various oral presentations and the Page-McCaw lab. The questions ranged from whether the cells are the primary target in the dextran sodium sulfate damage model to if the cells signal to elicit repair and everything in between. From chapter 2, we have shown that basement membrane damage precedes epithelial barrier functional loss. There are two distinct questions which I think are important to ask about the role cells play in the detection and recovery of the gut after dextran sodium sulfate damage. The first question is how do cells detect damage (if it is an active response)? The second question is how do cells participate in the repair?

If we have determined cells play an active role in response, we will want to start by asking how the cells are detecting the damage. If an above repair response is identified then we can look at the role the cells play in signaling the damage, which cells are signaling, and ask how do the cells detect the damage. The first thing the Page-McCaw lab will need to find if they wish to understand how the cells are detecting damage is a transcriptional reporter that is upregulated after basement membrane damage (Appendix E). Previously, I have shown peroxidasin transcriptional levels are upregulated after dextran sodium sulfate damage. The lab would then down knock integrins or dystroglycans, damage with dextran sodium sulfate then ask if there is still an upregulation in transcriptional levels. If we see the transcriptional levels have

returned to wild type levels then we know that these cell-basement membrane connections play an integral part of how the cells detect the damage.

The second question is how do cells participate in the repair? It is known cells are attached to basement membrane via integrins and dystroglycan receptors on the cell surface (S. Li et al. 2017). Therefore, we can knockdown these attachments using a large flip out clone to overexpress an RNAi against them to see if they are required for basement membrane repair after dextran sodium sulfate damage. As previously discussed in the introduction, simplified Drosophila genetics allows for these questions to be easily asked. Drosophila have two β-integrin genes, *mys* and *βv* (Lin et al. 2013) as well as a single dystroglycan gene (Schneider and Baumgartner 2008; Kucherenko et al. 2011). The Page-McCaw lab could conditionally knock down these genes specifically in the gut epithelium and in the peristalsis muscles then see if we still get a readout. If we determine the cells detect the damage then we can use our dextran sodium sulfate damaging protocol to test if integrins and/or dystroglycan are required for basement membrane repair.

Another cell type that may be important in basement membrane repair are hemocyte cells as they have been reported to be at the site of basement membrane damage in larvae (Pastor-Pareja, Wu, and Xu 2008) and are the source of Peroxidasin in embryos (Nelson, Fessler, Takagi, Blumberg, Keene, Olson, Parker, and Fessler 1994a). First, we can assess if the hemocytes are present at damaged basement membranes by staining for hemocytes after dextran sodium sulfate damage. We will follow the dextran sodium sulfate damage protocol to test for their necessity in the repair of the gut basement membrane. If the hemocytes are seen then the hemocytes will be selectively

killed in the adult flies by turning on a pro-apoptotic gene, hid (Charroux and Royet 2009), the dextran sodium sulfate damaging protocol will be administrated then we will assess the tissue by muscle aspect ratio to look for the requirement of hemocytes in repair. If hemocytes are necessary for the repair mechanism of the basement membrane, we can go on and ask if the above damage-induced repair response also requires hemocytes. We can then ask if hemocytes need integrins and/or dystroglycan for the basement membrane repair. Hemocytes may be necessary to deposit new basement membrane components.

Is mechanotransduction used by cells to detect damaged basement membranes?

We have established that dextran sodium sulfate damage results in reduced mechanical stiffness of the basement membrane and so one possibility is that the intestinal cells are able to sense the mechanical changes and detect damage. Cells lie on top of the basement membrane and are able to sense basement membrane stiffness by pulling on it via their actomyosin contractility (Discher, Janmey, and Wang 2005). The mechanotransduction of the epithelial cell layer has been previously altered in other labs by either activating or inactivating the nonmuscle myosin II (Rauskolb et al. 2014; Mason, Tworoger, and Martin 2013). Upon Rho kinase (rok) knock down, the myosin contractility is decreased, on the other hand when phosphomimemtic myosin II, Squash.EE is expressed then there is an increase in the amount of myosin contractility (Rauskolb et al. 2014; Mason, Tworoger, and Martin 2013).

Using Drosophila spatial and temporal drivers, we can conditionally express either *rok-RNAi* or Sqh.EE in the gut epithelium, muscles, and hemocytes then use the dextran sodium sulfate damage model to assess both basement membrane damage and repair. If the cells detect basement membrane damage by sensing changes in stiffness then if we knockdown the cell's ability to sense mechanical changes by decreasing tension (rok), this would reduce the cell's ability to detect basement membrane damage. Therefore, I expect repair to be inhibited and the previously discussed repair response to decrease. On the other hand, if Squash.EE is expressed then the cells will be under greater tension, which may lead to greater sensitivity of the cells. Therefore, we would predict a lower dose of dextran sodium sulfate would produce the same amount of response, measured by Peroxidasin upregulation. This experiment will help us determine whether or not mechanotransduction is important in detecting basement membrane damage and eliciting repair, in addition to if and which cells are necessary for the repair process. If mechanotransduction is important for repair, we can see if integrins and dystroglcans also play a role in this process.

Does the mechanical strength of the guts change throughout the course of repair?

Using two microneedles, the micromechanical properties of the basement membrane was tested in chapter two of this thesis. As previously described, for that experiment, the Malphigan tubules were used as opposed to the gut. Malphigan tubules, the excretory system of insects, are slender one-cell layer tubes that branch out

where the midgut turns into the hindgut. They consist of only basement membrane and a single cell layer, without any complicating muscles or exoskeleton. However, since dextran sodium sulfate becomes lodged in the basement membrane of the gut, all of these experiments were performed ex-vivo. This protocol would not allow for the assessment of the basement membrane as it repairs over the course of two days. Therefore, I propose to use microrheology to assess this question. Microrheology works by attaching fluorescently-labeled micrometer-sized chemically inert spherical beads to a substrate, here basement membrane (MacKintosh and Schmidt 1999; Helfer et al. 2000). The fluorescently labeled beads will bind to the basement membrane via an antibody against the GFP in our collagen IV (vkg) GFP fly line. Employing passive microrheology, one can observe the natural thermal fluctuations of the system via the bead. Exploiting a two-bead technique the macro-movements of the whole system can be accounted for allowing them to be subtracted out, permitting for finite precision of the micro-movements. By tracking the small fluctuation in Brownian motion, we can calculate the stiffness of the basement membrane.

In addition to passive microrheology, the lab would be able to utilize active microrheology techniques, both magnetic and optical tweezers, which are available at Vanderbilt University. Active microrheology allows forces to be applied to the system. Active microrheology is often used in rigid systems as it is harder to tease apart smaller differences in stiffness. The fluorescent beads are magnetic in nature allowing us to apply a given magnetic force to pull the beads, and the recoil of the beads is measured (Neuman and Nagy 2008; Tanase, Biais, and Sheetz 2007). By mapping the fluctuations of the bead movement, the stiffness of the system can be calculated. The

same principles are used in optical-tweezer experiments (Tanase, Biais, and Sheetz 2007). Using these techniques, the question about changes in mechanical stiffness throughout the course of repair can be assessed. I expect the basement membrane that is damaged by dextran sodium sulfate will slowly return to its normal mechanical strength as it repairs.

Another way to assess if the mechanical strength of the gut is compromised throughout repair is to use a bursting assay. This assay would not only provide scientific insight, but would also be a fun assay to assess damage. The guts fed either sucrose or dextran sodium sulfate would be exposed to osmotic shock by soaking them in deionized water. As the water diffuses into the gut's cells, it will cause the cells to swell before eventually bursting. When basement membranes have weakened mechanical strength, they burst quicker than their control counter parts (Wolfstetter et al. 2019). Therefore, I hypothesize the guts fed dextran sodium sulfate will burst at a quicker rate than controls. I also predict that as the guts recover their mechanical strength will slowly return to normal over 48 hours and we will be able to see this in the increase in time before the gut cells burst.

Are Matrix metalloproteinases necessary for the repair of the basement membrane after dextran sodium sulfate damage?

Matrix metalloproteinases are extracellular proteases that degrade the extracellular matrix (Page-McCaw, Ewald, and Werb 2007). Previous work from the Page-McCaw

lab showed that Matrix metalloproteinase 1 and 2 are required to aid in the reepithelialization in the epidermis of the fly by promoting basement membrane repair in addition to aiding in cell elongation, the reorganization of the actin cytoskeleton, and activating the Jun N-terminal kinase (JNK) pathway (Stevens and Page-McCaw 2012). Drosophila is an ideal organism to study the role of matrix metalloproteinases in as they possess 2 non-redundant genes while mammals possess 24 matrix metalloproteinase genes. For this reason, we asked if either of the matrix metalloproteinases were necessary for repair of the gut basement membrane after two days of dextran sodium sulfate damage. I hypothesized that the basement membrane would be necessary for repair as they would cleave and remove the damaged basement membrane components in order for the new basement membrane components to be deposited. We started by knocking down matrix metalloproteinase 1 and 2, separately, for ten days after they have reached adulthood, as matrix metalloproteinases are necessary for embryogenesis, then looking at collagen IV. Surprisingly, the collagen IV basement membrane signal disappeared from under the enterocytes, while the GFP signal could still be seen on the hemolymph side (Appendix D). When the guts were stained with an anti-NC1 antibody, we saw the same patterning (Kimberly LaFever, preliminary data). However, when matrix metalloproteinase 1 or 2 was knocked down and we looked at LanB1 GFP, we saw the converse with the GFP basement membrane signal under the cells, but absent from the hemolymph side (Kimberly LaFever, preliminary data). When we looked at perlecan expression, we saw no difference in the GFP expression on either side of the gut.

These surprising results led to many questions. Since we are unable to see both

sides of the basement membrane concurrently using epifluorescent microscopy, it may be worth the time and money to procure electron microscopy images of these knockdown flies. These images may show that when either of the matrix metalloproteinases are knocked down, we see a thinner basement membrane compared to control flies, corresponding to the loss of GFP-tagged protein. This would be a logical hypothesis as when the proteinases are knocked down we are unable to see the collagen IV protein on the luminal side of the gut and unable to see Laminin on the hemolymph side. Electron microscopy images could give us insight into whether the proteins are truly being degraded and removed from the basement membrane.

The Page-McCaw lab should next look at the localization of the matrix metalloproteinases proteins as well as where they are transcribed. Matrix metalloproteinase 1 has an excellent antibody with which they can stain the gut and visualize its localization. For matrix metalloproteinase 2, they would have to use the GFP tagged protein. As for looking for the transcriptional location, a possible experiment is to express matrix metalloproteinase 1 and 2 LacZ and staining with the various cell type markers and look for co-localization. The LacZ can be visualized by a Beta-galactosidase antibody. Co-localization of the Beta-galactosidase and a cellular antibody would tell us which cell is transcribing the matrix metalloproteinase. If we know which cells are transcribing the two matrix metalloproteinases, we can start to ask questions of if there is an upregulation in one matrix metalloproteinase if the other one is knocked down.

Tissue inhibitor of metalloproteinase (TIMP) is an inhibitor of the Drosophila matrix metalloproteinases (Godenschwege et al. 2000; Wei et al. 2003). TIMP overexpression

should recapitulate the matrix metalloproteinase RNAi experiments. The Page-McCaw lab would first need to determine how long TIMP needs to be overexpressed then they could proceed with the dextran sodium sulfate damaging protocol. I hypothesize we will see the same missing protein phenotype as above. If we do not then this tells us that either the matrix metalloproteinases or TIMP have multiple pathways or the RNAis are leaky. The lab can also knock down both the matrix metalloproteinases to determine if they are working in the same pathway as each other. Based on the fact we see the same results when 1 and 2 are knocked down, I would predict the double knock down would phenocopy the individual knockdowns.

If I could ask and answer one more question during my graduate career at Vanderbilt it would what is the mechanism behind collagen IV and laminin disappearing from the opposite sides of the basement membrane in the absence of matrix metalloproteinase 1 and 2. I do not believe we have enough information on the matrix metalloproteinase expression, homeostasis or the RNAis at this moment to be able to propose an experiment. In our lab, Kimi LaFever is working towards understanding what the half-life of the basement membrane proteins at the two sides of the muscle. She is also going to inhibit the Mmps by using a drug cocktail to determine if the matrix metalloproteinases affect matrix turnover, using the GFP technique described earlier. I feel both of these experiments are key to start to narrow down how to ask the question I propose. I look forward to the Page-McCaw lab discovering the answers to these questions and more in the upcoming years.

REFERENCES

Albrecht, Simone C, Ana Gomes Barata, Jörg Grosshans, Aurelio A Teleman, and Tobias P Dick. 2011. “In Vivo Mapping of Hydrogen Peroxide and Oxidized Glutathione Reveals Chemical and Regional Specificity of Redox Homeostasis..” *Cell Metabolism* 14 (6): 819–29. doi:10.1016/j.cmet.2011.10.010.

Amcheslavsky, Alla, Jin Jiang, and Y Tony Ip. 2009. “Tissue Damage-Induced Intestinal Stem Cell Division in Drosophila..” *Cell Stem Cell* 4 (1): 49–61. doi:10.1016/j.stem.2008.10.016.

Andersen, Darcy, and Sally Horne-Badovinac. 2016. “Influence of Ovarian Muscle Contraction and Oocyte Growth on Egg Chamber Elongation in Drosophila..” *Development (Cambridge, England)* 143 (8). Oxford University Press for The Company of Biologists Limited: 1375–87. doi:10.1242/dev.131276.

Arahata, K, H Ishii, and Y K Hayashi. 1995. “Congenital Muscular Dystrophies..” *Current Opinion in Neurology* 8 (5): 385–90.

ARAHATA, Kiichi, Yukiko K HAYASHI, Ritsuko KOGA, Kanako GOTO, Je Hyeon LEE, Yuko MIYAGOE, Hiroko ISHII, et al. 1993. “Laminin in Animal Models for Muscular Dystrophy Defect of Laminin M in Skeletal and Cardiac Muscles and Peripheral Nerve of the Homozygous Dystrophic Dy/Dy Mice..” *Proceedings of the Japan Academy. Ser. B: Physical and Biological Sciences* 69 (10). The Japan Academy: 259–64. doi:10.2183/pjab.69.259.

Aumailley, M, and B Gayraud. 1998. “Structure and Biological Activity of the Extracellular Matrix..” *Journal of Molecular Medicine (Berlin, Germany)* 76 (3-4): 253–65.

Avery, L, and H R Horvitz. 1989. “Pharyngeal Pumping Continues After Laser Killing of the Pharyngeal Nervous System of C. Elegans..” *Neuron* 3 (4): 473–85.

Bateman, J, R S Reddy, H Saito, and D Van Vactor. 2001. “The Receptor Tyrosine Phosphatase Dlar and Integrins Organize Actin Filaments in the Drosophila Follicular Epithelium..” *Current Biology : CB* 11 (17): 1317–27.

Bhave, Gautam, Christopher F Cummings, Roberto M Vanacore, Chino Kumagai-Cresse, Isi A Ero-Tolliver, Mohamed Rafi, Jeong-Suk Kang, et al. 2012. “Peroxidasin Forms Sulfilimine Chemical Bonds Using Hypohalous Acids in Tissue Genesis..” *Nature Chemical Biology* 8 (9): 784–90. doi:10.1038/nchembio.1038.

Bhave, Gautam, Selene Colon, and Nicholas Ferrell. 2017. “The Sulfilimine Cross-Link of Collagen IV Contributes to Kidney Tubular Basement Membrane Stiffness.” *American Journal of Physiology-Renal Physiology* 313 (3). American Physiological Society Bethesda, MD: F596–F602. doi:10.1152/ajprenal.00096.2017.

Blake, Derek J, Andrew Weir, Sarah E Newey, and Kay E Davies. 2002. “Function and Genetics of Dystrophin and Dystrophin-Related Proteins in Muscle..” *Physiological Reviews* 82 (2): 291–329. doi:10.1152/physrev.00028.2001.

Bunt, Stephanie, Clare Hooley, Nan Hu, Catherine Scahill, Helen Weavers, and Helen Skaer. 2010. “Hemocyte-Secreted Type IV Collagen Enhances BMP Signaling to Guide Renal Tubule Morphogenesis in Drosophila.” *Developmental Cell* 19 (2): 296–306. doi:10.1016/j.devcel.2010.07.019.

Butcher, Darci T, Tamara Alliston, and Valerie M Weaver. 2009. “A Tense Situation: Forcing Tumour Progression..” *Nature Reviews. Cancer* 9 (2): 108–22. doi:10.1038/nrc2544.

Campbell, K P. 1995. “Three Muscular Dystrophies: Loss of Cytoskeleton-Extracellular Matrix Linkage..” *Cell* 80 (5): 675–79.

Candiello, Joseph, Manimalha Balasubramani, Emmanuel M Schreiber, Gregory J Cole, Ulrike Mayer, Willi Halfter, and Hai Lin. 2007. “Biomechanical Properties of Native Basement Membranes..” *The FEBS Journal* 274 (11). John Wiley & Sons, Ltd: 2897–2908. doi:10.1111/j.1742-4658.2007.05823.x.

Cetera, Maureen, and Sally Horne-Badovinac. 2015. “Round and Round Gets You Somewhere: Collective Cell Migration and Planar Polarity in Elongating Drosophila Egg Chambers..” *Current Opinion in Genetics & Development* 32 (June): 10–15. doi:10.1016/j.gde.2015.01.003.

Charroux, Bernard, and Julien Royet. 2009. “Elimination of Plasmatocytes by Targeted Apoptosis Reveals Their Role in Multiple Aspects of the Drosophila Immune Response..” *Proceedings of the National Academy of Sciences of the United States of America* 106 (24): 9797–9802. doi:10.1073/pnas.0903971106.

Chassaing, Benoit, Jesse D Aitken, Madhu Malleshappa, and Matam Vijay-Kumar. 2001. *Dextran Sulfate Sodium (DSS)-Induced Colitis in Mice*. *Current Protocols in Immunology*. Vol. 40. Hoboken, NJ, USA: John Wiley & Sons, Inc. doi:10.1002/0471142735.im1525s104.

Cordero, Julia B, Rhoda K Stefanatos, Alessandro Scopelliti, Marcos Vidal, and Owen J Sansom. 2012. “Inducible Progenitor-Derived Wingless Regulates Adult Midgut Regeneration in Drosophila..” *The EMBO Journal* 31 (19). EMBO Press: 3901–17. doi:10.1038/emboj.2012.248.

Costell, M, E Gustafsson, A Aszódi, M Mörgelin, W Bloch, E Hunziker, K Addicks, R Timpl, and R Fässler. 1999. “Perlecan Maintains the Integrity of Cartilage and Some Basement Membranes..” *The Journal of Cell Biology* 147 (5). The Rockefeller University Press: 1109–22.

Csiszar, K. 2001. “Lysyl Oxidases: a Novel Multifunctional Amine Oxidase Family..” *Progress in Nucleic Acid Research and Molecular Biology* 70: 1–32.

Cummings, Christopher F, Vadim Pedchenko, Kyle L Brown, Selene Colon, Mohamed Rafi, Celestial Jones-Paris, Elena Pokydeshava, et al. 2016. “Extracellular Chloride Signals Collagen IV Network Assembly During Basement Membrane Formation..” *The Journal of Cell Biology* 213 (4). Rockefeller University Press: 479–94. doi:10.1083/jcb.201510065.

Dai, Jianli, Beatriz Estrada, Sofie Jacobs, Besaiz J Sánchez-Sánchez, Jia Tang, Mengqi Ma, Patricia Magadán-Corpas, Jose C Pastor-Pareja, and Maria D Martín-Bermudo. 2018. “Dissection of Nidogen Function in Drosophila Reveals Tissue-Specific Mechanisms of Basement Membrane Assembly.” Edited by Claude Desplan. *PLOS Genetics* 14 (9): e1007483. doi:10.1371/journal.pgen.1007483.

Daley, William P, and Kenneth M Yamada. 2013. “ECM-Modulated Cellular Dynamics as a Driving Force for Tissue Morphogenesis..” *Current Opinion in Genetics & Development* 23 (4): 408–14. doi:10.1016/j.gde.2013.05.005.

Discher, Dennis E, Paul Janmey, and Yu-Li Wang. 2005. “Tissue Cells Feel and Respond to the Stiffness of Their Substrate..” *Science (New York, N.Y.)* 310 (5751): 1139–43. doi:10.1126/science.1116995.

Durbeej, Madeleine. 2015. “Laminin-A2 Chain-Deficient Congenital Muscular Dystrophy: Pathophysiology and Development of Treatment..” *Current Topics in Membranes* 76. Elsevier: 31–60. doi:10.1016/bs.ctm.2015.05.002.

Ekblom, P, M Ekblom, L Fecker, G Klein, H Y Zhang, Y Kadoya, M L Chu, U Mayer, and R Timpl. 1994. “Role of Mesenchymal Nidogen for Epithelial Morphogenesis in Vitro..” *Development (Cambridge, England)* 120 (7): 2003–14.

Engel, J, E Odermatt, A Engel, J A Madri, H Furthmayr, H Rohde, and R Timpl. 1981. “Shapes, Domain Organizations and Flexibility of Laminin and Fibronectin, Two Multifunctional Proteins of the Extracellular Matrix..” *Journal of Molecular Biology* 150 (1): 97–120.

Engler, Adam J, Shamik Sen, H Lee Sweeney, and Dennis E Discher. 2006. “Matrix Elasticity Directs Stem Cell Lineage Specification..” *Cell* 126 (4): 677–89. doi:10.1016/j.cell.2006.06.044.

Evans, Cory J, Ting Liu, and Utpal Banerjee. 2014. “Drosophila Hematopoiesis: Markers and Methods for Molecular Genetic Analysis..” *Methods (San Diego, Calif.)* 68 (1): 242–51. doi:10.1016/j.ymeth.2014.02.038.

Fata, Jimmie E, Zena Werb, and Mina J Bissell. 2004. “Regulation of Mammary Gland Branching Morphogenesis by the Extracellular Matrix and Its Remodeling Enzymes..” *Breast Cancer Research : BCR* 6 (1). BioMed Central: 1–11. doi:10.1186/bcr634.

Fessler, J H, N Shigaki, and L I Fessler. 1985. “Biosynthesis and Properties of Procollagens v..” *Annals of the New York Academy of Sciences* 460: 181–86.

Fessler, L I, and J H Fessler. 1982. “Identification of the Carboxyl Peptides of Mouse Procollagen IV and Its Implications for the Assembly and Structure of Basement Membrane Procollagen..” *The Journal of Biological Chemistry* 257 (16): 9804–10.

Fidler, A L, R M Vanacore, and S V Chetyrkin. 2014. “A Unique Covalent Bond in Basement Membrane Is a Primordial Innovation for Tissue Evolution.” doi:10.1073/pnas.1318499111.

Fidler, Aaron L, Carl E Darris, Sergei V Chetyrkin, Vadim K Pedchenko, Sergei P Boudko, Kyle L Brown, W Gray Jerome, Julie K Hudson, Antonis Rokas, and Billy G Hudson. 2017. “Collagen IV and Basement Membrane at the Evolutionary Dawn of Metazoan Tissues..” *eLife* 6 (April): e15040. doi:10.7554/eLife.24176.

Flood-Page, Patrick, Andrew Menzies-Gow, Simon Phipps, Sun Ying, Arun Wangoo, Mara S Ludwig, Neil Barnes, Douglas Robinson, and A Barry Kay. 2003. “Anti-IL-5 Treatment Reduces Deposition of ECM Proteins in the Bronchial Subepithelial Basement Membrane of Mild Atopic Asthmatics..” *The Journal of Clinical Investigation* 112 (7). American Society for Clinical Investigation: 1029–36. doi:10.1172/JCI17974.

Fox, J W, U Mayer, R Nischt, M Aumailley, D Reinhardt, H Wiedemann, K Mann, R Timpl, T Krieg, and J Engel. 1991. “Recombinant Nidogen Consists of Three Globular Domains and Mediates Binding of Laminin to Collagen Type IV..” *The EMBO Journal* 10 (11). European Molecular Biology Organization: 3137–46.

Furuya, Kazuo. 2008. “Nanofabrication by Advanced Electron Microscopy Using Intense and Focused Beam∗..” *Science and Technology of Advanced Materials* 9 (1). Taylor & Francis: 014110. doi:10.1088/1468-6996/9/1/014110.

Gersdorff, N, S Otto, M Roediger, J Kruegel, and N Miosge. 2007. “The Absence of One or Both Nidogens Does Not Alter Basement Membrane Composition in Adult Murine Kidney..” *Histology and Histopathology* 22 (10): 1077–84. doi:10.14670/HH-22.1077.

Godenschwege, T A, N Pohar, S Buchner, and E Buchner. 2000. “Inflated Wings, Tissue Autolysis and Early Death in Tissue Inhibitor of Metalloproteinases Mutants of Drosophila..” *European Journal of Cell Biology* 79 (7): 495–501. doi:10.1078/0171-9335-00072.

Gustafsson, Mats G L, Lin Shao, Peter M Carlton, C J Rachel Wang, Inna N Golubovskaya, W Zacheus Cande, David A Agard, and John W Sedat. 2008. “Three-Dimensional Resolution Doubling in Wide-Field Fluorescence Microscopy by Structured Illumination..” *Biophysical Journal* 94 (12): 4957–70. doi:10.1529/biophysj.107.120345.

Haigo, Saori L, and David Bilder. 2011. “Global Tissue Revolutions in a Morphogenetic Movement Controlling Elongation..” *Science (New York, N.Y.)* 331 (6020): 1071–74. doi:10.1126/science.1199424.

Halfter, Willi, Joseph Candiello, Haiyu Hu, Peng Zhang, Emanuel Schreiber, and Manimalha Balasubramani. 2013. “Protein Composition and Biomechanical Properties of in Vivo-Derived Basement Membranes..” *Cell Adhesion & Migration* 7 (1). Taylor & Francis: 64–71. doi:10.4161/cam.22479.

Helbling-Leclerc, A, Helbling-Leclerc, Anne, X Zhang, Xu Zhang, H Topaloglu, Haluk Topaloglu, Corinne Cruaud, et al. 1995. “Mutations in the Laminin A2–Chain Gene (LAMA2) Cause Merosin–Deficient Congenital Muscular Dystrophy.” *Nature Genetics* 11 (2). Nature Publishing Group: 216–18. doi:10.1038/ng1095-216.

Helfer, E, S Harlepp, L Bourdieu, J Robert, F C MacKintosh, and D Chatenay. 2000. “Microrheology of Biopolymer-Membrane Complexes..” *Physical Review Letters* 85 (2). American Physical Society: 457–60. doi:10.1103/PhysRevLett.85.457.

Hohenester, Erhard, and Peter D Yurchenco. 2013. “Laminins in Basement Membrane Assembly..” *Cell Adhesion & Migration* 7 (1). Taylor & Francis: 56–63. doi:10.4161/cam.21831.

Hopf, M, W Göhring, E Kohfeldt, Y Yamada, and R Timpl. 1999. “Recombinant Domain IV of Perlecan Binds to Nidogens, Laminin-Nidogen Complex, Fibronectin, Fibulin-2 and Heparin..” *European Journal of Biochemistry* 259 (3): 917–25.

Horne-Badovinac, Sally. 2014. “The Drosophila Egg Chamber-a New Spin on How Tissues Elongate..” *Integrative and Comparative Biology* 54 (4): 667–76. doi:10.1093/icb/icu067.

Huber, A R, and S J Weiss. 1989. “Disruption of the Subendothelial Basement Membrane During Neutrophil Diapedesis in an in Vitro Construct of a Blood Vessel Wall..” *The Journal of Clinical Investigation* 83 (4). American Society for Clinical Investigation: 1122–36. doi:10.1172/JCI113992.

Ihara, Shinji, Elliott J Hagedorn, Meghan A Morrissey, Qiuyi Chi, Fumio Motegi, James M Kramer, and David R Sherwood. 2011. “Basement Membrane Sliding and Targeted Adhesion Remodels Tissue Boundaries During Uterine-Vulval Attachment in Caenorhabditis Elegans..” *Nature Cell Biology* 13 (6). Nature Publishing Group: 641–51. doi:10.1038/ncb2233.

Isabella, Adam J, and Sally Horne-Badovinac. 2015a. “Building From the Ground Up: Basement Membranes in Drosophila Development..” *Current Topics in Membranes* 76. Elsevier: 305–36. doi:10.1016/bs.ctm.2015.07.001.

Isabella, Adam J, and Sally Horne-Badovinac. 2015b. “Dynamic Regulation of Basement Membrane Protein Levels Promotes Egg Chamber Elongation in Drosophila..” *Developmental Biology* 406 (2): 212–21. doi:10.1016/j.ydbio.2015.08.018.

Jöbsis, G J, H Keizers, J P Vreijling, M de Visser, M C Speer, R A Wolterman, F Baas, and P A Bolhuis. 1996. “Type VI Collagen Mutations in Bethlem Myopathy, an Autosomal Dominant Myopathy with Contractures..” *Nature Genetics* 14 (1). Nature Publishing Group: 113–15. doi:10.1038/ng0996-113.

Kalluri, Raghu. 2003. “Basement Membranes: Structure, Assembly and Role in Tumour Angiogenesis..” *Nature Reviews. Cancer* 3 (6): 422–33. doi:10.1038/nrc1094.

Karpowicz, Phillip, Jessica Perez, and Norbert Perrimon. 2010. “The Hippo Tumor Suppressor Pathway Regulates Intestinal Stem Cell Regeneration..” *Development (Cambridge, England)* 137 (24): 4135–45. doi:10.1242/dev.060483.

Kelemen-Valkony, Ildikó, Márton Kiss, Judit Csiha, András Kiss, Urs Bircher, János Szidonya, Péter Maróy, et al. 2012. “Drosophila Basement Membrane Collagen Col4a1 Mutations Cause Severe Myopathy.” *Matrix Biology* 31 (1): 29–37. doi:10.1016/j.matbio.2011.09.004.

Khoshnoodi, Jamshid, Vadim Pedchenko, and Billy G Hudson. 2008. “Mammalian Collagen IV..” *Microscopy Research and Technique* 71 (5): 357–70. doi:10.1002/jemt.20564.

Kim, S, and W G Wadsworth. 2000. “Positioning of Longitudinal Nerves in C. Elegans by Nidogen..” *Science (New York, N.Y.)* 288 (5463): 150–54.

Kivirikko, K I, L Ryhänen, H Anttinen, P Bornstein, and D J Prockop. 1973. “Further Hydroxylation of Lysyl Residues in Collagen by Protocollagen Lysyl Hydroxylase in Vitro..” *Biochemistry* 12 (24): 4966–71.

Kleinman, H K, M L McGarvey, J R Hassell, V L Star, F B Cannon, G W Laurie, and G R Martin. 1986. “Basement Membrane Complexes with Biological Activity..” *Biochemistry* 25 (2): 312–18.

Kleinman, Hynda K, and George R Martin. 2005. “Matrigel: Basement Membrane Matrix with Biological Activity..” *Seminars in Cancer Biology* 15 (5): 378–86. doi:10.1016/j.semcancer.2005.05.004.

Kleinman, Hynda K, Mary L McGarvey, Lance A Liotta, Pamela Gehron Robey, Karl Tryggvason, and George R Martin. 1982. “Isolation and Characterization of Type IV Procollagen, Laminin, and Heparan Sulfate Proteoglycan From the EHS Sarcoma.” *Biochemistry* 21 (24). American Chemical Society: 6188–93. doi:10.1021/bi00267a025.

Kucherenko, Mariya M, April K Marrone, Valentyna M Rishko, Helena de Fatima Magliarelli, and Halyna R Shcherbata. 2011. “Stress and Muscular Dystrophy: a Genetic Screen for Dystroglycan and Dystrophin Interactors in Drosophila Identifies Cellular Stress Response Components.” *Developmental Biology* 352 (2): 228–42. doi:10.1016/j.ydbio.2011.01.013.

Kühn, L C, and J P Kraehenbuhl. 1981. “The Membrane Receptor for Polymeric Immunoglobulin Is Structurally Related to Secretory Component. Isolation and Characterization of Membrane Secretory Component From Rabbit Liver and Mammary Gland..” *The Journal of Biological Chemistry* 256 (23): 12490–95.

Langeveld, J P, M E Noelken, K Hård, P Todd, J F Vliegenthart, J Rouse, and B G Hudson. 1991. “Bovine Glomerular Basement Membrane. Location and Structure of the Asparagine-Linked Oligosaccharide Units and Their Potential Role in the Assembly of the 7 S Collagen IV Tetramer..” *The Journal of Biological Chemistry* 266 (4): 2622–31.

Lerner, David W, Darcy McCoy, Adam J Isabella, Anthony P Mahowald, Gary F Gerlach, Thymur A Chaudhry, and Sally Horne-Badovinac. 2013. “A Rab10-Dependent Mechanism for Polarized Basement Membrane Secretion During Organ Morphogenesis..” *Developmental Cell* 24 (2): 159–68. doi:10.1016/j.devcel.2012.12.005.

Lewellyn, Lindsay, Maureen Cetera, and Sally Horne-Badovinac. 2013. “Misshapen Decreases Integrin Levels to Promote Epithelial Motility and Planar Polarity in Drosophila.” *The Journal of Cell Biology* 200 (6). Rockefeller University Press: 721–29. doi:10.1083/jcb.201209129.

Li, Hongjie, Yanyan Qi, and Heinrich Jasper. 2013. “Dpp Signaling Determines Regional Stem Cell Identity in the Regenerating Adult Drosophila Gastrointestinal Tract.” *Cell Reports* 4 (1): 10–18. doi:10.1016/j.celrep.2013.05.040.

Li, Shaohua, David Harrison, Salvatore Carbonetto, Reinhard Fassler, Neil Smyth, David Edgar, and Peter D Yurchenco. 2002. “Matrix Assembly, Regulation, and Survival Functions of Laminin and Its Receptors in Embryonic Stem Cell Differentiation..” *The Journal of Cell Biology* 157 (7): 1279–90. doi:10.1083/jcb.200203073.

Li, Shaohua, Yanmei Qi, Karen McKee, Jie Liu, June Hsu, and Peter D Yurchenco. 2017. “Integrin and Dystroglycan Compensate Each Other to Mediate Laminin-

Dependent Basement Membrane Assembly and Epiblast Polarization.." *Matrix Biology : Journal of the International Society for Matrix Biology* 57-58 (January): 272–84. doi:10.1016/j.matbio.2016.07.005.

Liefhebber, Jolanda Mp, Simone Punt, Willy Jm Spaan, and Hans C van Leeuwen. 2010. "The Human Collagen Beta(1-O)Galactosyltransferase, GLT25D1, Is a Soluble Endoplasmic Reticulum Localized Protein.." *BMC Cell Biology* 11 (1). BioMed Central: 33. doi:10.1186/1471-2121-11-33.

Lin, Guonan, Xi Zhang, Juan Ren, Zhimin Pang, Chenhui Wang, Na Xu, and Rongwen Xi. 2013. "Integrin Signaling Is Required for Maintenance and Proliferation of Intestinal Stem Cells in Drosophila.." *Developmental Biology* 377 (1): 177–87. doi:10.1016/j.ydbio.2013.01.032.

Lunstrum, G P, H P Bächinger, L I Fessler, K G Duncan, R E Nelson, and J H Fessler. 1988. "Drosophila Basement Membrane Procollagen IV. I. Protein Characterization and Distribution.." *The Journal of Biological Chemistry* 263 (34): 18318–27.

Maartens, Aidan P, and Nicholas H Brown. 2015. "The Many Faces of Cell Adhesion During Drosophila Muscle Development.." *Developmental Biology* 401 (1): 62–74. doi:10.1016/j.ydbio.2014.12.038.

MacKintosh, F C, and C F Schmidt. 1999. "Microrheology." *Current Opinion in Colloid & Interface Science* 4 (4): 300–307. doi:10.1016/S1359-0294(99)90010-9.

Mason, Frank M, Michael Tworoger, and Adam C Martin. 2013. "Apical Domain Polarization Localizes Actin-Myosin Activity to Drive Ratchet-Like Apical Constriction.." *Nature Cell Biology* 15 (8). Nature Publishing Group: 926–36. doi:10.1038/ncb2796.

Mayer, Ulrike. 2003. "Integrins: Redundant or Important Players in Skeletal Muscle?." *The Journal of Biological Chemistry* 278 (17): 14587–90. doi:10.1074/jbc.R200022200.

McCall, A Scott, Christopher F Cummings, Gautam Bhave, Roberto Vanacore, Andrea Page-McCaw, and Billy G Hudson. 2014. "Bromine Is an Essential Trace Element for Assembly of Collagen IV Scaffolds in Tissue Development and Architecture." *Cell* 157 (6). Elsevier Inc.: 1380–92. doi:10.1016/j.cell.2014.05.009.

Mercuri, Eugenio, and Francesco Muntoni. 2013. "Muscular Dystrophies." *The Lancet* 381 (9869): 845–60. doi:10.1016/S0140-6736(12)61897-2.

Michele, Daniel E, and Kevin P Campbell. 2003. "Dystrophin-Glycoprotein Complex: Post-Translational Processing and Dystroglycan Function.." *The Journal of Biological Chemistry* 278 (18). American Society for Biochemistry and Molecular Biology: 15457–60. doi:10.1074/jbc.R200031200.

Miner, Jeffrey H, and Peter D Yurchenco. 2004. “Laminin Functions in Tissue Morphogenesis..” *Annual Review of Cell and Developmental Biology* 20 (1): 255–84. doi:10.1146/annurev.cellbio.20.010403.094555.

Morrissey, Meghan A, and David R Sherwood. 2015. “An Active Role for Basement Membrane Assembly and Modification in Tissue Sculpting..” *Journal of Cell Science* 128 (9): 1661–68. doi:10.1242/jcs.168021.

Morrissey, Meghan A, Daniel P Keeley, Elliott J Hagedorn, Shelly T H McClatchey, Qiuyi Chi, David H Hall, and David R Sherwood. 2014. “B-LINK: a Hemicentin, Plakin, and Integrin- Dependent Adhesion System That Links Tissues by Connecting Adjacent Basement Membranes.” *Developmental Cell* 31 (3). Elsevier Inc.: 319–31. doi:10.1016/j.devcel.2014.08.024.

Murray, P, and D Edgar. 2000. “Regulation of Programmed Cell Death by Basement Membranes in Embryonic Development..” *The Journal of Cell Biology* 150 (5). The Rockefeller University Press: 1215–21.

Nagarkar-Jaiswal, Sonal, Pei-Tseng Lee, Megan E Campbell, Kuchuan Chen, Stephanie Anguiano-Zarate, Manuel Cantu Gutierrez, Theodore Busby, et al. 2015. “A Library of MiMICs Allows Tagging of Genes and Reversible, Spatial and Temporal Knockdown of Proteins in Drosophila..” *eLife* 4 (March): 2743. doi:10.7554/eLife.05338.

Nelson, R E, L I Fessler, Y Takagi, B Blumberg, D R Keene, P F Olson, C G Parker, and J H Fessler. 1994a. “Peroxidasin: a Novel Enzyme-Matrix Protein of Drosophila Development..” *The EMBO Journal* 13 (15): 3438–47. http://eutils.ncbi.nlm.nih.gov/entrez/eutils/elink.fcgi?dbfrom=pubmed&id=8062820&retmode=ref&cmd=prlinks.

Nelson, R E, L I Fessler, Y Takagi, B Blumberg, D R Keene, P F Olson, C G Parker, and J H Fessler. 1994b. “Peroxidasin: a Novel Enzyme-Matrix Protein of Drosophila Development..” *The EMBO Journal* 13 (15): 3438–47. http://eutils.ncbi.nlm.nih.gov/entrez/eutils/elink.fcgi?dbfrom=pubmed&id=8062820&retmode=ref&cmd=prlinks.

Neuman, Keir C, and Attila Nagy. 2008. “Single-Molecule Force Spectroscopy: Optical Tweezers, Magnetic Tweezers and Atomic Force Microscopy..” *Nature Methods* 5 (6). Nature Publishing Group: 491–505. doi:10.1038/nmeth.1218.

Niethammer, Philipp, Clemens Grabher, A Thomas Look, and Timothy J Mitchison. 2009. “A Tissue-Scale Gradient of Hydrogen Peroxide Mediates Rapid Wound Detection in Zebrafish..” *Nature* 459 (7249): 996–99. doi:10.1038/nature08119.

Noonan, D M, A Fulle, P Valente, S Cai, E Horigan, M Sasaki, Y Yamada, and J R Hassell. 1991. “The Complete Sequence of Perlecan, a Basement Membrane Heparan Sulfate Proteoglycan, Reveals Extensive Similarity with Laminin a Chain, Low Density Lipoprotein-Receptor, and the Neural Cell Adhesion Molecule..” *The Journal of Biological Chemistry* 266 (34): 22939–47.

Norose, K, W K Lo, J I Clark, E H Sage, and C C Howe. 2000. “Lenses of SPARC-Null Mice Exhibit an Abnormal Cell Surface-Basement Membrane Interface..” *Experimental Eye Research* 71 (3): 295–307. doi:10.1006/exer.2000.0884.

Nyström, Alexander, Olivier Bornert, and Tobias Kühl. 2017. “Cell Therapy for Basement Membrane-Linked Diseases..” *Matrix Biology : Journal of the International Society for Matrix Biology* 57-58 (January): 124–39. doi:10.1016/j.matbio.2016.07.012.

Page-McCaw, Andrea, Andrew J Ewald, and Zena Werb. 2007. “Matrix Metalloproteinases and the Regulation of Tissue Remodelling..” *Nature Reviews. Molecular Cell Biology* 8 (3): 221–33. doi:10.1038/nrm2125.

Page-McCaw, Andrea, Julia Serano, Joshua M Santé, and Gerald M Rubin. 2003. “Drosophila Matrix Metalloproteinases Are Required for Tissue Remodeling, but Not Embryonic Development..” *Developmental Cell* 4 (1): 95–106.

Parsons, Michael J, Isabel Campos, Elizabeth M A Hirst, and Derek L Stemple. 2002. “Removal of Dystroglycan Causes Severe Muscular Dystrophy in Zebrafish Embryos..” *Development (Cambridge, England)* 129 (14): 3505–12.

Pastor-Pareja, J C, M Wu, and T Xu. 2008. “An Innate Immune Response of Blood Cells to Tumors and Tissue Damage in Drosophila.” *Disease Models & Mechanisms* 1 (2-3): 144–54. doi:10.1242/dmm.000950.

Pastor-Pareja, José Carlos, and Tian Xu. 2011. “Shaping Cells and Organs in Drosophila by Opposing Roles of Fat Body-Secreted Collagen IV and Perlecan..” *Developmental Cell* 21 (2): 245–56. doi:10.1016/j.devcel.2011.06.026.

Poritz, Lisa S, Kristian I Garver, Cecelia Green, Leo Fitzpatrick, Francesca Ruggiero, and Walter A Koltun. 2007. “Loss of the Tight Junction Protein ZO-1 in Dextran Sulfate Sodium Induced Colitis..” *The Journal of Surgical Research* 140 (1): 12–19. doi:10.1016/j.jss.2006.07.050.

Pöschl, Ernst, Ursula Schlötzer-Schrehardt, Bent Brachvogel, Kenji Saito, Yoshifumi Ninomiya, and Ulrike Mayer. 2004. “Collagen IV Is Essential for Basement Membrane Stability but Dispensable for Initiation of Its Assembly During Early Development..” *Development (Cambridge, England)* 131 (7). Oxford University Press for The Company of Biologists Limited: 1619–28. doi:10.1242/dev.01037.

Preil, Simone A R, Lars P Kristensen, Hans C Beck, Pia S Jensen, Patricia S Nielsen, Torben Steiniche, Marina Bjørling-Poulsen, Martin R Larsen, Maria L Hansen, and Lars M Rasmussen. 2015. “Quantitative Proteome Analysis Reveals Increased Content of Basement Membrane Proteins in Arteries From Patients with Type 2 Diabetes Mellitus and Lower Levels Among Metformin Users..” *Circulation. Cardiovascular Genetics* 8 (5). American Heart Association, Inc.: 727–35. doi:10.1161/CIRCGENETICS.115.001165.

Raghavan, S, C Bauer, G Mundschau, Q Li, and E Fuchs. 2000. “Conditional Ablation of Beta1 Integrin in Skin. Severe Defects in Epidermal Proliferation, Basement Membrane Formation, and Hair Follicle Invagination..” *The Journal of Cell Biology* 150 (5). The Rockefeller University Press: 1149–60.

Ramos-Lewis, William, and Andrea Page-McCaw. 2018. “Basement Membrane Mechanics Shape Development: Lessons From the Fly..” *Matrix Biology : Journal of the International Society for Matrix Biology*, April. doi:10.1016/j.matbio.2018.04.004.

Ramos-Lewis, William, Kimberly S LaFever, and Andrea Page-McCaw. 2018. “A Scar-Like Lesion Is Apparent in Basement Membrane After Wound Repair in Vivo..” *Matrix Biology : Journal of the International Society for Matrix Biology*, July. doi:10.1016/j.matbio.2018.07.004.

Rauskolb, Cordelia, Shuguo Sun, Gongping Sun, Yuanwang Pan, and Kenneth D Irvine. 2014. “Cytoskeletal Tension Inhibits Hippo Signaling Through an Ajuba-Warts Complex..” *Cell* 158 (1): 143–56. doi:10.1016/j.cell.2014.05.035.

Razzell, William, Iwan Robert Evans, Paul Martin, and Will Wood. 2013. “Calcium Flashes Orchestrate the Wound Inflammatory Response Through DUOX Activation and Hydrogen Peroxide Release..” *Current Biology : CB* 23 (5): 424–29. doi:10.1016/j.cub.2013.01.058.

Reilly, Gwendolen C, and Adam J Engler. 2010. *Journal of Biomechanics* 43 (1). Elsevier: 55–62. doi:10.1016/j.jbiomech.2009.09.009.

Ren, Fangfang, Bing Wang, Tao Yue, Eun-Young Yun, Y Tony Ip, and Jin Jiang. 2010. “Hippo Signaling Regulates Drosophila Intestine Stem Cell Proliferation Through Multiple Pathways..” *Proceedings of the National Academy of Sciences of the United States of America* 107 (49): 21064–69. doi:10.1073/pnas.1012759107.

Ren, Fangfang, Qing Shi, Yongbin Chen, Alice Jiang, Y Tony Ip, Huaqi Jiang, and Jin Jiang. 2013. “Drosophila Myc Integrates Multiple Signaling Pathways to Regulate Intestinal Stem Cell Proliferation During Midgut Regeneration..” *Cell Research* 23 (9). Nature Publishing Group: 1133–46. doi:10.1038/cr.2013.101.

Ries, A, W Göhring, J W Fox, R Timpl, and T Sasaki. 2001. “Recombinant Domains of Mouse Nidogen-1 and Their Binding to Basement Membrane Proteins and Monoclonal Antibodies..” *European Journal of Biochemistry* 268 (19): 5119–28.

Risteli, J, and K I Kivirikko. 1974. “Activities of Prolyl Hydroxylase, Lysyl Hydroxylase, Collagen Galactosyltransferase and Collagen Glucosyltransferase in the Liver of Rats with Hepatic Injury..” *The Biochemical Journal* 144 (1). Portland Press Ltd: 115–22.

Risteli, J, H P Bächinger, J Engel, H Furthmayr, and R Timpl. 1980. “7-S Collagen: Characterization of an Unusual Basement Membrane Structure..” *European Journal of Biochemistry* 108 (1): 239–50.

Ross, M Elizabeth. 2002. “Full Circle to Cobbled Brain..” *Nature* 418 (6896). Nature Publishing Group: 376–77. doi:10.1038/418376a.

Sanes, Joshua R. 2003. “The Basement Membrane/Basal Lamina of Skeletal Muscle..” *The Journal of Biological Chemistry* 278 (15): 12601–4. doi:10.1074/jbc.R200027200.

Schegg, Belinda, Andreas J Hülsmeier, Christoph Rutschmann, Charlotte Maag, and Thierry Hennet. 2009. “Core Glycosylation of Collagen Is Initiated by Two Beta(1-O)Galactosyltransferases..” *Molecular and Cellular Biology* 29 (4): 943–52. doi:10.1128/MCB.02085-07.

Schneider, Martina, and Stefan Baumgartner. 2008. “Differential Expression of Dystroglycan-Spliceforms with and Without the Mucin-Like Domain During Drosophila Embryogenesis..” *Fly* 2 (1): 29–35. http://eutils.ncbi.nlm.nih.gov/entrez/eutils/elink.fcgi?dbfrom=pubmed&id=18820475&retmode=ref&cmd=prlinks.

Sherwood, David R. 2015. “A Developmental Biologist's “Outside-the-Cell” Thinking..” *The Journal of Cell Biology* 210 (3): 369–72. doi:10.1083/jcb.201501083.

Shimamoto, Yuta, and Tarun M Kapoor. 2012. “Microneedle-Based Analysis of the Micromechanics of the Metaphase Spindle Assembled in Xenopus Laevis Egg Extracts” 7 (5). Nature Publishing Group, a division of Macmillan Publishers Limited. All Rights Reserved.: 959–69. doi:10.1038/nprot.2012.033.

SIEBOLD, Bernhard, Rainer DEUTZMANN, and Klaus KUHN. 1988. “The Arrangement of Intra- and Intermolecular Disulfide Bonds in the Carboxyterminal, Non-Collagenous Aggregation and Cross-Linking Domain of Basement-Membrane Type IV Collagen.” *European Journal of Biochemistry* 176 (3). John Wiley & Sons, Ltd: 617–24. doi:10.1111/j.1432-1033.1988.tb14321.x.

Soudi, Monika, Marcel Zamocky, Christa Jakopitsch, Paul G Furtmüller, and Christian Obinger. 2012. “Molecular Evolution, Structure, and Function of Peroxidasins..” *Chemistry & Biodiversity* 9 (9). Wiley-Blackwell: 1776–93. doi:10.1002/cbdv.201100438.

Spiro, R G, and M J Spiro. 1971. “Studies on the Biosynthesis of the Hydroxylysine-Linked Disaccharide Unit of Basement Membranes and Collagens. 3. Tissue and Subcellular Distribution of Glycosyltransferases and the Effect of Various Conditions on the Enzyme Levels..” *The Journal of Biological Chemistry* 246 (16): 4919–25.

Sricholpech, Marnisa, Irina Perdivara, Megumi Yokoyama, Hideaki Nagaoka, Masahiko Terajima, Kenneth B Tomer, and Mitsuo Yamauchi. 2012. “Lysyl Hydroxylase 3-Mediated Glucosylation in Type I Collagen: Molecular Loci and Biological Significance..” *The Journal of Biological Chemistry* 287 (27). American Society for Biochemistry and Molecular Biology: 22998–3009. doi:10.1074/jbc.M112.343954.

Stevens, Laura J, and Andrea Page-McCaw. 2012. “A Secreted MMP Is Required for Reepithelialization During Wound Healing.” Edited by Marcos Gonzalez-Gaitan. *Molecular Biology of the Cell* 23 (6): 1068–79. doi:10.1091/mbc.e11-09-0745.

Stramer, Brian, Will Wood, Michael J Galko, Michael J Redd, Antonio Jacinto, Susan M Parkhurst, and Paul Martin. 2005. “Live Imaging of Wound Inflammation in Drosophila Embryos Reveals Key Roles for Small GTPases During in Vivo Cell Migration..” *The Journal of Cell Biology* 168 (4): 567–73. doi:10.1083/jcb.200405120.

Sugimoto, Hikaru, Thomas M Mundel, Malin Sund, Liang Xie, Dominic Cosgrove, and Raghu Kalluri. 2006. “Bone-Marrow-Derived Stem Cells Repair Basement Membrane Collagen Defects and Reverse Genetic Kidney Disease..” *Proceedings of the National Academy of Sciences of the United States of America* 103 (19): 7321–26. doi:10.1073/pnas.0601436103.

Sugimoto, Hikaru, Thomas M Mundel, Mark W Kieran, and Raghu Kalluri. 2006. “Identification of Fibroblast Heterogeneity in the Tumor Microenvironment..” *Cancer Biology & Therapy* 5 (12): 1640–46.

Suleiman, Hani, Lei Zhang, Robyn Roth, John E Heuser, Jeffrey H Miner, Andrey S Shaw, and Adish Dani. 2013. “Nanoscale Protein Architecture of the Kidney Glomerular Basement Membrane.” *eLife* 2 (October). eLife Sciences Publications Limited: 1471. doi:10.7554/eLife.01149.

Takagi, Junichi, Yuting Yang, Jin-Huan Liu, Jia-Huai Wang, and Timothy A Springer. 2003. “Complex Between Nidogen and Laminin Fragments Reveals a Paradigmatic Beta-Propeller Interface..” *Nature* 424 (6951). Nature Publishing Group: 969–74. doi:10.1038/nature01873.

Tanase, Monica, Nicolas Biais, and Michael Sheetz. 2007. “Magnetic Tweezers in Cell Biology.” In *Cell Mechanics*, 83:473–93. Methods in Cell Biology. Elsevier. doi:10.1016/S0091-679X(07)83020-2.

Thomas, Tim, and Marie Dziadek. 1993. “Differential Expression of Laminin, Nidogen and Collagen IV Genes in the Midgestation Mouse Placenta.” *Placenta* 14 (6): 701–13. doi:10.1016/S0143-4004(05)80387-X.

Thomas, Tim, and Marie Dziadek. 1994. “Expression of Collagen A1(IV), Laminin and Nidogen Genes in the Embryonic Mouse Lung: Implications for Branching Morphogenesis.” *Mechanisms of Development* 45 (3): 193–201. doi:10.1016/0925-4773(94)90007-8.

Tian, Aiguo, and Jin Jiang. 2014. “Intestinal Epithelium-Derived BMP Controls Stem Cell Self-Renewal in Drosophila Adult Midgut..” *eLife* 3 (March). eLife Sciences Publications Limited: e01857. doi:10.7554/eLife.01857.

Tian, Aiguo, Qing Shi, Alice Jiang, Shuangxi Li, Bing Wang, and Jin Jiang. 2015. “Injury-Stimulated Hedgehog Signaling Promotes Regenerative Proliferation of Drosophila Intestinal Stem Cells..” *The Journal of Cell Biology* 208 (6): 807–19. doi:10.1083/jcb.201409025.

TIMPL, RUPERT, and ROBERT W GLANVILLE. 1981. “The Aminopropeptide of Collagen.” *Clinical Orthopaedics and Related Research* &NA; (158). Clinical Orthopaedics and Related Research: 224???242–42. doi:10.1097/00003086-198107000-00032.

Tsilibary, Effie C. 2003. “Microvascular Basement Membranes in Diabetes Mellitus..” Edited by Fred T Bosman and Ivan Stamenkovic 200 (4). Wiley-Blackwell: 537–46. doi:10.1002/path.1439.

Urbano, Jose M, Catherine N Torgler, Cristina Molnar, Ulrich Tepass, Ana López-Varea, Nicholas H Brown, Jose F de Celis, and Maria D Martín-Bermudo. 2009. “Drosophila Laminins Act as Key Regulators of Basement Membrane Assembly and Morphogenesis..” *Development (Cambridge, England)* 136 (24): 4165–76. doi:10.1242/dev.044263.

Vanacore, Roberto, Amy-Joan L Ham, Markus Voehler, Charles R Sanders, Thomas P Conrads, Timothy D Veenstra, K Barry Sharpless, Philip E Dawson, and Billy G Hudson. 2009. “A Sulfilimine Bond Identified in Collagen IV..” *Science (New York, N.Y.)* 325 (5945): 1230–34. doi:10.1126/science.1176811.

Vila, Maria C, Sree Rayavarapu, Marshall W Hogarth, Jack H Van der Meulen, Adam Horn, Aurelia Defour, Shin'ichi TAKEDA, et al. 2017. “Mitochondria Mediate Cell Membrane Repair and Contribute to Duchenne Muscular Dystrophy.” *Cell Death*

and Differentiation 24 (2). Nature Publishing Group: 330–42. doi:10.1038/cdd.2016.127.

Walker, F. 1972. “Basement-Membrane Turnover in the Rat..” *The Journal of Pathology* 107 (2): 119–21. doi:10.1002/path.1711070206.

Wang, Su, Yuan Gao, Xiaoqing Song, Xing Ma, Xiujuan Zhu, Ying Mao, Zhihao Yang, et al. 2015. “Wnt Signaling-Mediated Redox Regulation Maintains the Germ Line Stem Cell Differentiation Niche..” *eLife* 4 (October): e08174. doi:10.7554/eLife.08174.

Wang, Xiaomeng, Robin E Harris, Laura J Bayston, and Hilary L Ashe. 2008. “Type IV Collagens Regulate BMP Signalling in Drosophila..” *Nature* 455 (7209): 72–77. doi:10.1038/nature07214.

Wei, Shuo, Zhihong Xie, Elena Filenova, and Keith Brew. 2003. “Drosophila TIMP Is a Potent Inhibitor of MMPs and TACE: Similarities in Structure and Function to TIMP-3..” *Biochemistry* 42 (42): 12200–12207. doi:10.1021/bi035358x.

Willem, Michael, Nicolai Miosge, Willi Halfter, Neil Smyth, Iris Jannetti, Elke Burghart, RUPERT TIMPL, and Ulrike Mayer. 2002. “Specific Ablation of the Nidogen-Binding Site in the Laminin Gamma1 Chain Interferes with Kidney and Lung Development..” *Development (Cambridge, England)* 129 (11): 2711–22.

Wolfstetter, Georg, Ina Dahlitz, Kathrin Pfeifer, Uwe Töpfer, Joscha Arne Alt, Daniel Christoph Pfeifer, Reinhard Lakes-Harlan, Stefan Baumgartner, Ruth H Palmer, and Anne Holz. 2019. “Characterization of Drosophila Nidogen/Entactin Reveals Roles in Basement Membrane Stability, Barrier Function and Nervous System Patterning..” *Development (Cambridge, England)* 146 (2). Oxford University Press for The Company of Biologists Limited: dev168948. doi:10.1242/dev.168948.

Xiao, Yu Shu, Frieder Schöck, and Nicanor González-Morales. 2017. “Rapid IFM Dissection for Visualizing Fluorescently Tagged Sarcomeric Proteins..” *Bio-Protocol* 7 (22). doi:10.21769/BioProtoc.2606.

Xu, H, X R Wu, U M Wewer, and E Engvall. 1994. “Murine Muscular Dystrophy Caused by a Mutation in the Laminin Alpha 2 (Lama2) Gene..” *Nature Genetics* 8 (3). Nature Publishing Group: 297–302. doi:10.1038/ng1194-297.

Yan, Xiaohe, Sibylle Sabrautzki, Marion Horsch, Helmut Fuchs, Valerie Gailus-Durner, Johannes Beckers, Martin Hrabě de Angelis, and Jochen Graw. 2014. “Peroxidasin Is Essential for Eye Development in the Mouse..” *Human Molecular Genetics* 23 (21): 5597–5614. doi:10.1093/hmg/ddu274.

You, Jia, Yan Zhang, Zhouhua Li, Zhefeng Lou, Longjin Jin, and Xinhua Lin. 2014. “Drosophila Perlecan Regulates Intestinal Stem Cell Activity via Cell-Matrix Attachment..” *Stem Cell Reports* 2 (6): 761–69. doi:10.1016/j.stemcr.2014.04.007.

Yurchenco, P D, E C Tsilibary, A S Charonis, and H Furthmayr. 1985. “Laminin Polymerization in Vitro. Evidence for a Two-Step Assembly with Domain Specificity..” *The Journal of Biological Chemistry* 260 (12): 7636–44.

Yurchenco, P D, Y S Cheng, and H Colognato. 1992. “Laminin Forms an Independent Network in Basement Membranes..” *The Journal of Cell Biology* 117 (5). The Rockefeller University Press: 1119–33.

Yurchenco, Peter D. 2011. “Basement Membranes: Cell Scaffoldings and Signaling Platforms..” *Cold Spring Harbor Perspectives in Biology* 3 (2): a004911–11. doi:10.1101/cshperspect.a004911.

Yurchenco, Peter D, and Heinz Furthmayr. 1984. “Self-Assembly of Basement Membrane Collagen.” *Biochemistry* 23 (8). American Chemical Society: 1839–50. doi:10.1021/bi00303a040.

Zang, Yiran, Ming Wan, Min Liu, Hongmei Ke, Shuangchun Ma, Lu-Ping Liu, Jian-Quan Ni, and José Carlos Pastor-Pareja. 2015. “Plasma Membrane Overgrowth Causes Fibrotic Collagen Accumulation and Immune Activation in Drosophila Adipocytes..” *eLife* 4 (June). eLife Sciences Publications Limited: e07187. doi:10.7554/eLife.07187.

Zhu, Xianmin, Shaad M Ahmad, Anton Aboukhalil, Brian W Busser, Yongsok Kim, Terese R Tansey, Adrian Haimovich, Neal Jeffries, Martha L Bulyk, and Alan M Michelson. 2012. “Differential Regulation of Mesodermal Gene Expression by Drosophila Cell Type-Specific Forkhead Transcription Factors..” *Development (Cambridge, England)* 139 (8): 1457–66. doi:10.1242/dev.069005.

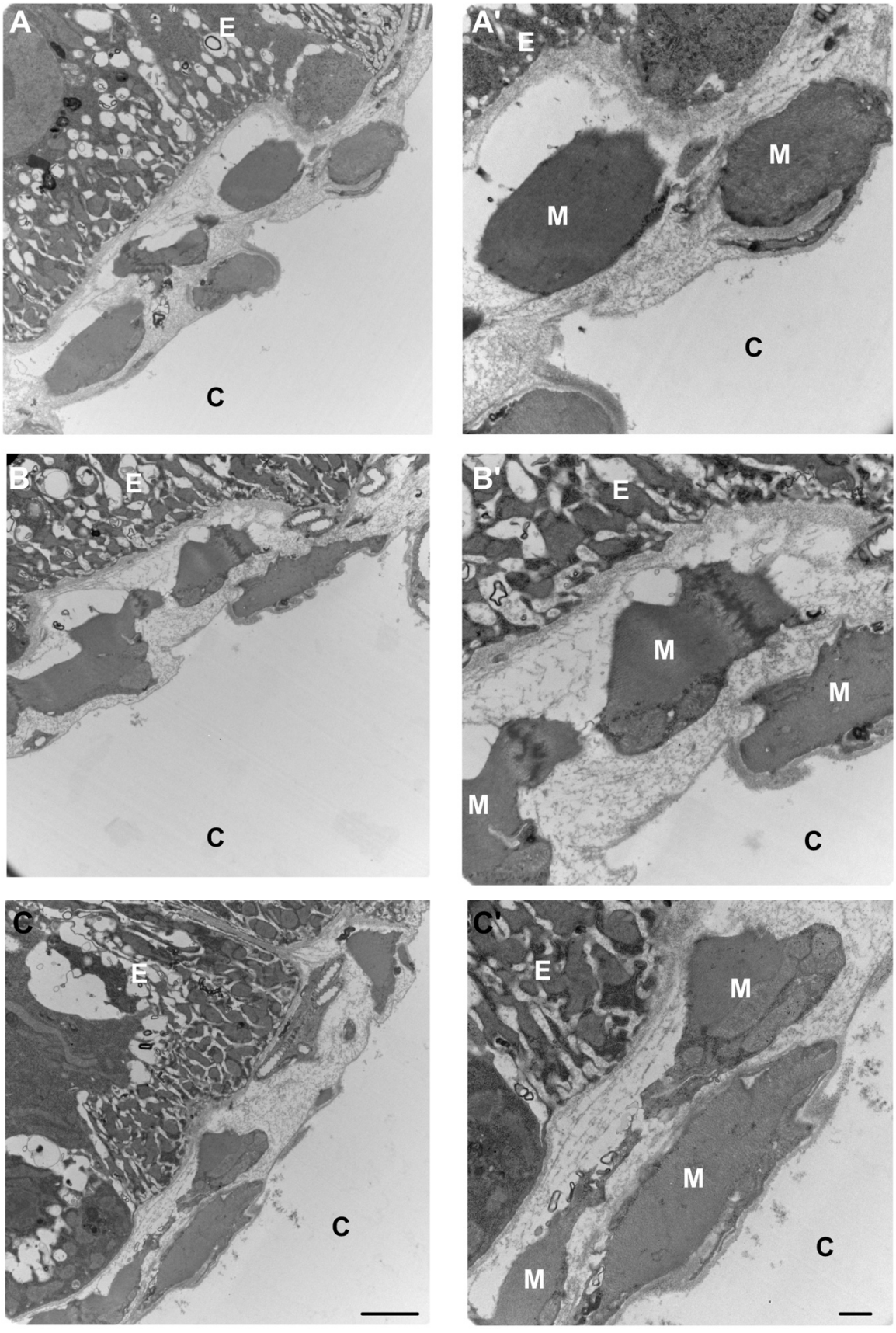
A
E
C
A'
E
M
M
C
B
E
C
B'
E
M
M
M
C
C
E
C
C'
E
M
M
M
C

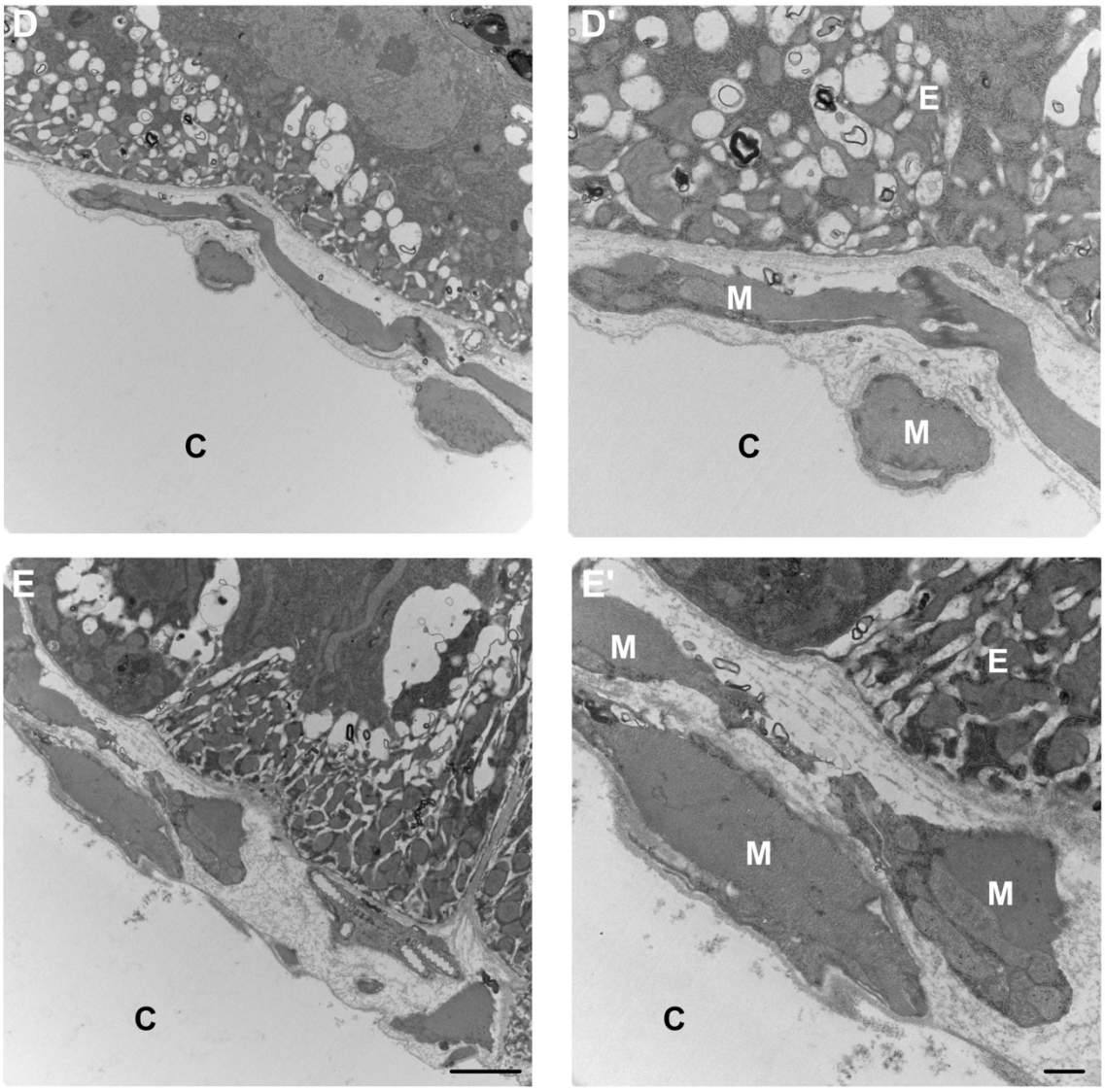

Appendix A- The basement membranes of Sucrose fed fly midguts show a variety of morphologies.

A-E. TEM images of control wild-type (w^{1118}) midguts, fed 48 h on a sucrose diet. The longitudinal and circumferential muscles are perpendicularly oriented to each other. In TEM images, the longitudinal muscles appear stretched in towards the lumen in cross-section, whereas circumferential muscles appear long, because guts were cut in cross-section.

A-E 6500x magnification of TEM images. **A'-E'** 15000x magnification of the left images.

E- enterocyte epithelial layer.

C- body cavity.

M - muscle.

A-E Scale bar = 2 μm A'-E' Scale bar = 500 nm

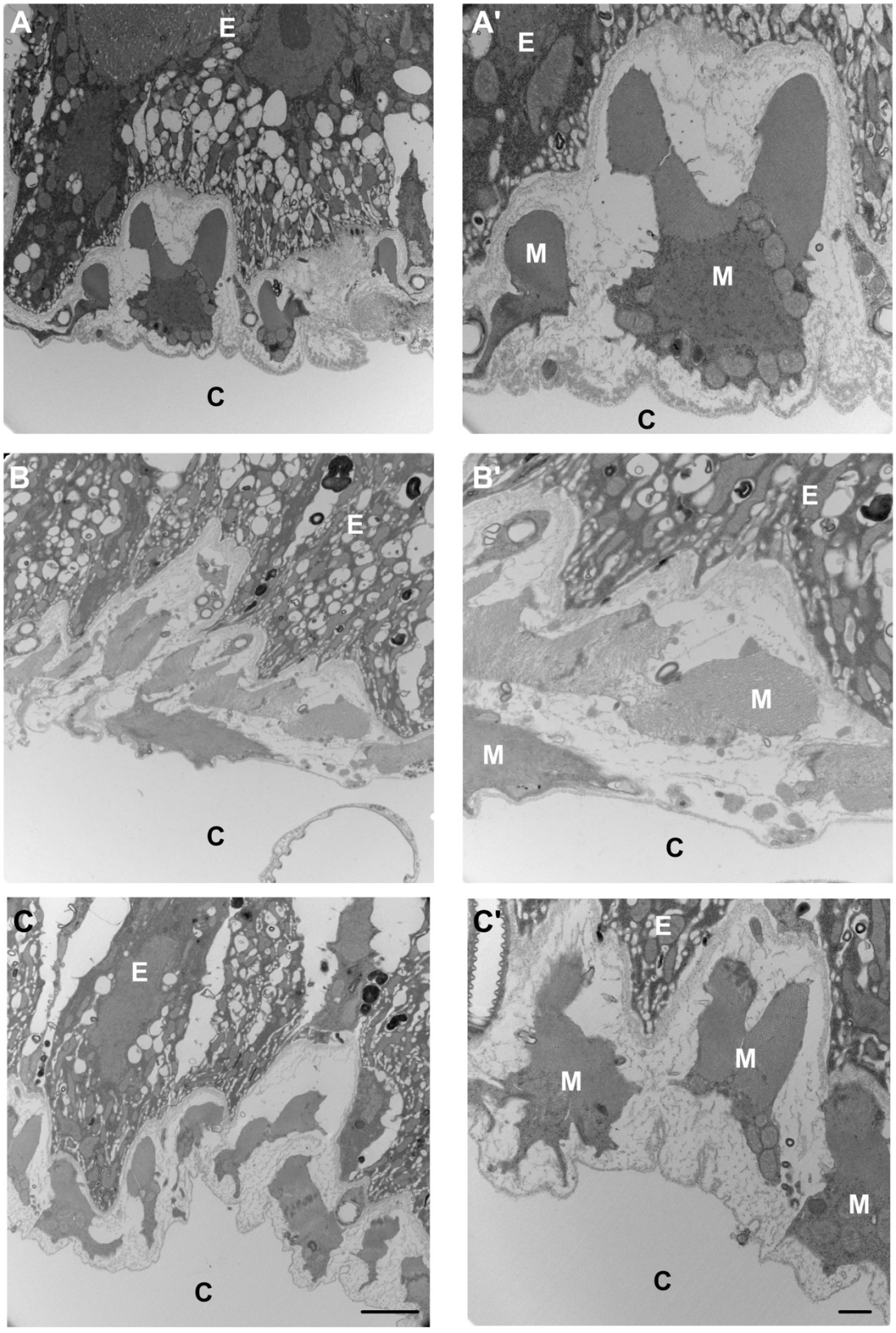
A
E
C
A'
E
M
M
C
B
E
C
B'
E
M
M
C
C
E
C
C'
E
M
M
M
C

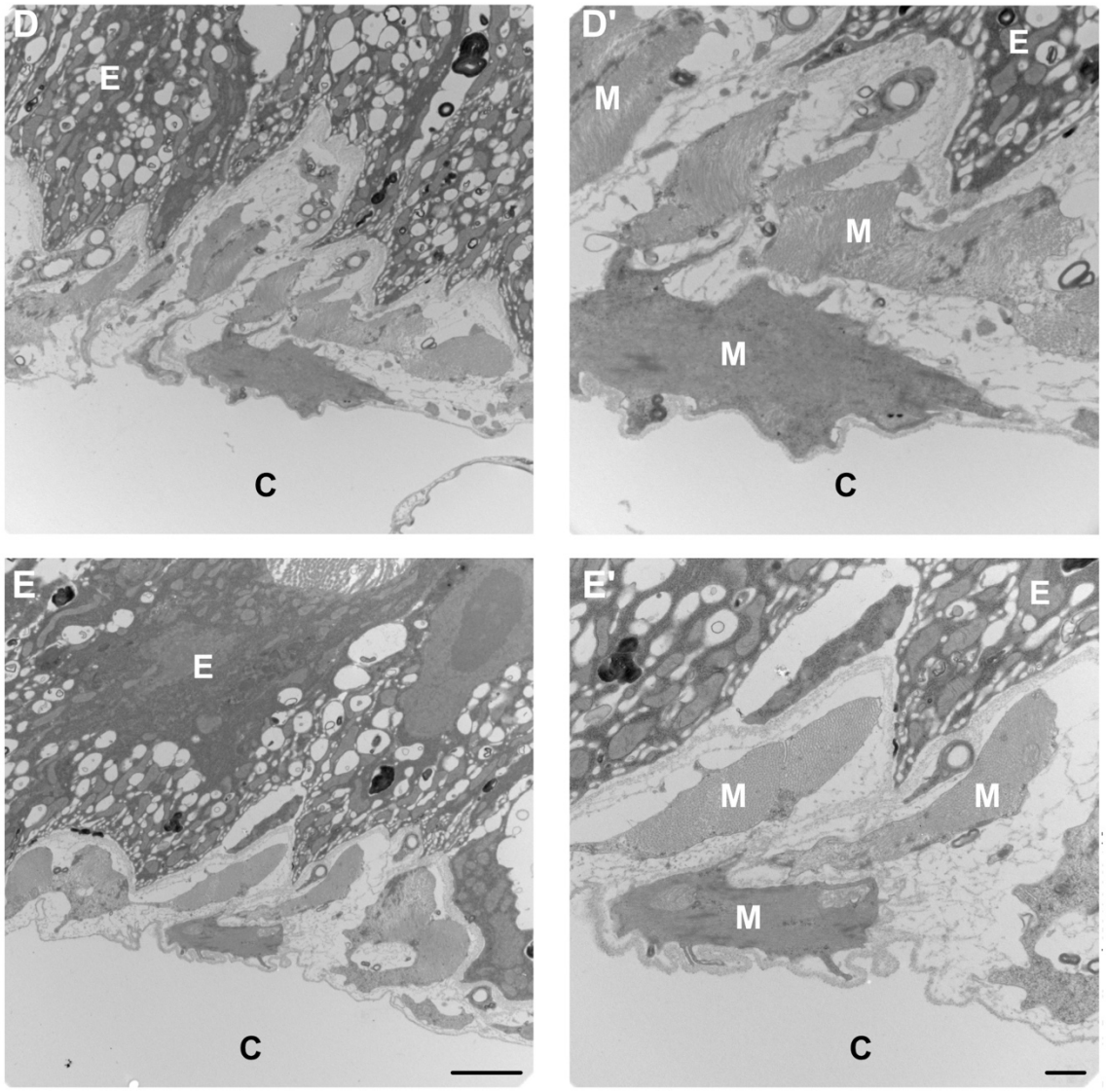

Appendix B- The basement membranes of DSS fed fly midguts show a variety of morphologies.

A-E. TEM images of control wild-type (*w*^{1118}) midguts, fed 48 h on a DSS diet. The longitudinal and circumferential muscles are perpendicularly oriented to each other. In TEM images, the longitudinal muscles appear stretched in towards the lumen in cross-section, whereas circumferential muscles appear long, because guts were cut in cross-section.

A-E 6500x magnification of TEM images. **A'-E'** 15000x magnification of the left images.

E- enterocyte epithelial layer.

C- body cavity.

M - muscle.

A-E Scale bar = 2 μm A'-E' Scale bar = 500 nm

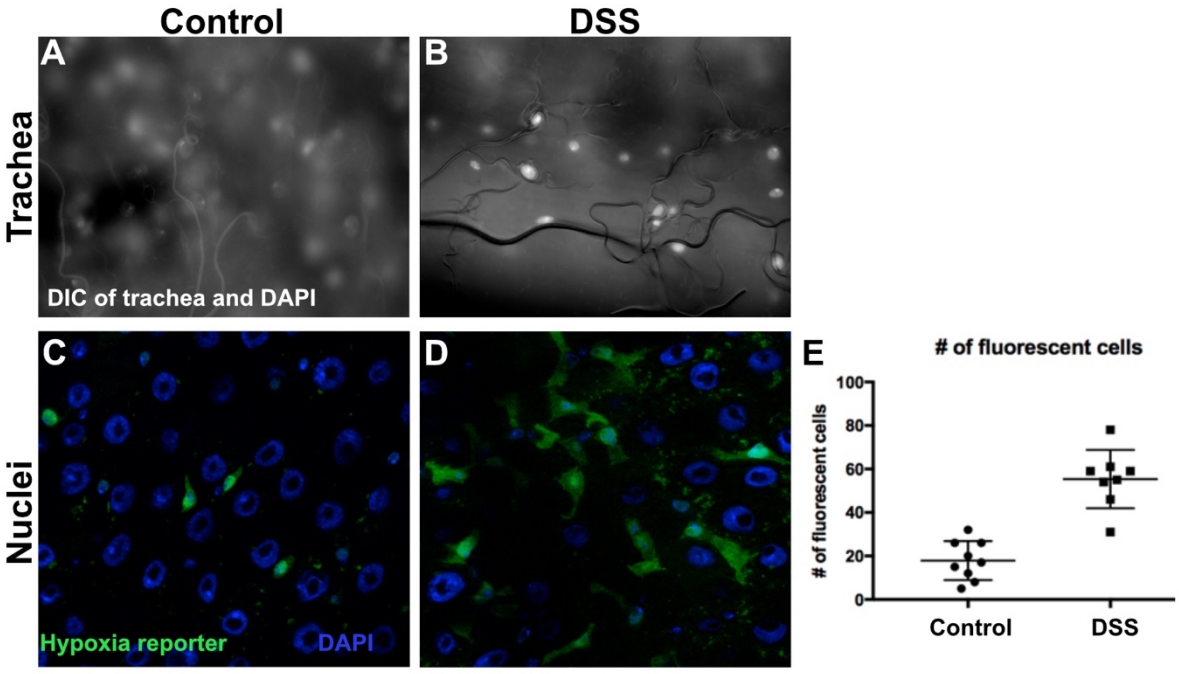

Appendix C - DSS induces a hypoxic response in the gut of *Drosophila*

(A) Brightfield image showing trachea and DAPI of control fed fly. **(B)** Brightfield images showing trachea wrapped around the nuclei staining. This wrapping can be indicative of a hypoxia response. **(C-D)** A hypoxia response element (HRE) reporter fly was used to assess if there was a hypoxic response in the fly guts. **(D)** DSS fed flies show a upregulation in the hypoxia response element. **(E)** Quantification of number of cells positive for the hypoxia response element. n = 9 for control flies. n = 8 for DSS fed flies.

Fly Line- HRE-Gal4/TM3

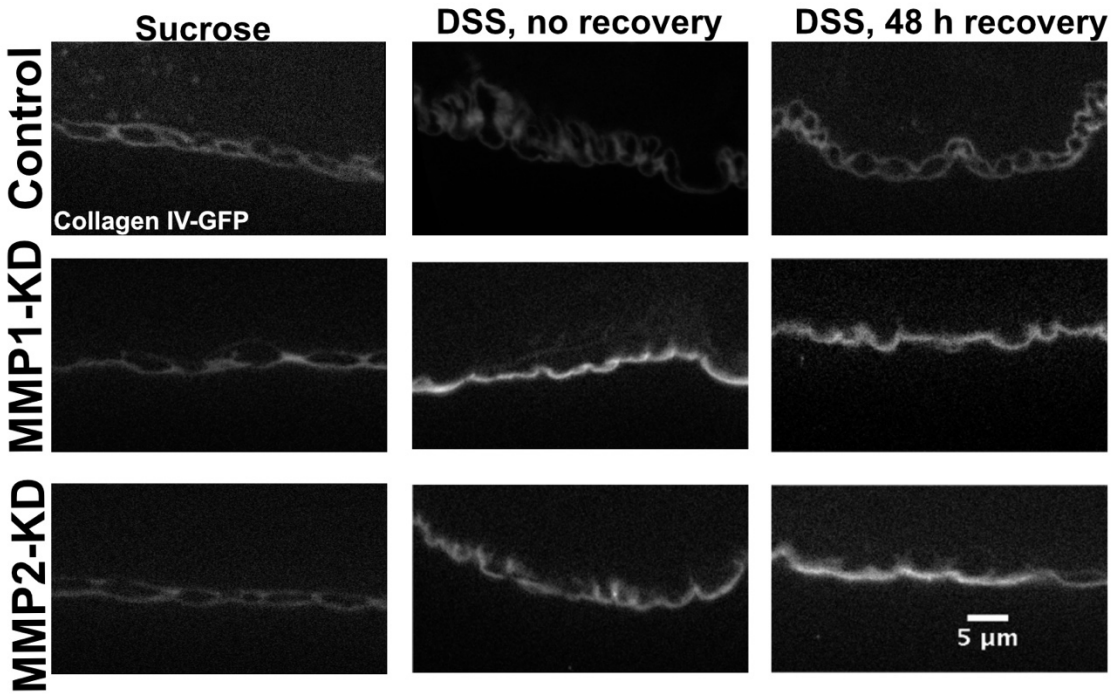

Appendix D- Basement membrane repair requires matrix metalloproteinase 1 and 2

(A-I) Epifluorescence microscopy images of Col IV-GFP showing the basement membrane and muscle morphology before, during, or after DSS feeding. When *Mmp 1* or *Mmp2* is knocked down for 11 days prior to feeding in adults, basement membranes do not repair as inferred from the muscle morphology Scale bar= 5 um.

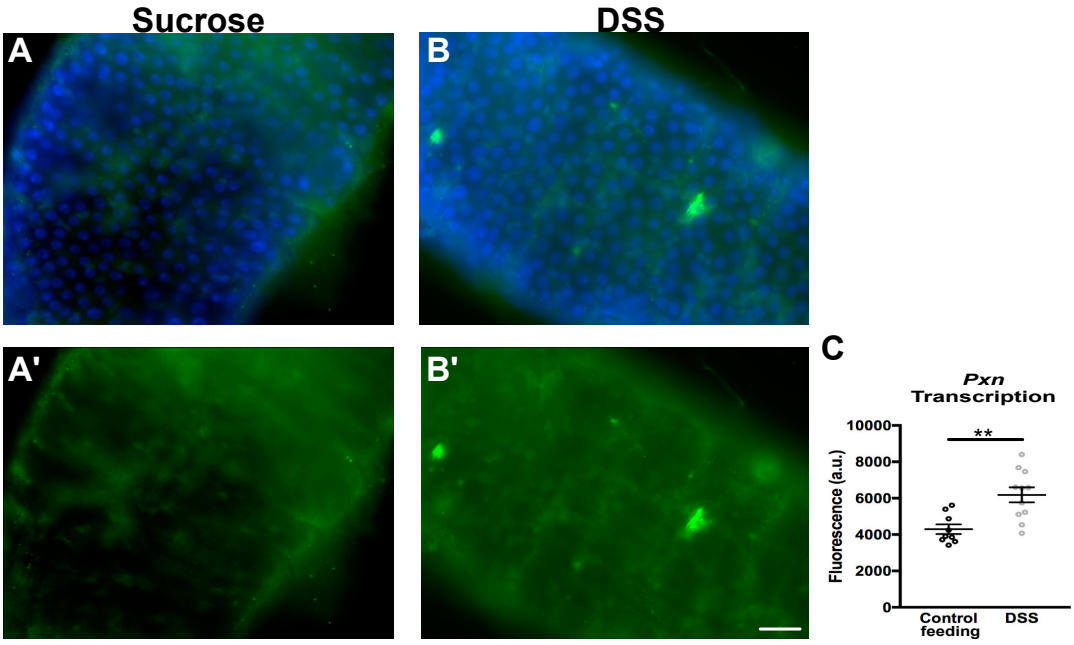

Appendix E- Peroxidasin transcriptional levels increase in gut epithelium upon DSS damage

(A-B')A *Pxn-Gal4* reporter driving *UAS-GFP* allows visualization of the transcription of *peroxidasin* in the gut epithelium. Blue = DAPI Green = GFP (direct fluorescence). **(A-A')** A representative control image of the peroxidasin transcriptional reporter. **(B-B')** A representative DSS fed image of the peroxidasin transcriptional reporter.**(C)** *Pxn* transcription is increased in the gut epithelium in response to DSS, assayed by a *Pxn-Gal4* reporter driving *UAS-GFP*. scale bar = 50 μm

Quantification Method- Single optical sections were captured at 20 x as above. Using imageJ, I manually outlined the gut region within the image, and then the mean fluorescence intensity was measured. Each dot represents a different gut.

Round 1 Cohort 1
Started - 11/11/15

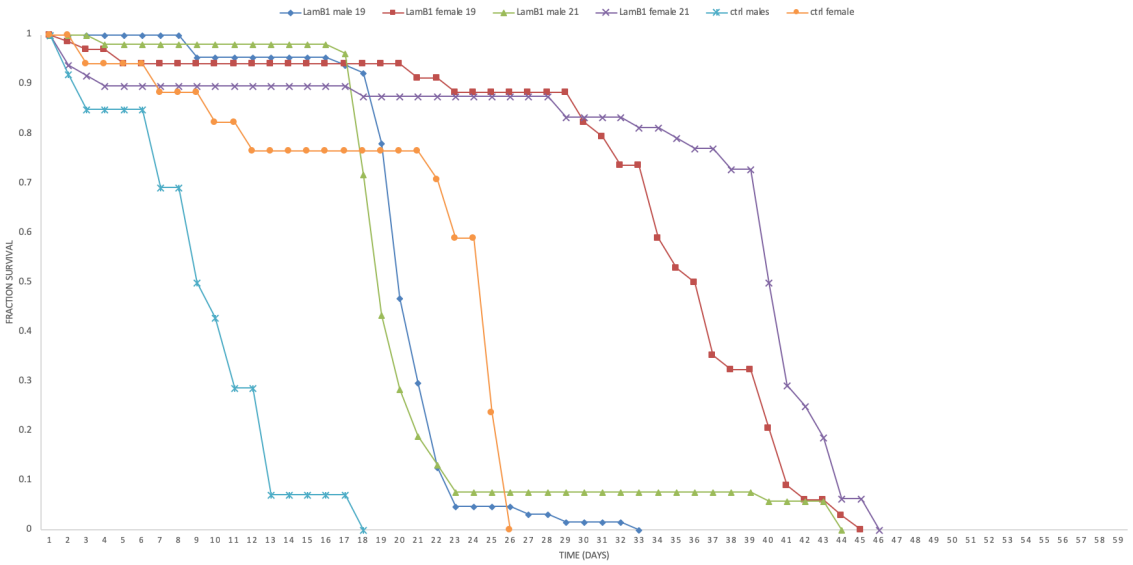

Round 1 Cohort 2
Started - 11/11/15

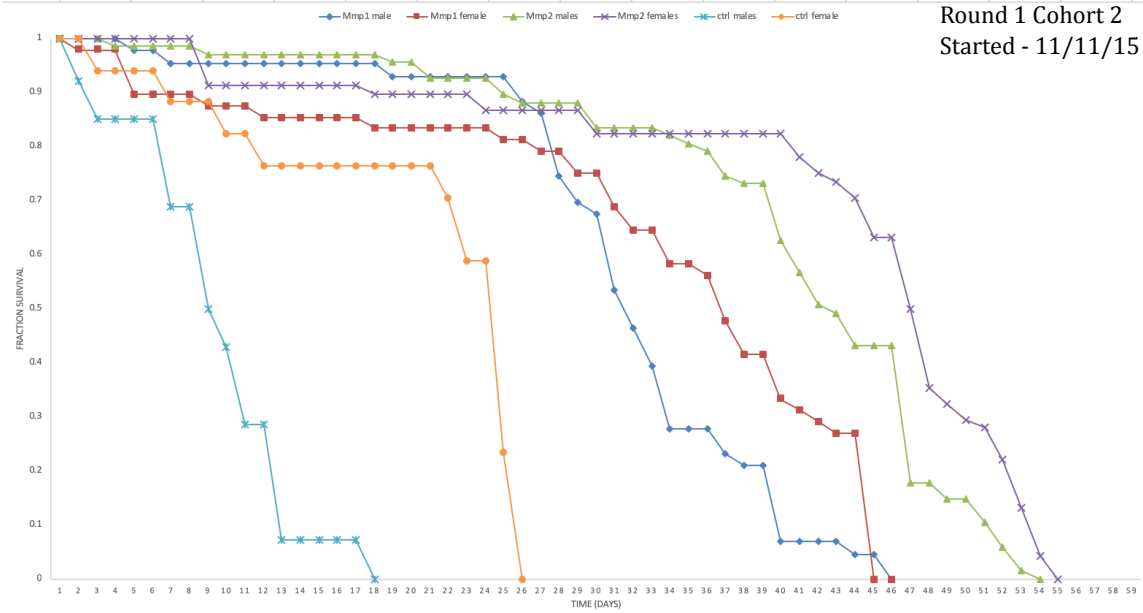

Round 1 Cohort 3
Started - 11/11/15

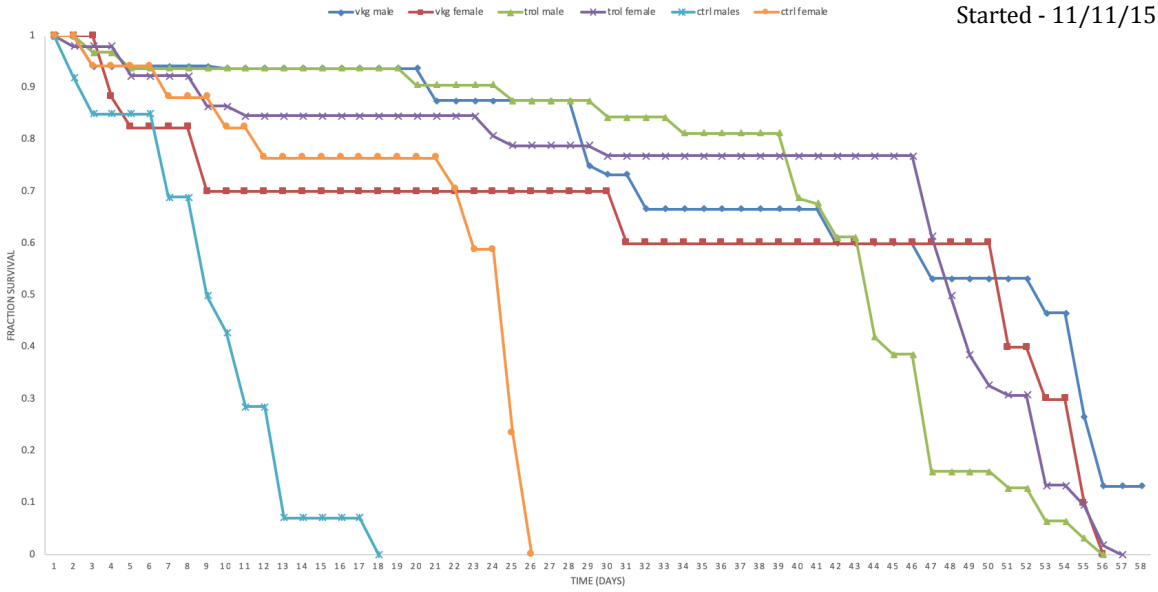

Round 2 Cohort 1
Started - 12/15/15

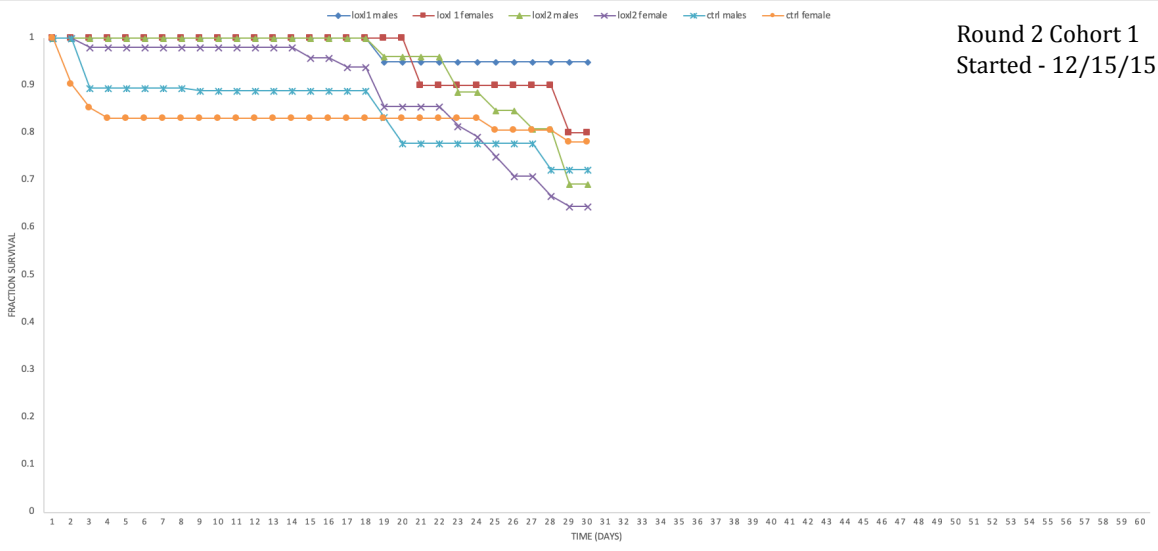

Appendix F- Longevity data of the basement membrane components knocked down
Three to Five day old mated female drosophila knock down lines crossed to tubgal4-tubgal80ts at 29 C and observed longevity.

Methods for RNAi longevity data-

Three to five-day old mated female flies or male flies were collected and fed varying feeding conditions in separate vials. The flies were flipped every 24 hours into a new vial of food at which time the number of dead flies were counted. If a fly flew out of the vial this fly was subtracted from the denominator and was not counted as a dead fly. For the first round of RNAi knockdowns, I used controls flies over a balancer, which was an inappropriate control. I used the fly TubGal4,TubGal80/TM3, but in the second round, I used TubGal4,TubGal80/+.

LamB1 19	**VDRC 23119**
LamB1 21	**VDRC 23121**
MMP1	**VDRC 101505**
MMP2	**VDRC 104713**
vkg	**VDRC 111668**
trol	**VDRC 105502**
Tubgal4 tubgal80^{ts}/TM3	**stock**
Loxl1	**VDRC 106503**
Loxl2	**VDRC 102170**
Tubgal4 tubgal80^{ts}/+	**stock**

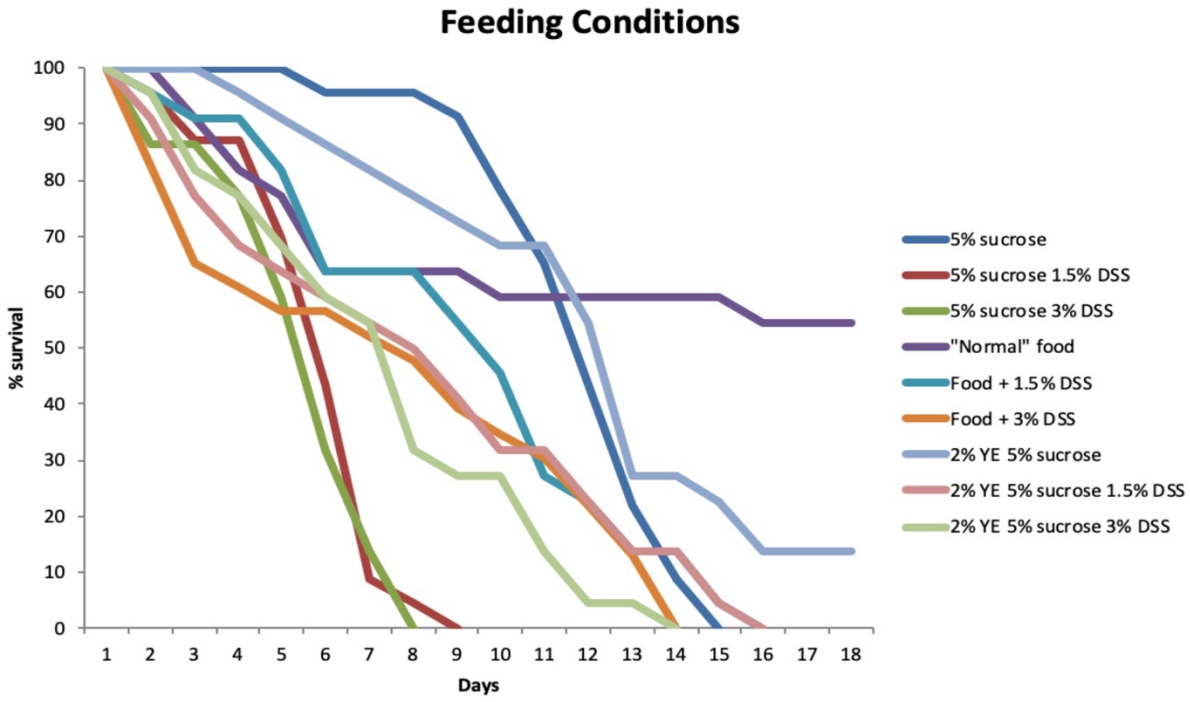

Appendix G- Varying feeding conditions
Three to five day old w^{1118} mated female drosophila fed various feeding conditions.
N = 23 flies for 5% sucrose, 5% + 1.5% DSS, and food + 3% DSS. N = 22 flies for all other feeding conditions.

Method- Three to five day old mated female flies were collected and fed varying feeding conditions. The female flies were flipped every 24 hours into a new vial of food at which time the number of dead flies were counted. If a fly flew out of the vial this fly was subtracted from the denominator and was not counted as a dead fly. The flies would consistently get stuck to the yeast extract as it was extremely sticky. Therefore, we decided to discontinue feeding the flies yeast extract.

DSS = dextran sodium sulfate
YE = yeast extract

Creating fly food
68 mL H2O
320 mg of agar
1.2 g of Redstar yeast
4 mL of dark molasses

Directions:
1. bring H2O to a slight boil
2. Add agar & bring it back to a rolling boil
3. Bring H2O down
4. Add yeast to the mixture
5. Finally add molasses
6. Heat for ~30 - 45 m
7. Divide the mixture
8. Allow to partially cool & add chemicals (phg or DSS)
9. Divide into plastic vials (~2-3 mL/vial)
10. Allow to cool overnight with cheese grate
11. Cap the next day